General Disclaimer

One or more of the Following Statements may affect this Document

- This document has been reproduced from the best copy furnished by the organizational source. It is being released in the interest of making available as much information as possible.

- This document may contain data, which exceeds the sheet parameters. It was furnished in this condition by the organizational source and is the best copy available.

- This document may contain tone-on-tone or color graphs, charts and/or pictures, which have been reproduced in black and white.

- This document is paginated as submitted by the original source.

- Portions of this document are not fully legible due to the historical nature of some of the material. However, it is the best reproduction available from the original submission.

EXPERIMENTS FOR IMPROVED POSITIONING BY MEANS OF INTEGRATED DOPPLER SATELLITE OBSERVATIONS AND THE NNSS BROADCAST EPHEMERIS

by

Manohar G. Arur

Prepared for

National Aeronautics and Space Administration
Washington, D.C.

OSU

The Ohio State University
Research Foundation
Columbus, Ohio   43212

October, 1977

EXPERIMENTS FOR IMPROVED POSITIONING BY MEANS OF INTEGRATED DOPPLER SATELLITE OBSERVATIONS AND THE NNSS BROADCAST EPHEMERIS

by

Manohar G. Arur

Dedicated to the Loving Memory

of my Grandfather

SHIVRAO NARAYAN ARUR

who was also my first Teacher

PREFACE

This project is under the supervision of Professor Ivan I. Mueller, Department of Geodetic Science, The Ohio State University, and under the technical direction of Mr. James P. Murphy, Special Programs, Office of Applications, Code ES, NASA Headquarters, Washington, D.C. The contract is administered by the Office of University Affairs, NASA, Washington, D.C. 20546.

ABSTRACT

The Navy Navigation Satellite System (NNSS) is over fifteen years old and has well established its utility in position determination, from the knowledge of the satellite ephemeris and the observations of the Doppler shifts at the receiver.

The satellite ephemeris is available in two forms. The broadcast ephemeris which can be received on real time basis is predictive and has larger uncertainties than the post fitted precise ephemeris whose availability is restrictive.

This study is an effort to improve station position recovery using broadcast ephemeris in Doppler data reduction.

Comparison of precise and broadcast ephemerides, treating the former as the standard, yields information about the state disturbance that can be associated with the broadcast ephemeris. Statistical information about the state disturbance has been used with current observational data for improved position recovery.

The rank deficiency problem encountered in the Short Arc Geodetic Adjustment (SAGA) procedure has been analysed and it has been deduced that the fundamental rank deficiency is six, scale information being derivable from the wavelength of transmission. Coordinate differences between stations coobserving a pass are estimable.

The uncertainty of the broadcast ephemeris, now in the WGS72 system, has been assessed. It is conservatively estimated that its positional uncertainty may vary between 19 to 26 m in-track, 15 to 20 m cross-track and 9 to 10 m in radial directions depending on the incidence of the epoch of observations in the interinjection period.

iv

The broadcast ephemeris indicates a radial bias of -5 m, which appears to be the consequence of

(a) a 9.8 m offset of the origin of the coordinate system, with respect to the geocentre, in the direction of 90°W longitude,

(b) a scale correction of -1.4 ppm required to make it compatible with a terrestrial system obtainable from a scale corrected precise ephemeris.

Considering the state disturbance as a signal, sample autocovariances have been computed for acceleration, velocity, and position.

Two specific experiments have been conducted. In the first experiment in which three stations coobserve 12 passes, the removal of the radial bias, resulted in bringing a chord distance in better agreement with ground survey though the uncertainties were unchanged.

In the second experiment, the station positions of the first experiment, simulated range rate observations and the autocovariance function of the acceleration signal in the Cartesian coordinate system has been used in an adaptive filtering procedure to improve the state of the satellite for one pass. The position improved by only 0.6 m while the positional uncertainty improved by about 4 meters. Much better results are expected with the use of positional signal in the polar coordinate system which could also evaluate the in-track, out-of-plane and radial biases in the individual passes. The experiment has demonstrated the feasibility of this approach.

ACKNOWLEDGEMENTS

TABLE OF CONTENTS

LIST OF TABLES

LIST OF FIGURES

1. INTRODUCTION

1.1 General Background and Brief Description of Present Study

The Navy Navigation Satellite System (NNSS) also known as the TRANSIT system is over fifteen years old and has well established its utility in position determination.

The operational satellites of this system (currently five) in near polar orbit broadcast a pair of signals with a fixed frequency relationship which is received at ground stations and examined for Doppler shift due to the relative motion between the satellite and the receiver. From the integrated Doppler shift position of the receiver antenna can be computed with the knowledge of the satellite ephemeris.

The major factors affecting the accuracy of a receiver position in Doppler survey are the following:

(1) the type of Doppler receiver and the design of the observations

(2) the accuracy of orbital ephemerides

(3) the method of data reduction including the corrections for atmospheric refraction.

The satellite ephemeris for the NNSS is available from two sources:

(a) on a real time basis, broadcast as a message from the satellite,

(b) in a more precise form, maintained by the Defense Mapping Agency (DMA).

The precise ephemeris is a set of values for earth-fixed positions and velocities at one-minute intervals computed by fitting 48-hour orbital arcs to Doppler data from a world-wide network [Sims, 1972]. The broadcast ephemeris injected into satellite memories twice per day and broadcast automatically to users is computed by fitting 36-hour orbital arcs to Doppler data from the four U.S. Naval Astronautics Group (NAG) stations in Maine, Minnesota,

1

California, and Hawaii and extrapolating these arcs 16 hours beyond the time of the last data used [Piscane et al., 1973].

The broadcast ephemeris differs from the precise ephemeris in the following respects:

(i) The broadcast ephemeris is available on real time basis and is predictive, while the precise ephemeris is a post-fitted ephemeris.

(ii) The broadcast ephemeris is based on Doppler data from only four stations in the U.S. and generated by the NAG (independently of DMA), while the precise ephemeris is based on Doppler data from over 20 stations around the globe including the four stations tracking the satellites for the broadcast ephemeris.

(iii) There are variations in the mathematical models, the parameters used, and truncation errors between the precise and broadcast ephemerides (e.g., the corrections to semi-major axis and out-of-plane orbit components are broadcast to the nearest ten meters) [Moffett, 1973].

(iv) The broadcast ephemeris is available for all satellites, while the precise ephemeris is available for only two satellites (which differ from time to time) and only after a time lag.

(v) The precise ephemeris is believed to have uncertainties of two meters in each coordinate [Anderle, 1976], while the broadcast ephemeris is expected to have an uncertainty of 12 - 28 m.

There has, therefore, been an ongoing effort to improve station position recovery using broadcast ephemeris in Doppler data reduction. The approaches tried out so far can be considered to fall into one of the following categories:

(i) Approaches in which the broadcast ephemeris is allowed to adjust by assigning suitable a priori variances to the ephemeris in a computation in which up to six unknowns (satellite state vector) are also solved for in each pass. For example, the short arc procedure [Brown, 1976] falls in this category.

2

(ii) Approaches in which the data is examined pass by pass in the "Guier Plane" to account for certain biases and to edit the data before subsequent adjustment taking advantage of the fact that both refraction and ephemeris errors are correlated between stations which track the same satellite. For example, the procedures in [Kouba and Wells, 1976] fall in this category.

Further approaches appear to be available. If the post-fitted precise ephemeris is considered to represent the true state of the satellite, the comparison between the precise ephemeris and the predicted broadcast ephemeris (generated by an independent agency) over a length of time may yield statistical information which when suitably used with observational data, broadcast ephemeris and procedures in stochastic filtering theory (where necessary) may give an improved state of the satellite and consequently an improved recovery of station positions. An effort in this direction is the central theme of this study.

The study has been carried out in the following sequence: Most geodetic problems are intimately connected with reference frames and solutions where adequate precautions are not taken would yield values which may not necessarily refer to the reference frame of interest. One cause for this is the rank deficiency encountered in a normal matrix formed without introducing appropriate constraints and is closely related to the mathematical model used to relate the observables with the unknowns for the solution of the geodetic problem. An understanding of the rank deficiency encountered helps in ensuring that appropriate constraints are enforced. An analytical study of the rank deficiency problem in Doppler survey in the short arc mode which has been used in this study has, therefore, first been carried out and described in Chapter 2 along with a discussion about the estimable quantities in Doppler survey.

The next step in the study was to assess the uncertainty of the broadcast ephemeris by comparing it with the precise ephemeris. Studies of this nature carried out by Wells [1974] and White et al. [1975] were based on data pertaining to the period before the computational procedure of the broadcast ephemeris was upgraded in December, 1975. It was, therefore, felt

3

appropriate to carry out a fresh assessment as part of this study. This is described in Chapter 3. The data used for this purpose refers partly to the pre-1975 period and partly to 1976.

Considering that the broadcast ephemeris provides the nominal state of the satellite which is sought to be improved, comparisons between the precise and broadcast ephemerides may be considered to yield information about the state disturbance. Considering the state disturbance as a signal, the procedures for obtaining the statistics of the signal by normal sampling methods have been described along with the results obtained in Chapter 4.

Based on the above, two specific experiments have been carried out and are described with their results in Chapter 5. The first experiment was designed to study the influence of removing the radial bias in the broadcast ephemeris noticed in the investigations in Chapters 3 and 4. With JMR 1 receiver data from three stations, station positions have been obtained from 12 coobserved passes, both before and after removing the radial bias, and the results have been compared. The second experiment was designed to judge the feasibility of using the adaptive filtering technique for local orbit improvement. With the station positions obtained in the first experiment held fixed, the precise and broadcast ephemeris state vectors for one pass of satellite 19 and the parameters of the sample signal autocovariance obtained in Chapter 4 have been input to an adaptive filtering program. This program uses simulated range rate observations to determine the error and uncertainty of the broadcast state vector after processing three new observations at every integration step treating the precise ephemeris state vector as errorless for this purpose.

Conclusions and recommendations are made in Chapter 6.

1.2 Brief Description of Data Utilized

The data utilized in this study was received from several sources, a brief description of which is given below. The first data set (hereafter referred to as Data Set L) consists of precise and NAG predicted state vectors for

1

satellite nos. 13 and 19 for several passes during a period in September, 1974. This data was received from Defense Mapping Agency Aerospace Center (DMAAC). The data is in the earth-fixed coordinate system of NWL 9D as described in [White et al., 1975]. As mentioned earlier since 1975 the broadcase ephemeris system has been upgraded. Along with changes in computational procedures, the coordinate system adopted has been changed to the Department of Defense World Geodetic System 1972 (WGS 72) which differs by a small amount from the NWL 9D system in which the precise ephemeris continues to be maintained.

The second data set, hereafter referred to as Data Set D, was received from DBA Systems, Inc. It consists of Doppler observational data from three ground stations in Florida acquired during a period in January, 1976. As JMR 1 receivers were used, the broadcast ephemeris for the satellites tracked was also available in a message form. The precise ephemeris of satellite nos. 19 and 20 for the related period was obtained from DMA.

The third data set, hereafter referred to as Data Set S, was received from the National Geodetic Survey (NGS). It consists of the precise ephemeris for satellite nos. 12 and 19 tracked during October, 1976. The broadcase ephemeris of the satellites for the related period was received separately from the NAG.

1.3 Brief Description of Computer Software Utilized

This study has required a considerable amount of data processing for which software from the following sources was used after due modifications.

For obtaining station positions with Doppler observational data, the Short Arc Geodetic Adjustment Program (SAGA) as received at The Ohio State University and described in [Kumar, 1976] was used along with the stand-alone program SAMVAP received from Air Force Geophysics Laboratory. For decoding the JMR 1 receiver ephemeris message, a routine obtained from Mr. White, DMAAC, was useful. For Kalman filtering procedures, the program "EARTHOD" from the University of Texas at Austin was suitably modified.

1.4 Coordinate Systems Used

For formulations related to satellite dynamics, an earth-centered inertial coordinate system (ECI) has been used as defined below:

The X and Z axes are directed, respectively, to the true vernal equinox and the true North celestial pole at a selected epoch t_0. The Y axis forms a right-handed system with Z and X.

The precise and broadcast ephemerides provide the satellite state vectors in an earth-fixed system (EF), through there is a small difference in the scale and longitude definition between the two. The earth-fixed coordinate system is defined with the X axis oriented to the Greenwich Mean Astronomical Meridian, and the Z axis passing through the Conventional International Origin (CIO), both as defined by the Bureau International de l'Heure (BIH). The Y axis forming the right-handed system defines with X the average geodetic equator.

For observations, topocentric systems which are parallel to the above but passing through the observer position instead of being geocentric are also used.

Variations from the above where they arise, and actual symbols used, have been explained in the text. All vector quantities have an overbar.

2. RANK DEFICIENCY PROBLEM IN THE DOPPLER SYSTEM

2.1 Introductory Remarks

One of the practical aims of geodesy is that of the determination of positions of points on the earth's surface. The latter aim has dictated the need for adopting a frame of reference (or coordinate system) with respect to which locations of points could be determined. Having adopted a reference frame, it is imperative that for the results to be fully meaningful the coordinate system is maintained.

Unfortunately, one kind of geometric observation cannot provide all the necessary information about the coordinate system. For example, range observations can give information about the scale but not the origin or orientation of a coordinate system. When an adjustment is carried out with such observations by the usual method of observation equations [Uotila, 1967] with the mathematical model

$$\overline{Y}_a \;-\; G(\overline{X}_a) \tag{2.1}$$

where G is a vector function relating the u × 1 parameter vector $\overline{X}_a$ with $\overline{Y}_a$, the n × 1 observation vector, the following linearized form is obtained

$$\overline{V} \;=\; H\overline{X} + \overline{Y} \tag{2.2}$$

where

$\overline{V}$ is the n × 1 vector of observational residuals

H is the n × u matrix $\partial G/\partial \overline{X}_a$, the matrix of partials of the observables with respect to the parameters evaluated at the nominal value of the parameters $\overline{X}_0$

$\overline{X}$ is the u × 1 vector of unknown corrections to $\overline{X}_0$

7

and

$$\overline{Y} = \overline{Y}_0 - \overline{Y}_b \text{ is the difference between the computed observations}$$

$\overline{Y}_0 \cdot G(\overline{X}_0)$ and the observations $\overline{Y}_b$.

Generally in all geodetic adjustments $n > u$, and the rank of the H matrix becomes less than u if no parameters are constrained.

So in the normal equations

$$N\overline{X} \qquad -\overline{U} \qquad\qquad\qquad (2.3)$$

where

$N \qquad H^T PH$, the $u \times u$ normal matrix

$P \qquad n \times n$ weight matrix of the observations

$\overline{U} \qquad H^T P \overline{Y}$

the rank of N is less than u, and a Cayley inverse cannot be obtained for N, which could give the unique solution $\overline{X} \qquad -N^{-1}\overline{U}$, as the unbiased estimator of the parameters.

This is because the lack of information about the reference frame in the observations leads to a rank defect of the design matrix H and the singularity of the normal matrix.

To overcome this situation, additional information about the coordinate system lacking in the observations is needed in the form of constraints on parameters. This additional information may be introduced in the form of (a) inner constraints, (b) weighted constraints, or (c) absolute constraints. The nature of the constraints enforced influences the coordinate system in which the solution vector is obtained.

For making decisions in this matter, the rank deficiency encountered in the short arc mode of Doppler data reduction used in this study has been derived in this chapter and the decisions regarding the constraints have been explained.

2.2 Rank Defect in the Short Arc Mode

Primarily, the rank defect in a design matrix depends on the type of observations. However, the rank defect may increase due to the additional parameters used in the mathematical model other than the station positions and/or numerical problems, which may generate dependence between the columns of the design matrix.

Therefore, only the minimum rank defect situation has been analyzed, taking into consideration a simplified form of the mathematical model used in the SAGA program with the Doppler data reduction [Brown, 1969, 1973], and this is termed the fundamental rank deficiency.

In its simplest form the integrated Doppler shift is modeled as

$$D = \Delta f (t_2 - t_1) + (\rho_{P2} - \rho_{P1})/\lambda \qquad (2.4)$$

where

λ is the wave length of the adopted frequency of transmission

D is the observable Doppler count at one ground station P during the motion of a satellite from position 1 to position 2

t_1, t_2 are the epochs corresponding to satellite positions 1 and 2

Δf is the unknown frequency offset given by $f_t - f_s$, where f_t is the ground reference frequency and f_s is the frequency transmitted by the satellite

ρ_{P2}, ρ_{P1} are the slant ranges corresponding to positions 2 and 1 from P.

In terms of the computed range difference, the observation equation in a functional form is given by

$$(\rho_{P2} - \rho_{P1})^c + d\rho_{12} (d\overline{X}_P, d\overline{X}_1, d\overline{X}_2) = (\rho_{P2} - \rho_{P1})^0 + V_{12} \qquad (2.5)$$

where

$(\rho_{P2} - \rho_{P1})^c$ is the computed range difference

$(\rho_{P2} - \rho_{P1})^0$ is the observed range difference

$$[D - \Delta f (t_2 - t_1)] \lambda$$

$$\approx \lambda [D - \Delta f^0 (t_2 - t_1)] - \lambda (t_2 - t_1) d\Delta f$$

$\rho_{12} \qquad = \rho_{P2} - \rho_{P1}$

$d\rho_{12}$ is the change in range difference due to changes in coordinates of station and satellite positions

V_{12} is the observational residual corresponding to station P and satellite positions 1 and 2

$d\overline{X}_P$ are the three ground station unknowns at P

$d\overline{X}_1$ are the three unknowns for satellite position 1

$d\overline{X}_2$ are the three unknowns for the satellite position 2

$d\Delta f$ is the unknown frequency offset correction to the nominal value Δf^0

For the study of rank deficiency it is necessary to examine the structure of the design matrix H, arising from the left member in the observation equation of the resulting form

$$d\rho_{12} (d\overline{X}_P, \ d\overline{X}_1, \ d\overline{X}_2) + \lambda (t_2 - t_1) \, d\Delta f =$$
$$\lambda [D - \Delta f^0 (t_2 - t_1)] - (\rho_{P2} - \rho_{P1})^c + V_{12} \qquad (2.6)$$

and to determine the number of independent columns therein. For doing this, the form of H matrix in a range observation will be considered first since the formulation for range difference observation follows easily from it.

2.2.1 H Matrix for Range Observation

The formulation of the H matrix is simplified in the system of topocentric right ascension and declination. Let

$$\overline{X}_P \qquad \begin{bmatrix} X_P \\ Y_P \\ Z_P \end{bmatrix} \quad \text{be the earth-fixed coordinates of ground station P, and}$$

$$\overline{X}_1 \qquad \begin{bmatrix} X_1 \\ Y_1 \\ Z_1 \end{bmatrix} \quad \text{be the earth-fixed coordinates of the satellite at epoch 1}$$

If α_1 and δ_1 are the topocentric right ascension and declination of the satellite at position 1, then

10

$$\begin{bmatrix} X_P - X_1 \\ Y_P - Y_1 \\ Z_P - Z_1 \end{bmatrix} = \begin{bmatrix} 1 & 0 & x_n \\ 0 & 1 & -y_n \\ -x_n & y_n & 1 \end{bmatrix} R_3(\theta_{G1}) \begin{bmatrix} \rho_{P1} \cos \delta_1 \cos \alpha_1 \\ \rho_{P1} \cos \delta_1 \sin \alpha_1 \\ \rho_{P1} \sin \delta_1 \end{bmatrix} \qquad (2.7)$$

[Krakiwsky et al., 1967]

where

$R_3(\theta_{G1})$ is the transformation matrix for rotation around the third

axis given by
$$\begin{bmatrix} \cos \theta_{G1} & \sin \theta_{G1} & 0 \\ -\sin \theta_{G1} & \cos \theta_{G1} & 0 \\ 0 & 0 & 1 \end{bmatrix}$$

θ_{G1} is the Greenwich apparent sidereal time at epoch 1

x_n, y_n are the components of polar motion

Denoting the polar motion matrix by C^T, equation (2.7) can be differentiated treating the slant range ρ_{P1} and the position vectors $\overline{X}_P$ and $\overline{X}_1$ as variables.

Neglecting second-order terms, C^T is orthogonal. Therefore,

$$C \begin{bmatrix} dX_P - dX_1 \\ dY_P - dY_1 \\ dZ_P - dZ_1 \end{bmatrix} = \begin{bmatrix} \cos(\alpha_1 - \theta_{G1}) \cos \delta_1 \\ \sin(\alpha_1 - \theta_{G1}) \cos \delta_1 \\ \sin \delta_1 \end{bmatrix} d\rho_{P1}$$

Therefore,

$$[\cos(\alpha_1 - \theta_{G1}) \cos \delta_1 \mathrel{\vdots} \sin(\alpha_1 - \theta_{G1}) \cos \delta_1 \mathrel{\vdots} \sin \delta_1] \; C \begin{bmatrix} dX_P - dX_1 \\ dY_P - dY_1 \\ dZ_P - dZ_1 \end{bmatrix} = d\rho_{P1}$$

$$(2.8)$$

This is the familiar observation equation form.

Denoting

$$d\overline{X}_1 = \begin{bmatrix} dX_1 \\ dY_1 \\ dZ_1 \end{bmatrix} \qquad d\overline{X}_P = \begin{bmatrix} dX_P \\ dY_P \\ dZ_P \end{bmatrix}$$

equation (2.8) can be rewritten as

11

$$d\rho_{P1} = \begin{bmatrix} h_{P1} & -h_{P1} \end{bmatrix} \begin{bmatrix} d\overline{X}_P \\ d\overline{X}_1 \end{bmatrix} \qquad (2.9)$$

where h_{P1} is a 1×3 submatrix given by

$$h_{P1} = [\cos(\alpha_1 - \theta_{G1})\cos\delta_1 + x_\text{s}\sin\delta_1 \;\; \sin(\alpha_1 - \theta_{G1})\cos\delta_1 - y_\text{s}\sin\delta_1$$
$$- x_\text{s}\cos(\alpha_1 - \theta_{G1})\cos\delta_1 + y_\text{s}\sin(\alpha_1 - \theta_{G1})\cos\delta_1 + \sin\delta_1]$$

This equation gives the structure of the design matrix in the case of a slant range observation ρ_{P1}.

2.2.2 H Matrix for Range Difference Observations of Doppler System

To obtain the structure of the design matrix in the case of a range difference observation, equation (2.9) is extended to consider corrections to ranges $d\rho_{P1}$ and $d\rho_{P2}$. Corresponding to (2.9) for $d\rho_{P1}$,

$$d\rho_{P2} = \begin{bmatrix} h_{P2} & -h_{P2} \end{bmatrix} \begin{bmatrix} d\overline{X}_P \\ d\overline{X}_2 \end{bmatrix}$$

Hence $d\rho_{12}$, the variation in range difference due to variation in position of station P and satellite positions 1 and 2, is given by

$$d\rho_{12} = d\rho_{P1} - d\rho_{P2} =$$

$$= \begin{bmatrix} h_{P1} & -h_{P1} & 0 \end{bmatrix} \begin{bmatrix} d\overline{X}_P \\ d\overline{X}_1 \\ d\overline{X}_2 \end{bmatrix} - \begin{bmatrix} h_{P2} & 0 & -h_{P2} \end{bmatrix} \begin{bmatrix} d\overline{X}_P \\ d\overline{X}_1 \\ d\overline{X}_2 \end{bmatrix} =$$

$$\begin{bmatrix} (h_{P1} - h_{P2}) & -h_{P1} & h_{P2} \end{bmatrix} \begin{bmatrix} d\overline{X}_P \\ d\overline{X}_1 \\ d\overline{X}_2 \end{bmatrix} \qquad (2.10)$$

The variation of the range difference due to variation of the last unknown $d\Delta f$ is now considered. This is readily seen from equation (2.6) as $\lambda(t_2 - t_1)$. Thus, the structure of the H matrix for a Doppler observation for one ground station, two satellite position unknowns, and a frequency offset unknown will be

$$
\begin{bmatrix}
\overset{(i)}{\cos(\alpha_1 - \theta_{G1})\cos\delta_1} & \overset{(ii)}{\sin(\alpha_1 - \theta_{G1})\cos\delta_1} \\
\;\; -\cos(\alpha_2 - \theta_{G2})\cos\delta_2 & \;\; -\sin(\alpha_2 - \theta_{G2})\cos\delta_2
\end{bmatrix}
$$

$$
\overset{(iii)}{\sin\delta_1 - \sin\delta_2} \qquad \overset{(iv)}{-\cos(\alpha_1 - \theta_{G1})\cos\delta_1} \qquad \overset{(v)}{-\sin(\alpha_1 - \theta_{G1})\cos\delta_1}
$$

$$
\overset{(vi)}{-\sin\delta_1} \qquad \overset{(vii)}{\cos(\alpha_2 - \theta_{G2})\cos\delta_2} \qquad \overset{(viii)}{\sin(\alpha_2 - \theta_{G2})\cos\delta_2}
$$

$$
\overset{(ix)}{\sin\delta_2} \qquad \overset{(x)}{\lambda(t_2 - t_1)} \Big] \tag{2.11}
$$

treating the polar motion components as known and leaving them out of consideration for rank deficiency analysis.

Now the addition of a second range difference observation for satellite positions 2 and 3 will imply three more unknowns. Denoting $\omega_i = \alpha_i - \theta_{Gi}$, the structure of H matrix for the 13 unknowns with two observations will be

$$
\begin{bmatrix}
\overset{(i)}{\cos\omega_1 \cos\delta_1} & \overset{(ii)}{\sin\omega_1 \cos\delta_1} & \overset{(iii)}{\sin\delta_1 - \sin\delta_2} & \overset{(iv)}{-\cos\omega_1 \cos\delta_1} \\
-\cos\omega_2 \cos\delta_2 & -\sin\omega_2 \cos\delta_2 & & \\[4pt]
\cos\omega_2 \cos\delta_2 & \sin\omega_2 \cos\delta_2 & \sin\delta_2 - \sin\delta_3 & 0 \\
-\cos\omega_3 \cos\delta_3 & -\sin\omega_3 \cos\delta_3 & &
\end{bmatrix}
$$

$$
\begin{array}{ccccc}
\overset{(v)}{-\sin\omega_1 \cos\delta_1} & \overset{(vi)}{-\sin\delta_1} & \overset{(vii)}{\cos\omega_2 \cos\delta_2} & \overset{(viii)}{\sin\omega_2 \cos\delta_2} & \overset{(ix)}{\sin\delta_2} \\
0 & 0 & -\cos\omega_2 \cos\delta_2 & -\sin\omega_2 \cos\delta_2 & -\sin\delta_2
\end{array}
$$

$$
\begin{array}{cccc}
\overset{(x)}{0} & \overset{(xi)}{0} & \overset{(xii)}{0} & \overset{(xiii)}{\lambda(t_2 - t_1)} \\
\cos\omega_3 \cos\delta_3 & \sin\omega_3 \cos\delta_3 & \sin\delta_3 & \lambda(t_3 - t_2)
\end{array} \Big] \tag{2.12}
$$

2.2.3 H Matrix in SAGA

It can readily be seen that the above procedure gives three more unknowns for every additional observation, and an overdetermined system required for adjustment cannot be obtained. This situation is remedied either by increasing the number of coobserving stations or restricting the number of satellite unknowns

per pass. In SAGA, the satellite unknowns are restricted to six per pass (three for position and three for velocity) by assuming the force model to be known. In this investigation the same procedure has been followed.

Adopting the following compact notation

$$CC_i = \cos \omega_i \cos \delta_i$$

$$SC_i = \sin \omega_i \cos \delta_i$$

$$S_i = \sin \delta_i$$

the problem is extended to one ground station and four consecutive satellite positions. Following equation (2.12), the structure of H matrix for three observations and 16 unknowns assuming one frequency offset per pass, will appear as

$$
\begin{array}{ccccccccc}
\text{(i)} & \text{(ii)} & \text{(iii)} & \text{(iv)} & \text{(v)} & \text{(vi)} & \text{(vii)} & \text{(viii)} & \text{(ix)} \\
CC_1 \; -CC_2 & SC_1 \; -SC_2 & S_1 \; -S_2 & -CC_1 & -SC_1 & -S_1 & CC_2 & SC_2 & S_2 \\
CC_2 \; -CC_3 & SC_2 \; -SC_3 & S_2 \; -S_3 & 0 & 0 & 0 & -CC_2 & -SC_2 & -S_2 \\
CC_3 \; -CC_4 & SC_3 \; -SC_4 & S_3 \; -S_4 & 0 & 0 & 0 & 0 & 0 & 0
\end{array}
$$

$\longleftarrow$ ----------- $d\overline{X}_P$ ------------- $\longrightarrow$ $($------ $d\overline{X}_1$ ------$)$ $($------ $d\overline{X}_2$ ----$)$

$$
\begin{array}{ccccccc}
\text{(x)} & \text{(xi)} & \text{(xii)} & \text{(xiii)} & \text{(xiv)} & \text{(xv)} & \text{(xvi)} \\
0 & 0 & 0 & 0 & 0 & 0 & \lambda\,(t_2 - t_1) \\
CC_3 & SC_3 & S_3 & 0 & 0 & 0 & \lambda(t_3 - t_2) \\
-CC_3 & -SC_3 & -S_3 & CC_4 & SC_4 & S_4 & \lambda\,(t_4 - t_3)
\end{array}
$$
(2.13)

$($------ $d\overline{X}_3$ ----$)$ $($------ $d\overline{X}_4$ -------$)$ $($---$d\Delta f$---$)$

The unknowns for satellite positions are now reduced to six, viz., $d\overline{X}_0$, $d\dot{\overline{X}}_0$, the corrections to assumed values of position and velocity components at an adopted epoch t_0 (preferably taken as the epoch t_0 at midarc of the pass). This approach gives the following linear transformation [Brown, 1969, p. 20] for satellite position i at epoch t_i:

$$
d\overline{X}_i \quad \underset{31}{} \quad \underset{33}{R^i} \quad \underset{36}{\Omega^i}
\begin{bmatrix}
d\overline{X}_0 \\
d\dot{\overline{X}}_0
\end{bmatrix}
$$
(2.14)

$$
\underset{61}{}
$$

where $[\overline{X}_0^T \quad \dot{\overline{X}}_0^T]$ $[X_0 \quad Y_0 \quad Z_0 \quad \dot{X}_0 \quad \dot{Y}_0 \quad \dot{Z}_0]$, and Ω^1 is the matrizant in the inertial system given by

$$\Omega^1 = \frac{\partial \ (X_1, \ Y_1, \ Z_1, \ T)_1}{\partial \ (X_0, \ Y_0, \ Z_0, \ \dot{X}_0, \ \dot{Y}_0, \ \dot{Z}_0)}$$

where

X_1, Y_1, Z_1 are the geocentric inertial coordinates of the satellite at T, with $T_1 = t_1 - t_0$

$X_0, Y_0, Z_0, \dot{X}_0, \dot{Y}_0, \dot{Z}_0$ are the assumed initial conditions at T 0

The inertial coordinate system is defined as the coordinate system which is coincident with the earth-fixed system at $T = 0$.

Ω is obtained in SAGA with the help of the orbital integrator developed by Hartwell [1968]. It employs a power series solution to the equations of motion in the inertial system, in a recursive algorithm, which can be represented by the following for an arbitrary T_1:

$$\begin{bmatrix} X_1 & \dot{X}_1 \\ Y_1 & \dot{Y}_1 \\ Z_1 & \dot{Z}_1 \end{bmatrix}_1 \quad \begin{bmatrix} a_0 & a_1 & a_2 & \ldots & a_q \\ b_0 & b_1 & b_2 & \ldots & b_q \\ c_0 & c_1 & c_2 & \ldots & c_q \end{bmatrix} \begin{bmatrix} 1 & 0 \\ T & 1 \\ T^2 & 2T \\ \vdots & \vdots \\ T^q & qT^{q-1} \end{bmatrix}_1 \tag{2.15}$$

where the coefficients a_j, b_j, c_j, j 0, 1, ..., q are functions of the six initial conditions at T 0, $(X_0, Y_0, Z_0, \dot{X}_0, \dot{Y}_0, \dot{Z}_0)$ and the earth gravitational coefficients. q is the index of the power series at which the series is truncated when a prespecified tolerance (0.001 m) is reached for T_m, the maximum value of T to be exercised.

From (2.15), Ω can be seen as

$$\Omega^1 \quad \begin{bmatrix} \Omega_{11} & \Omega_{12} & \ldots & \Omega_{16} \\ \Omega_{21} & \Omega_{2v} & \ldots & \Omega_{2v} \\ \Omega_{31} & \Omega_{3v} & \ldots & \Omega_{36} \end{bmatrix}_1$$

where Ω_{1n} is, in turn, a polynomial 1 1, 3; n 1, 6.

15

$$\Omega_{in} = (\alpha_0 \quad \alpha_1 \quad \ldots \quad \alpha_q)_{in} \begin{bmatrix} 1 \\ \tau \\ \cdot \\ \cdot \\ \tau^q \end{bmatrix}_i \tag{2.16}$$

with $(\alpha_0)_{in}$ as the dominant term. The correspondence between the α coefficients of (2.16) and (a,b,c) coefficients of (2.15) is easily seen. For example, taking Ω_{11}, $(\alpha_0)_{11} = \partial a_0 \, \partial X_0$.

$$R^i = \begin{bmatrix} \cos\psi \, \tau_i & \sin\psi \, \tau_i & 0 \\ -\sin\psi \, \tau_i & \cos\psi \, \tau_i & 0 \\ 0 & 0 & 1 \end{bmatrix} \tag{2.17}$$

is the matrix which can transform the matrizant Ω^i to an earth-fixed system at t_i. ψ is the earth rotation rate.

For passes up to 20 minutes, $\tau_i \leq 10$ minutes, $\cos\psi \, \tau_i \approx 1.0$, and $\sin\psi \, \tau_i \approx 0$, so R^i is taken as an identity matrix for the purpose of rank deficiency analysis. Thus with the help of equation (2.14), equation (2.13) is used to obtain the corresponding portion of the H matrix for satellite position i in terms of the new satellite unknowns through the linear transformation

$$h_i \begin{bmatrix} d\overline{X}_i \end{bmatrix}_{1a \;\; 3 \;\; 1} = h_i \, \Omega^i \begin{bmatrix} d\overline{X}_0 \\ d\dot{\overline{X}}_0 \end{bmatrix}_{6 \;\; 1} \tag{2.18}$$

For the situation in (2.13), the unknowns will reduce from 16 to 10, and the new H matrix will have the structure

$$
\begin{bmatrix}
\overset{\text{(i)}}{CC_1-CC_2} & \overset{\text{(ii)}}{SC_1-SC_2} & \overset{\text{(iii)}}{S_1-S_2}
\end{bmatrix}
$$

$$CC_1-CC_2 \quad SC_1-SC_2 \quad S_1-S_2 \quad
\begin{aligned}
&-(CC_1)(\Omega^1_{11})-(SC_1)(\Omega^1_{21})-(S_1)(\Omega^1_{31})\\
&+(CC_2)(\Omega^2_{11})+(SC_2)(\Omega^2_{21})+(S_2)(\Omega^2_{31})
\end{aligned}$$

$$CC_2-CC_3 \quad SC_2-SC_3 \quad S_2-S_3 \quad
\begin{aligned}
&-(CC_2)(\Omega^2_{11})-(SC_2)(\Omega^2_{21})-(S_2)(\Omega^2_{31})\\
&+(CC_3)(\Omega^3_{11})+(SC_3)(\Omega^3_{21})+(S_3)(\Omega^3_{31})
\end{aligned}$$

$$CC_3-CC_4 \quad SC_3-SC_4 \quad S_3-S_4 \quad
\begin{aligned}
&-(CC_3)(\Omega^3_{11})-(SC_3)(\Omega^3_{21})-(S_3)(\Omega^3_{31})\\
&+(CC_4)(\Omega^4_{11})+(SC_4)(\Omega^4_{21})+(S_4)(\Omega^4_{31})
\end{aligned}$$

(v)

$$
\begin{aligned}
&-(CC_1)(\Omega^1_{12})-(SC_1)(\Omega^1_{22})-(S_1)(\Omega^1_{32})\\
&+(CC_2)(\Omega^2_{12})+(SC_2)(\Omega^2_{22})+(S_2)(\Omega^2_{32})
\end{aligned}
$$

$$
\begin{aligned}
&-(CC_2)(\Omega^2_{12})-(SC_2)(\Omega^2_{22})-(S_2)(\Omega^2_{32})\\
&+(CC_3)(\Omega^3_{12})+(SC_3)(\Omega^3_{22})+(S_3)(\Omega^3_{32})
\end{aligned}
$$

$$
\begin{aligned}
&-(CC_3)(\Omega^3_{12})-(SC_3)(\Omega^3_{22})-(S_3)(\Omega^3_{32})\\
&+(CC_4)(\Omega^4_{12})+(SC_4)(\Omega^4_{22})+(S_4)(\Omega^4_{32})
\end{aligned}
$$

(vi)

$$
\begin{aligned}
&-(CC_1)(\Omega^1_{13})-(SC_1)(\Omega^1_{23})-(S_1)(\Omega^1_{33})\\
&+(CC_2)(\Omega^2_{13})+(SC_2)(\Omega^2_{23})+(S_2)(\Omega^2_{33})
\end{aligned}
$$

$$
\begin{aligned}
&-(CC_2)(\Omega^2_{13})-(SC_2)(\Omega^2_{23})-(S_2)(\Omega^2_{33})\\
&+(CC_3)(\Omega^3_{13})+(SC_3)(\Omega^3_{23})+(S_3)(\Omega^3_{33})
\end{aligned}
$$

$$
\begin{aligned}
&-(CC_3)(\Omega^3_{13})-(SC_3)(\Omega^3_{23})-(S_3)(\Omega^3_{33})\\
&+(CC_4)(\Omega^4_{13})+(SC_4)(\Omega^4_{23})+(S_4)(\Omega^4_{33})
\end{aligned}
$$

(vii)

$$
\begin{aligned}
&-(CC_1)(\Omega^1_{14})-(SC_1)(\Omega^1_{24})-(S_1)(\Omega^1_{34})\\
&+(CC_2)(\Omega^2_{14})+(SC_2)(\Omega^2_{24})+(S_2)(\Omega^2_{34})
\end{aligned}
$$

$$
\begin{aligned}
&-(CC_2)(\Omega^2_{14})-(SC_2)(\Omega^2_{24})-(S_2)(\Omega^2_{34})\\
&+(CC_3)(\Omega^3_{14})+(SC_3)(\Omega^3_{24})+(S_3)(\Omega^3_{34})
\end{aligned}
$$

$$
\begin{aligned}
&-(CC_3)(\Omega^3_{14})-(SC_3)(\Omega^3_{24})-(S_3)(\Omega^3_{34})\\
&+(CC_4)(\Omega^4_{14})+(SC_4)(\Omega^4_{24})+(S_4)(\Omega^4_{34})
\end{aligned}
$$

(viii)

$$
\begin{aligned}
&-(CC_1)(\Omega^1_{15})-(SC_1)(\Omega^1_{25})-(S_1)(\Omega^1_{35})\\
&+(CC_2)(\Omega^2_{15})+(SC_2)(\Omega^2_{25})+(S_2)(\Omega^2_{35})
\end{aligned}
$$

$$
\begin{aligned}
&-(CC_2)(\Omega^2_{15})-(SC_2)(\Omega^2_{25})-(S_2)(\Omega^2_{35})\\
&+(CC_3)(\Omega^3_{15})+(SC_3)(\Omega^3_{25})+(S_3)(\Omega^3_{35})
\end{aligned}
$$

$$
\begin{aligned}
&-(CC_3)(\Omega^3_{15})-(SC_3)(\Omega^3_{25})-(S_3)(\Omega^3_{35})\\
&+(CC_4)(\Omega^4_{15})+(SC_4)(\Omega^4_{25})+(S_4)(\Omega^4_{35})
\end{aligned}
$$

17

$$
\begin{array}{c|c}
\text{(ix)} & \text{(x)} \\[4pt]
\begin{aligned}
&-(CC_1)(\Omega^1{}_{16})-(SC_1)(\Omega^1{}_{26})-(S_1)(\Omega^1{}_{36}) \\
&+(CC_2)(\Omega^2{}_{16})+(SC_2)(\Omega^2{}_{26})+(S_2)(\Omega^2{}_{36})
\end{aligned}
& \lambda(t_2 - t_1) \\[20pt]
\begin{aligned}
&-(CC_2)(\Omega^2{}_{16})-(SC_2)(\Omega^2{}_{26})-(S_2)(\Omega^2{}_{36}) \\
&+(CC_3)(\Omega^3{}_{16})+(SC_3)(\Omega^3{}_{26})+(S_3)(\Omega^3{}_{36})
\end{aligned}
& \lambda(t_3 - t_2) \\[20pt]
\begin{aligned}
&-(CC_3)(\Omega^3{}_{16})-(SC_3)(\Omega^3{}_{26})-(S_3)(\Omega^3{}_{36}) \\
&+(CC_4)(\Omega^4{}_{16})+(SC_4)(\Omega^4{}_{26})+(S_4)(\Omega^4{}_{36})
\end{aligned}
& \lambda(t_4 - t_3)
\end{array}
\tag{2.19}
$$

Using index u for the satellite position and v for the column of the matrizant Ω, and denoting

$$
CC_u\,\Omega^u{}_{1v} + SC_u\,\Omega^u{}_{2v} + S_u\,\Omega^u{}_{3v} \qquad \text{by} \qquad m_u\,\Omega^u{}_v
$$

and $(t_{u+1} - t_u)$ by $\tau_{u+1,\,u}$

the above matrix takes the following more compact form

$$
\begin{array}{ccc|cc}
\text{(i)} & \text{(ii)} & \text{(iii)} & \text{(iv)} & \text{(v)} \\[4pt]
CC_1-CC_2 & SC_1-SC_2 & S_1-S_2 & -m_1\Omega^1{}_1 + m_2\Omega^2{}_1 & -m_1\Omega^1{}_2 + m_2\Omega^2{}_2 \\[10pt]
CC_2-CC_3 & SC_2-SC_3 & S_2-S_3 & -m_2\Omega^2{}_1 + m_3\Omega^3{}_1 & -m_2\Omega^2{}_2 + m_3\Omega^3{}_2 \\[10pt]
CC_3-CC_4 & SC_3-SC_4 & S_3-S_4 & -m_3\Omega^3{}_1 + m_4\Omega^4{}_1 & -m_3\Omega^3{}_2 + m_4\Omega^4{}_2
\end{array}
$$

$$
\underbrace{\hspace{5cm}}_{d\overline{X}_p} \qquad \underbrace{\hspace{5cm}}_{d\overline{X}_o}
$$

18

$$
\begin{array}{cccc}
-m_1\,\Omega^1_3 + m_2\,\Omega^2_3 & -m_1\,\Omega^1_4 + m_2\,\Omega^2_4 & -m_1\,\Omega^1_5 + m_2\,\Omega^2_5 & -m_1\,\Omega^1_6 + m_2\,\Omega^2_6 \\[2ex]
-m_2\,\Omega^2_3 + m_3\,\Omega^3_3 & -m_2\,\Omega^2_4 + m_3\,\Omega^3_4 & -m_2\,\Omega^2_5 + m_3\,\Omega^3_5 & -m_2\,\Omega^2_6 + m_3\,\Omega^3_6 \\[2ex]
-m_3\,\Omega^3_3 + m_4\,\Omega^4_3 & -m_3\,\Omega^3_4 + m_4\,\Omega^4_4 & -m_3\,\Omega^3_5 + m_4\,\Omega^4_5 & -m_3\,\Omega^3_6 + m_4\,\Omega^4_6
\end{array}
$$

$$\underbrace{\hphantom{\qquad\qquad\qquad\qquad\qquad\qquad\qquad\qquad}}_{\displaystyle \dot{\overline{dX}}_\varrho}$$

(x)

$$
\left.
\begin{array}{c}
\lambda\,\tau_{21} \\[3ex]
\lambda\,\tau_{32} \\[3ex]
\lambda\,\tau_{43} \\[1ex]
d\Delta f
\end{array}
\right]
$$

(2.20)

2.2.4 Rank Defect Analysis

As further observations are taken in the same pass from the same station P, the number of unknowns do not increase, and only more rows will be added to the above H matrix (2.20) which can now be analyzed for rank deficiency.

Examining the first row, it can be seen that

$$
\begin{aligned}
\text{element } h_{14} &= -m_1\,\Omega^1_1 + m_2\,\Omega^2_1 \\[1ex]
&= -(\cos\omega_1\cos\delta_1)\,\Omega^1_{11} - (\sin\omega_1\cos\delta_1)\,\Omega^1_{21} - (\sin\delta_1)\,\Omega^1_{31} \\[1ex]
&\quad + (\cos\omega_2\cos\delta_2)\,\Omega^2_{11} + (\sin\omega_2\cos\delta_2)\,\Omega^2_{21} + (\sin\delta_2)\,\Omega^2_{31} \\[1ex]
&\simeq -h_{11}\,\Omega^1_{11} - h_{12}\,\Omega^1_{21} - h_{13}\,\Omega^1_{31}
\end{aligned}
$$

(2.21)

19

as $\Omega_{11}^1 \simeq \Omega_{11}^2$; $\Omega_{21}^1 \simeq \Omega_{21}^2$; $\Omega_{31}^1 \simeq \Omega_{31}^2$. $\Omega_{11}^1 \simeq \Omega_{11}^2$ as they are monotone decreasing series with coefficients which alternate in sign [Hartwell and Lewis, 1967] and have the same first dominant term $(\alpha_0)_{11}$ independent of τ as seen from (2.16). Similarly, $\Omega_{21}^1 \simeq \Omega_{21}^2$ and $\Omega_{31}^1 \simeq \Omega_{31}^2$, as they have the same first dominant terms $(\alpha_0)_{21}$ and $(\alpha_0)_{31}$, respectively.

Therefore, h_{14} is a linear combination of h_{11}, h_{12}, and h_{13}. Similarly, it can be shown that h_{15}, h_{16}, h_{17}, h_{18}, and h_{19} are linear combinations of h_{11}, h_{12}, and h_{13}. And this holds for every row of H (e.g., $h_{24} \simeq -h_{21}\Omega_{11}^2 - h_{22}\Omega_{21}^2 - h_{23}\Omega_{31}^2$). Also, from row 1 to row 2, the scalars in the linear combination will be approximately equal in a short arc, e.g., $\Omega_{11}^1 \approx \Omega_{11}^2$, as explained earlier. The same argument holds from one row to the next, and columns 4, 5, 6, 7, 8, and 9 become dependent columns leaving only four independent columns.

If more stations observe the same pass, there will be three more station unknowns per station, but the above arguments about rank deficiency will hold. It can therefore be concluded that the fundamental rank deficiency in a Doppler system, short arc mode, is 6.

It is assumed that the scale information is obtainable in the system from λ, the wave length of transmission, as seen from the tenth column of the H matrix above. Having determined the fundamental rank deficiency in the system, an effort will now be made to determine what quantities are estimable in the above situation. But it is obvious that a rank deficient matrix like H above will lead to a singular normal matrix N.

2.3 Estimable Quantities in Doppler Observations

It is known that if a normal matrix N is singular and a solution is obtained with a pseudo-inverse N^+, the solution vector $X_a = -N^+ U$ is not estimable since $E(X_a) \neq X$, the parameter vector.

As derived by Rao [1973], any arbitrary matrix G can make GX_a estimable, in a linear system, if the condition

$$G[I - (N)^+(N)] = 0 \qquad (2.22)$$

is satisfied, where I is the identity matrix.

So if a change can be made in the parametrization of the mathematical model obtaining an H matrix which is not rank deficient, $(N)^+ = (N)^{-1}$, and the new parameters will be estimable. This can be done in the Doppler system considering the form of the H matrix given by (2.20).

With the modified parameters

$$\Delta \overline{X}_{po} = \begin{bmatrix} X_p - X_o \\ Y_p - Y_o \\ Z_p - Z_o \end{bmatrix}$$

instead of $\overline{X}_p$ and $\overline{X}_o$, the restructured form of H will be as given below:

$$
\begin{array}{ccc}
\text{(i)} & \text{(ii)} & \text{(iii)} \\
CC_1 - CC_2 + m_1 \Omega^1_1 - m_2 \Omega^2_1 & SC_1 - SC_2 + m_1 \Omega^1_2 - m_2 \Omega^2_2 & S_1 - S_2 + m_1 \Omega^1_3 - m_2 \Omega^2_3 \\
CC_2 - CC_3 + m_2 \Omega^2_1 - m_3 \Omega^3_1 & SC_2 - SC_3 + m_2 \Omega^2_2 - m_3 \Omega^3_2 & S_2 - S_3 + m_2 \Omega^2_3 - m_3 \Omega^3_3 \\
CC_3 - CC_4 + m_3 \Omega^3_1 - m_4 \Omega^4_1 & SC_3 - SC_4 + m_3 \Omega^3_2 - m_4 \Omega^4_2 & S_3 - S_4 + m_3 \Omega^3_3 - m_4 \Omega^4_3
\end{array}
$$

$$d \Delta \overline{X}_{po}$$

$$
\begin{array}{cccc}
\text{(iv)} & \text{(v)} & \text{(vi)} & \text{(vii)} \\
-m_1 \Omega^1_4 + m_2 \Omega^2_4 & -m_1 \Omega^1_5 + m_2 \Omega^2_5 & -m_1 \Omega^1_6 + m_2 \Omega^2_6 & \lambda \tau_{21} \\
-m_2 \Omega^2_4 + m_3 \Omega^3_4 & -m_2 \Omega^2_5 + m_3 \Omega^3_5 & -m_2 \Omega^2_6 + m_3 \Omega^3_6 & \lambda \tau_{32} \\
-m_3 \Omega^3_4 + m_4 \Omega^4_4 & -m_3 \Omega^3_5 + m_4 \Omega^4_5 & -m_3 \Omega^3_6 + m_4 \Omega^4_6 & \lambda \tau_{43}
\end{array}
$$

$$d \overline{X}_o$$

21

In this matrix all the columns are independent, and the solution will be a vector of estimable quantities. Thus, it is concluded that in a Doppler system, the vector of coordinate differences between the observing station and the mid arc state vector of the pass, the velocity components of this state vector, and the frequency offset are estimable.

If more than one station is coobserving the same pass, the linear relation

$$\Delta \bar{X}_{PQ} = \begin{bmatrix} X_P \\ Y_P \\ Z_P \end{bmatrix} - \begin{bmatrix} X_Q \\ Y_Q \\ Z_Q \end{bmatrix} = \begin{bmatrix} X_P - X_O \\ Y_P - Y_O \\ Z_P - Z_O \end{bmatrix} - \begin{bmatrix} X_Q - X_O \\ Y_Q - Y_O \\ Z_Q - Z_O \end{bmatrix} = \Delta \bar{X}_{P_O} - \Delta \bar{X}_{Q_O}$$

can be used to conclude that interstation coordinate differences are estimable if the stations coobserve the same pass of the satellite in a short arc mode. The coordinate differences are independent of origin. The scale information comes from the wave length of transmission, and the orientation information comes from the force components enforced in the satellite dynamics.

3. EPHEMERIDES OF THE NNSS AND
THEIR ACCURACY ESTIMATES

3.1 Introductory Remarks

Having analyzed the rank deficiency problem in the previous chapter, the next step in the goal to achieve improved positioning is to assess the accuracy of the ephemerides of the NNSS. As mentioned in Section 1.1, the ephemeris of satellites of the NNSS are available in two forms, precise ephemeris computed after the fact by DMA and broadcast ephemeris which is obtainable on a real time basis from satellite transmissions.

These values can be treated as direct observations on the position and velocity of the satellites for applying conventional sampling techniques to obtain estimates of uncertainties. Estimates of precision or more correctly the prediction errors in the broadcast ephemeris can be found by comparing the two values of state vectors for common time points in the overlaps of successive orbit fits.

Since the precise ephemeris is known to be more accurate than the broadcast ephemeris, in the pursuit of improving the broadcast ephemeris, estimates of its accuracy have been computed by comparing it with the precise ephemeris. After a review about the satellite system and ephemerides, the results of this study will be presented.

3.2 The Navy Navigation Satellites

There are at present (May, 1977) five operational NNSS satellites in orbit. Their identification numbers are summarized in Table 3-1. Some typical orbital elements of the satellites as per the latest data set (Data Set S) are given in Table 3-2. The orbital elements tabulated are the mean motion (n),

Table 3-1

NNSS Satellite Identification Numbers

Launch Date	Apr 14, 1967	May 18, 1967	Sep 25, 1967	Mar 2, 1968	Aug 27, 1970	Oct 29, 1973
Precise Ephemeris Identification Number	58	59	60	61 ♦	68	77
Operational Ephemeris Identification Number	30120	30130	30140	30180	30190	30200
Number Used in This Study	12	13	14	18	19	20

   ♦ Satellite Number 18 has since been declared as non operational. But some data for this satellite was available in this study in Data Set D.

Table 3-2

Values for Selected Operational Ephemeris Parameters

for Selected Days in 1976

Satellite	Day	n(deg/min)	e	a(km)	cos i
12	329	3.3815808	.002166	7440.73	-0.004095
13	316	3.3663808	.001978	7463.11	0.006719
14	316	3.3729148	.004009	7453.47	0.013237
19	329	3.3657248	.017800	7464.09	-0.002161
20	330	3.4106865	.015782	7398.34	-0.002291

eccentricity (e), semi-major axis (a), and the cosine of inclination (cos i).
All NNSS satellites follow a near circular polar orbit.

3.3 Precise Ephemeris

Precise ephemerides for one or more Navy Navigation Satellites are
computed on alternate days based on 48 hours of observation made at over 20
stations distributed around the world [Anderle, 1976].

The equations of motion of the satellite and the variational equations for
the forces are numerically integrated by a tenth-order Cowell process with UTC
time as the argument of integration. The force equation includes terms for the
gravitational field of the earth, moon, and sun, the lunar and solid earth tide
effects, atmospheric drag, and solar radiation pressure. The gravitational
field of the earth is given in a spherical harmonic expansion containing about
400 terms, and the earth tides are based on a Love's number of 0.26. The
gravity field revised in January, 1973 (NWL-10E) is in current usage.

The precise ephemeris is believed to have periodic errors of about 2m
in each coordinate due to uncertainties in the earth's gravitational field and
effects of variations in atmospheric density on the computed satellite positions.
It is maintained in the NWL-9D coordinate system which is believed to be related
to the NWL-10F system (consistent with WGS 72) as follows:

longitude $\quad\quad\quad\quad\quad\lambda_{10F} \cong \lambda_{9D} + 0\overset{''}{.}260,$ λ is positive East

geocentric latitude $\quad\Psi_{10F} \cong \Psi_{9D}$

radius $\quad\quad\quad\quad\quad\quad\xi_{10F} \cong \xi_{9D} - 5.27 \text{ m}$

[Anderle, 1976]

Based on the above approximate relations Vincenty [1976] has derived the
transformation parameters given in section 3.5.2, which have been used in
this investigation.

The precise ephemeris is made available at one-minute intervals in the
geocentric earth-fixed system in the form of position and velocity components.

3.4 Broadcast Ephemeris

The broadcast ephemeris is computed as already explained in Chapter 1. Each satellite has a memory which can hold 16 hours of orbit prediction data. This predicted ephemeris is injected into the satellite memory about every twelve hours.

The broadcast ephemeris is received at an observing station in the form of coded parameters from which earth-fixed satellite positions can be calculated [Moffett, 1973]. These parameters are divided into 14 fixed orbit parameters whose values change only twice a day and four sets of variable orbit parameters whose values change every two minutes. These are listed in Tables 3-3 and 3-4 as taken from [Wells, 1974] and [Moffett, 1973].

The decoding of the parameters and the computation of the positions of the satellites in the earth-fixed coordinate system, at two-minute intervals, is done according to procedures described in [Moffett, 1973]. For velocities of the satellite, at two-minute intervals, time derivatives of the variable parameters are also required, and these have been obtained by a polynominal fit to a maximum of 16 consecutive values.

Since December, 1975, the broadcast ephemeris system has been upgraded [Black, 1976], some main features of which are given below:

(i) The previous APL 4.5 geopotential model has been replaced by the WGS 72 model.

(ii) The value of GM has been changed from $398\ 601.5 \pm 0.6\ km^3/sec^2$ to $398\ 600.8 \pm 0.4\ km^3/sec^2$.

(iii) Station coordinates of tracking stations have been changed by small amounts to bring greater internal consistency.

(iv) Implementing the main sun-moon-induced body tide corrections.

The (single pass) error budget is given in Table 3-5 both "before" and "after" the introduction of WGS 72. It is clear that the error budget will continue to be dominated by uncertainty in the geopotential model and incorrectly modeled surface forces.

Table 3-3   Fixed Orbit Parameters

Symbol	Definition	Broadcast Units (Current Resolution)*
tp	Time of first satellite perigee after last satellite injection	10^{-4} min UT
n	Mean motion (only fractional part is broadcast)	10^{-7} deg/min
ω(tp)	Argument of perigee at tp	10^{-4} deg
$|\dot{\omega}|$	Absolute value of precession rate of perigee	10^{-7} deg/min
e	Eccentricity of orbit ellipse	10^{-6}
$\bar{a}$	Mean semi-major axis of orbit ellipse	10 metres
Ω(tp)	Right ascension of ascending node at tp	10^{-4} deg
$\dot{\Omega}$	Precession rate of ascending node	10^{-7} deg/min
cos i	Cosine of inclination	10^{-6}
GAST(tp)	Greenwich apparent sidereal time at tp	10^{-4} deg
-	Satellite identification number	-
-	Day number and time of last satellite data injection	2 min UT
sin i	Sine of inclination	10^{-6}
-	Fractional satellite frequency offset $(f_o - f_s)/f_o$	parts in 10^9

* For each of these parameters there is a trailing zero digit which is not currently used, and which could be used to increase the resolution (the frequency offset has four trailing zeroes).

Note: The above table is based on Wells [1974].

Table 3-4

Variable Orbit Parameters

Symbol	Definition	Broadcast Units
t	Time in even minutes of UT, modulus one half hour	2 min UT
$\Delta E(t)$	Correction to eccentric anomaly at time t	10^{-4} deg
$\Delta a(t)$	Correction to semi-major axis at time t	10 metres
$\eta(t)$	Out of plane orbit component at time t*	10 metres

* $\eta(t)$ values are available only at four minute intervals (for times which when expressed in minutes UT are divisible by 4). $\Delta E(t)$ and $\Delta a(t)$ values are available at two minute intervals (for even minutes UT).

Note : The above table is based on Wells [1974].

Table 3-5   NNSS Error Budget * (Single Pass)

		Meters	
1	Uncorrected propagation effects (3rd order ionospheric and neglected tropospheric eff̄cts)	1 - 5	
2	Instrumentation (oscillator phase jitter)	1 - 6	
3	Uncertainty in the geopotential model	15 - 20 (APL 4.5)	5 - 10 (WGS - 72)
4	Incorrectly modeled surface forces (secular error growth due to incorrect period, drag and radiation pressure)	10 - 25	
5	Unmodeled UTI-UTC effects and incorrect coordinates of the pole	1	
6	Ephemeris rounding error (last digit of ephemeris is rounded)	5	
	Overall Uncertainty	19 - 33 m (APL4.5)	12 - 28 m (WGS-72)

*

Adapted from Staff of Applied Physics Laboratory [1975]

3.5 Accuracy Estimates

Accuracy estimates of the precise ephemeris have been mentioned in Section 3.3 above, as available in the literature. Estimates of precision of the broadcast ephemeris can be made by carrying out a comparison between the broadcast ephemerides based on two successive orbit fits, in the overlap period, at common epochs.

Estimates of accuracy of the broadcast ephemeris are possible to be found by comparison between the precise and broadcast ephemeris at common two-minute epochs if the precise ephemeris is considered errorless for this purpose.

3.5.1 Precision of Broadcast Ephemeris

Ephemerides of satellites for common epochs for the overlap portion of two successive orbital fits were available in two forms:

(i)   from Data Set D, from passes tracked during injection

(ii) from Data Set S, where complete injection information was available on tape, in coded form.

The comparisons between the state vectors of the satellites have been carried out in two forms:

(i)   comparison between the position and velocity components in the Cartesian system $(X, Y, Z, \dot{X}, \dot{Y}, \dot{Z})$

(ii) comparison between the position and velocity components in the polar coordinate system $(\lambda, \varphi, r, \dot{\lambda}, \dot{\varphi}, \dot{r})$

Since the satellite orbits are polar and near circular, the comparisons at (ii) yield results which would correspond very closely to out-of-plane, in-track and radial differences.

For the above computations, values for X, Y, Z and $\dot{X}$, $\dot{Y}$, $\dot{Z}$ were obtained from the ephemeris message as indicated in Section 3.4. From these, the corresponding λ, φ, r, $\dot{\lambda}$, $\dot{\varphi}$, $\dot{r}$ values are readily derived from the relations:

$$r = (X^2 + Y^2 + Z^2)^{\frac{1}{2}}$$

$$\tan \varphi = \frac{Z}{(X^2 + Y^2)^{\frac{1}{2}}} \qquad (3.1)$$

$$\tan \lambda = \frac{Y}{X}$$

and

$$
\begin{bmatrix} \dot{X} \\ \dot{Y} \\ \dot{Z} \end{bmatrix} =
\begin{bmatrix}
- r \cos\varphi \sin\lambda & - r \sin\varphi \cos\lambda & \cos\varphi \cos\lambda \\
r \cos\varphi \cos\lambda & - r \sin\varphi \sin\lambda & \cos\varphi \sin\lambda \\
0 & r \cos\varphi & \sin\varphi
\end{bmatrix}
\begin{bmatrix} \dot{\lambda} \\ \dot{\varphi} \\ \dot{r} \end{bmatrix} \qquad (3.2)
$$

which yields

$$
\begin{bmatrix} \dot{\lambda} \\ \dot{\varphi} \\ \dot{r} \end{bmatrix} =
\begin{bmatrix}
\dfrac{-\sin\lambda}{r \cos\varphi} & \dfrac{\cos\lambda}{r \cos\varphi} & 0 \\
\dfrac{-\sin\varphi \cos\lambda}{r} & \dfrac{-\sin\varphi \sin\lambda}{r} & \dfrac{\cos\varphi}{r} \\
\cos\varphi \cos\lambda & \cos\varphi \sin\lambda & \sin\varphi
\end{bmatrix}
\begin{bmatrix} \dot{X} \\ \dot{Y} \\ \dot{Z} \end{bmatrix} \qquad (3.3)
$$

when the transformation matrix is nonsingular.

Let M be the quantity whose precision estimate is being obtained. $\triangle M_i = M_{\bullet i} - M_{1i}$, where M_{1i} is the value of quantity M from broadcast ephemeris at epoch t_i as per later orbit fit; $M_{\bullet i}$ is the value at the same epoch t_i as per earlier orbit fit.

$$\overline{\triangle M} = \frac{\displaystyle\sum_{j=1}^{n} \triangle M_j}{n} \qquad (3.4)$$

$$= \text{ mean value of M}$$

where n is the number of data points.

$$\text{RMS} = \sqrt{\frac{\sum_{j=1}^{n} \Delta M_j^2}{n}} = \text{Root Mean Square value} \qquad (3.5)$$

$$\text{SD} = \sqrt{\frac{\sum_{j=1}^{n} (\Delta M_j - \overline{\Delta M})^2}{n-1}} = \text{Standard Deviation} \qquad (3.6)$$

The above values for X, Y, Z, $\dot{X}$, $\dot{Y}$, $\dot{Z}$, λ, φ, r, and $\dot{\lambda}$, $\dot{\varphi}$, $\dot{r}$ are given in Tables 3-6 to 3-9.

Based on the preceding results, the following observations can be made giving more weight to the values obtained in Data Set S, where the number of data points are over 300:

(i) Taking conservative estimates (based on maximum values), the internal consistency of broadcast ephemeris for positions can be taken as about 10 m, 11 m, and 15 m in the X, Y, and Z directions, respectively. But since X, Y, Z coordinates are correlated, it is more appropriate to consider the inconsistencies in the in-track, out-of-plane, and radial directions. The estimates for these are 19 m, 14 m, and 4 m in the in-track, cross-track, and radial directions, respectively.

Fluctuations to the above extent show no indication of a bias since the RMS values are very close to the values of standard deviation.

The above values have been arrived at after excluding from consideration the values for satellite 20 in Data Set S. The unusually high values for satellite 20 are due to the fact that, as ascertained through private communication, NAG has been experiencing periodic fluctuations in the dynamics of this particular satellite due possibly to its low perigee height. It does not, therefore, represent the general behavior of the Navy Navigation Satellites.

(ii) The corresponding conservative estimates, for internal consistency in velocity components may be taken as 0.2 m/sec each in the X, Y, and Z

Table 3-6

Precision Estimates of Broadcast Ephemeris for Position Components in Cartesian System

Data Set	Satellite No	No of Data Points	X			Y			Z		
			$\overline{\Delta X}$ (m)	RMS (m)	SD (m)	$\overline{\Delta Y}$ (m)	RMS (m)	SD (m)	$\overline{\Delta Z}$ (m)	RMS (m)	SD (m)
D	12	20	0.8	6.6	6.8	-8.0	11.4	8.4	-12.8	16.4	10.6
	13	15	1.5	7.4	7.5	0.9	1.5	1.2	0.0	3.2	3.3
	14	10	4.6	10.0	9.3	5.9	7.7	5.2	11.5	14.0	8.3
	19	15	3.7	7.5	6.7	0.3	1.7	1.7	-1.4	3.4	3.2
	• 20	15	3.0	7.0	6.6	-9.5	10.2	3.7	-21.0	22.4	8.1
S	12	373	-0.4	7.5	7.5	-1.2	7.7	7.6	-0.2	8.2	8.2
	13	378	0.3	6.5	6.5	0.2	7.7	7.7	0.8	10.1	10.1
	14	354	0.2	5.2	5.2	0.5	5.6	5.6	0.5	5.5	5.5
	19	421	0.4	9.3	9.3	0.4	10.2	10.2	-0.4	14.0	14.1
	• 20	416	1.1	18.0	18.0	2.1	20.8	20.7	0.8	28.8	28.8

• exceptional   vide remarks in section 3.5.1

Table 3-7

Precision Estimates of Broadcast Ephemeris for Velocity Components in Cartesian System

Data Set	Satellite No.	No of Data Points	$\dot{X}$ (m/s)			$\dot{Y}$ (m/s)			$\dot{Z}$ (m/s)		
			$\overline{\Delta \dot{X}}$	RMS	SD	$\overline{\Delta \dot{Y}}$	RMS	SD	$\overline{\Delta \dot{Z}}$	RMS	SD
	12	20	.028	.033	.016	-.010	.036	.036	-.018	.083	.083
	13	15	.054	.056	.014	.004	.038	.039	-.018	.080	.081
D	14	10	.024	.040	.034	.021	.040	.036	-.024	.073	.073
	19	15	.029	.039	.027	-.002	.046	.048	-.030	.100	.098
	20	15	.040	.045	.021	.002	.056	.058	-.010	.069	.071
	12	373	-.001	.096	.096	-.011	.133	.133	-.003	.154	.154
	13	378	.004	.136	.136	-.010	.160	.160	-.009	.188	.188
S	14	354	.003	.151	.151	-.012	.157	.157	-.013	.202	.202
	19	421	.000	.107	.107	-.000	.152	.152	-.018	.187	.186
	20	416	-.007	.147	.147	-.019	.170	.169	.012	.223	.223

Table 3-8

Precision Estimates of Broadcast Ephemeris for Position Components in Polar System

Data Set	Satellite No.	No. of Data Points	λ			φ			r		
			$\overline{\Delta\lambda}$ (")	RMS (")	SD (")	$\overline{\Delta\varphi}$ (")	RMS (")	SD (")	$\overline{\Delta r}$ (m)	RMS (m)	SD (m)
	12	20	.026	.224	.229	-.429	.543	.341	- .6	4.4	4.5
	13	15	.053	.232	.234	.007	.095	.098	- .2	.4	.3
D	14	10	.189	.320	.272	.385	.450	.245	- .4	3.0	3.2
	19	15	.138	.272	.243	-.048	.113	.106	- .0	.4	.4
	20	15	.049	.192	.192	-.650	.692	.246	-2.5	4.5	3.9
	12	373	-.021	.384	.384	-.020	.306	.306	.1	2.9	2.9
	13	378	.044	.320	.317	.020	.355	.355	.0	3.2	3.2
S	14	354	.056	.337	.333	.014	.193	.193	.0	2.8	2.8
	19	421	.070	.319	.312	-.005	.502	.503	.2	3.6	3.6
	*20	416	.000	.324	.325	.042	1.088	1.088	.2	3.3	3.3

* exceptional vide remarks in section 3.5.1

Table 3-9

Precision Estimates of Broadcast Ephemeris for Velocity Components in Polar System

Data Set	Satellite No.	No. of Data Points	$\dot{\lambda}$ (10^{-2} "/s)			$\dot{\varphi}$ (10^{-2} "/s)			$\dot{r}$ (m/s)		
			$\overline{\Delta\dot{\lambda}}$	RMS	SD	$\overline{\Delta\dot{\varphi}}$	RMS	SD	$\overline{\Delta\dot{r}}$	RMS	SD
D	12	20	.110	.127	.065	-.037	.169	.169	-.022	.069	.067
	13	15	.182	.187	.047	-.012	.128	.132	-.021	.077	.077
	14	10	.105	.143	.103	-.006	.095	.100	-.025	.073	.072
	19	15	.097	.126	.084	-.059	.227	.227	-.030	.076	.073
	20	15	.149	.175	.095	.008	.076	.078	-.028	.086	.084
S	12	373	-.024	.496	.496	-.029	.289	.288	-.001	.194	.194
	13	376	-.104	.900	.896	-.009	.342	.342	.001	.241	.241
	14	354	-.030	.815	.816	-.025	.361	.361	.000	.257	.257
	19	421	-.039	.339	.337	-.029	.385	.384	-.003	.218	.218
	20	416	-.014	.446	.447	.016	.424	.424	-.002	.270	.270

directions. The corresponding in-track, cross-track and radial components are 0.2, 0.4, and 0.3 m/sec, respectively.

(iii) At this stage it is also clarified that though estimates of precision have been arrived at by comparing ephemerides in the overlap period between successive injections, these values more appropriately represent the error of prediction over the inter-injection period. This point will be brought up again in a subsequent section while discussing the overall accuracy estimate of the broadcast ephemeris.

3.5.2 Accuracy Estimate of Broadcast Ephemeris

Estimates of accuracy of broadcast ephemeris have been obtained in two ways in the cases of Data Sets L, D and S by comparison of precise and broadcast ephemeris of the satellite for which a precise ephemeris was being maintained for the related period.

In the case of Data Set L, both the precise and predicted ephemerides (broadcast ephemeris prior to injection) were available in the form of earth-fixed position and velocity components $(X, Y, Z, \dot{X}, \dot{Y}, \dot{Z})$ in the same coordinate system (NWL 9D); and as explained in [White, 1975] the predicted ephemeris was provided by the Naval Astronautics Group directly and not derived from transmitted ephemeris in coded form. Comparisons have been made in the position and velocity components in the earth-fixed Cartesian system as well as in the spherical system in a procedure similar to that described in Section 3.5.1.

In the case of Data Sets D and S, the precise ephemeris was in the NWL 9D system, while the broadcast ephemeris was in the WGS 72 system. So a coordinate transformation was performed to bring the precise ephemeris into the WGS 72 system before carrying out the comparisons. With the parameters mentioned in Section 3.3, the equation for the transformation is given by

37

$$
\begin{bmatrix} X \\ Y \\ Z \end{bmatrix}_{\text{WGS 72}} = \begin{bmatrix} X \\ Y \\ Z \end{bmatrix}_{9D} + \begin{bmatrix} \Delta L & W & 0 \\ -W & \Delta L & 0 \\ 0 & 0 & \Delta L \end{bmatrix} \begin{bmatrix} X \\ Y \\ Z \end{bmatrix}_{9D}
$$

Since the transformation parameters are time independent

$$
\begin{bmatrix} \dot{X} \\ \dot{Y} \\ \dot{Z} \end{bmatrix}_{\text{WGS 72}} = \begin{bmatrix} \dot{X} \\ \dot{Y} \\ \dot{Z} \end{bmatrix}_{9D} + \begin{bmatrix} \Delta L & W & 0 \\ -W & \Delta L & 0 \\ 0 & 0 & \Delta L \end{bmatrix} \begin{bmatrix} \dot{X} \\ \dot{Y} \\ \dot{Z} \end{bmatrix}_{9D}
$$

where

$$\Delta L = -0.8263 \text{ ppm}$$
$$W = -0\overset{..}{\,}26 \qquad\qquad \text{[Vincenty, 1976]}$$

The broadcast ephemeris was derived from majority-voted ephemeris message from data collected at three stations in the case of Data Set D and from the coded ephemeris message provided on tape by NAG in the case of Data Set S. Where data pertains to an overlap between successive orbit fits, the more recent data has been used. The results of the comparisons are shown in Tables 3-10 to 3-13.

Based on the above finding, the following observations can be made about the accuracy estimates of the broadcast ephemeris in the WGS 72 system.

(i) Taking conservative estimates, the positional accuracy of the broadcast ephemeris, taking the precise ephemeris as the standard, can be taken as 10 m, 10 m, and 17 m in the X, Y, Z directions, respectively. The estimates for the in-track, out-of plane, and radial directions are 19 m, 15 m, and 9 m, respectively. The values obtained in a comparable procedure by White [1975], before upgrading of the broadcast ephemeris computational system, were 25 m, 15 m, and 10 m, respectively. The smaller values now obtained

38

Table 3-10

Accuracy Estimates of Broadcast Ephemeris for Position Components in Cartesian System

Data Set	Satellite No	No. of Data Points	X (m)			Y (m)			Z (m)		
			$\Delta \bar{x}$	RMS	SD	$\Delta \bar{Y}$	RMS	SD	$\overline{\Delta Z}$	RMS	SD
L	13	496	-3.2	10.1	9.8	8.2	13.8	11.1	-3.3	14.1	13.7
	19	506	-4.0	9.9	9.1	8.4	12.7	9.5	-4.9	16.0	15.2
D	19	199	-0.4	4.3	4.3	1.2	6.2	6.1	-6.9	11.5	9.2
	20	131	1.0	7.2	7.2	3.8	9.1	8.2	4.2	16.4	15.9
S	12	2005	6.2	9.2	6.8	-2.2	8.5	8.2	-4.5	12.2	11.3
	19	1879	7.5	9.3	5.6	-0.9	7.1	7.0	-7.7	11.3	8.2

Table 3-11

Accuracy Estimates of Broadcast Ephemeris for Velocity Components in Cartesian System

Data Set	Satellite No.	No. of Data Points	$\dot{X}$ (m/s)			$\dot{Y}$(m/s)			$\dot{Z}$(m/s)		
			$\overline{\Delta\dot{X}}$	RMS	SD	$\overline{\Delta\dot{Y}}$	RMS	SD	$\overline{\Delta\dot{Z}}$	RMS	SD
L	13	496	-.002	.014	.014	-.004	.015	.014	.001	.014	.014
	19	506	-.007	.016	.014	.000	.014	.014	.003	.014	.013
D	19	199	-.000	.041	.041	-.011	.140	.140	.009	.129	.129
	20	131	-.003	.030	.030	.008	.059	.058	-.007	.040	.039
S	12	2005	.014	.074	.073	.003	.103	.103	.013	.113	.112
	19	1579	.013	.080	.079	-.002	.111	.111	-.007	.128	.128

Table 3-12

Accuracy Estimates of Broadcast Ephemeris for Position Components in Polar System

Data Set	Satellite No.	No. of Data Points	$\lambda(")$			$\varphi(")$			$r_{(m)}$		
			$\overline{\Delta\lambda}$	RMS	SD	$\overline{\Delta\varphi}$	RMS	SD	$\overline{\Delta r}$	RMS	SD
L	13	496	-.198	.625	.593	.044	.451	.450	-7.4	9.1	5.4
	19	506	-.267	.667	.612	.022	.454	.454	-7.9	9.9	6.1
D	19	199	-.014	.147	.147	-.148	.324	.289	-4.9	6.1	3.7
	20	131	.070	.205	.193	.170	.509	.482	-4.5	6.1	4.2
S	12	2005	.282	.399	.282	-.107	.386	.371	-3.3	5.5	4.3
	19	1879	.298	.371	.221	-.105	.301	.283	-7.4	8.3	3.8

Table 3-13

Accuracy Estimates of Broadcast Ephemeris for Velocity Components in Polar System

Data Set	Satellite No.	No. of Data Points	$\dot\lambda(10^{-2}\ "/s)$			$\dot\varphi(10^{-2}\ "/s)$			$\dot r\ _{(m/s)}$		
			$\overline{\Delta\dot\lambda}$	RMS	SD	$\overline{\Delta\dot\varphi}$	RMS	SD	$\overline{\Delta\dot r}$	RMS	SD
L	13	496	.039	.258	.256	-.008	.028	.027	-.002	.011	.011
	19	506	-.056	.349	.345	.014	.031	.028	.001	.011	.011
D	19	199	-.013	.131	.131	.022	.380	.380	.001	.134	.135
	20	131	-.016	.127	.126	.006	.064	.064	.001	.064	.064
S	12	2005	.037	.280	.278	-.016	.207	.207	-.009	.143	.143
	19	1879	.033	.274	.272	-.022	.286	.285	-.004	.148	.148

would represent the effect of the improvements incorporated in the ephemerides since December, 1975. Previous study by Wells [1974] obtained 26 m, 10 m, and 5 m for the above estimates, in a slightly different procedure.

(ii) The values for the accuracy of the velocity components would be 0.1 , 0.2 , and 0.2 m/sec in the X, Y, Z directions, respectively. The corresponding values in the in-track, out-of-plane, and radial directions would be 0.2 , 0.1 , and 0.2 m/sec, respectively.

(iii) The RMS values for velocity differences are much smaller in the case of Data Set L though this refers to a period before incorporation of improvements in the computation of broadcast ephemerides. This is because in Data Set L the predicted state vectors of the satellites (both position and velocity components) were available directly on cards and referred to a precoded and preinjection stage, while in Data Sets D and S these have been derived from coded message and a fitting process for obtaining time derivatives of variable elements. So the velocities in Data Set L are free of truncation errors and errors of fitting.

(iv) At first sight it may appear irrational that the precision estimates are of the same order and, in some cases, even lower than the accuracy estimates. However, as pointed out in the previous section, the precision estimates in reality are the estimates of the prediction errors accumulated over the interinjection period. The overall uncertainty of the broadcast ephemeris as obtained by a user will depend on the relative position of the observation time in the interinjection period as well as the interinjection period itself, which was found to vary from about $9\frac{1}{2}$ to $13\frac{1}{2}$ hours in the data available in this study.

Thus, if a user happens to track a satellite just before injection, the uncertainty of the ephemeris obtainable by him would be a result of the compounding of the estimates of precision and accuracy given above. In this case, the positional uncertainty of the satellite is likely to be 26 m in-track, 20 m cross-track and 10 m in radial directions. However, for a user tracking a

satellite during or soon after injection, the uncertainties will be those given by the accuracy estimates above (i.e., about 19 m in-track, 15 m cross-track, and 9 m in radial directions). If prediction errors are not taken into account, the improvements in the Transit system in December, 1975, have brought the broadcast ephemeris closer to the precise ephemeris.

(v) Another observation which can be made is about the prominent negative value of $\overline{\Delta r}$ (between three to seven meters) in all data sets.

The possibility of a radial bias is evident and has been pursued in Chapters 4 and 5.

(vi) The existence of cross-track and in-track biases cannot be completely overruled. As regards cross-track bias, Data Set D indicated a bias of about -0''01 for satellite 19 and 0''07 for satellite 20. In Data Set S both satellites 12 and 19 indicated a bias of about 0''28 and 0''30, respectively. While in Data Set L the bias indicated is of the order -0''20 and -0''28. A similar situation is seen in the case of in-track bias. This led to the conclusion that in the data sets used in this study, a consistent evidence of the existence of in-track and cross-track bias is not available. These biases have, therefore, not been pursued further in this study, but a need does exist for identifying these biases with more data sets in the future.

This conclusion was also supported by the results of tests of hypothesis. Only in the case of radial bias the tests indicated that the hypothesis that the expectation of the bias is zero could be rejected at $\alpha = 0.05$, in the case of all data sets. The biases investigated here are in the nature of constant systematic effects that can be associated with the broadcast ephemeris irrespective of the satellite or its pass tracked. Other biases in individual satellite passes, if varying in magnitude and sign between passes, may average out to an insignificant value over a large number of satellite passes. These latter types of pass biases, referred to in the literature [Kouba and Wells, 1976], are viewed as signals which can be separated in an adaptive filtering procedure discussed in Chapter 5.

Based on the above, and taking into consideration the 2m uncertainty in each component of position expected of the precise ephemeris, it can be stated that the positional uncertainty of ephemeris as obtainable by a user just before injection is about 35 m. The positional uncertainty obtainable immediately after injection is about 25 m. The figures given in the literature places the single pass error budget for a surveyor at 12-28 m for the broadcast ephemeris in WGS 72.

4. STATISTICAL ANALYSIS OF EPHEMERIS DATA

4.1 Introductory Remarks

An immediate application for the accuracy estimates of the broadcast ephemeris, obtained in the study described in Chapter 3, lies in utilizing this information in the form of a diagonal matrix to assign appropriate weights to the orbit parameters in an adjustment procedure in which the main parameters of interest would still be the station positions.

In this method it is assumed that the uncertainty in the orbit is the result of a system "noise" arising from a random variable whose outcomes are independent and identically distributed with a zero expectation and finite variance. This is similar to the assumption invariably made about the observational "noise" or random observational "errors" in any least squares adjustment procedure, irrespective of whether a system "noise" is taken into consideration or not. In effect, the procedure amounts to adding the best known orbit parameter values as additional observations in the adjustment.

Though the mathematical treatment for system "noise" and observational "noise" is similar in the above situation, the distinction between the two is clear. A system "noise" arises from an inadequacy in the mathematical model, while an observational "noise" arises from the measurement process. Further in this study, system "noise" arises from two models, the model which describes the dynamics of satellite motion and the model which relates the observable quantity with the parameters. The first model is the concern of this chapter.

In many situations, such as the satellite orbit in this study, the successive outcomes of system noise are correlated, though their expectation may still be zero. In such situations estimates of the parameters of interest may improve if the system "noise" is modeled by a stochastic process in the form of a "signal" to be estimated along with the other parameters, instead of being

compensated for by weighting parameters.

The situation is well described by considering a physical system whose dynamic behavior can be modeled by the first-order linear differential equations

$$\dot{\overline{X}} = A(t)\overline{X} + G(t)\overline{W}(t) \qquad \text{for } t \geq t_0 \text{ where } \overline{X} = \overline{X}(t) \qquad (4.1)$$

Here $\overline{X}$ is an n vector called the state of the system. We say that $\overline{X}$ is a state vector if $\overline{X}(t_1)$ can be determined unambiguously from a knowledge of $\overline{X}(t_0)$, $t_1 \geq t_0$, and $A(t)$, $G(t)$, and $\overline{W}(t)$ for $t_0 \leq t \leq t_1$. $\overline{X}$ contains all the parameters of interest required to describe the system. $\overline{W}$ is an n x 1 "disturbance" vector, a term which implies a "noise" if the outcomes are uncorrelated and a "signal" if correlated, and t denotes time. A(t) and G(t) are n x n system matrices assumed to be continuous in time t. It is assumed that the initial time t_0 is fixed and initial state $\overline{X}(t_0)$ is known. The forms of the matrices A(t) and G(t) are also given.

The observation process is modeled as

$$\overline{Z}(t) = H(t)\overline{X}(t) + \overline{V}(t) \qquad (4.2)$$

where $\overline{Z}$ is a p vector of measurements, $\overline{V}$ is a P vector of measurement errors, and H(t) is a continuous p x n design matrix or measurement matrix of known form. A block diagram for the process implied by equations (4.1) and (4.2) is shown in Fig. 4.1 as adapted from [Meditch, 1969].
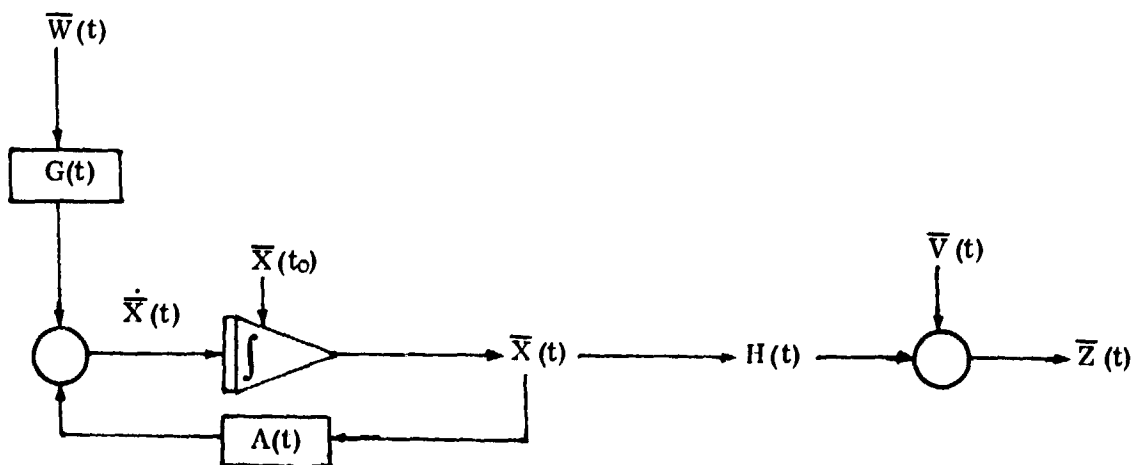
Fig. 4.1   Block diagram for continuous linear system description.

46

Estimation procedures in the above system require some knowledge about the statistics of the disturbance as well as the observational noise. In most cases where the former is not directly observable, observational residuals are the only source of information for determining the statistics of the disturbance as well as of the observational errors, and it is difficult to separate their effects. However, there are situations where disturbance is accessible to form some estimate about its statistics. Availability of precise and broadcast ephemerides of the same satellite gives rise to one such situation. The outcomes of this disturbance process are generally correlated, and it can more appropriately be termed as a signal.

Precise and broadcast ephemerides provide us information about the state of the same satellites at two-minute intervals for observation spans over a time period. Precise ephemeris is known to be much more accurate than broadcast ephemeris. So treating precise ephemeris as the standard, the small differences obtainable by comparing the two can be treated as the outcomes of the system signal inherent in broadcast ephemeris and their statistics estimated by the normal sampling procedures. Immediately, several possibilities arise as these comparisons can be carried out in different ways. The specific procedure for comparison depends on how the state disturbance is proposed to be viewed. For example, the state disturbance could be viewed as predominantly a consequence of uncompensated acceleration, in which case a stochastic process would be required to be added to the relevant first-order differential equation for acceleration in the dynamic model. Outcomes of this process would be computed by comparing the accelerations given by precise and broadcast ephemerides of the same satellite, at the same epochs, and in the same coordinate system for obtaining their statistics. Further, the uncompensated acceleration could be considered either in the Cartesian system or a spherical system.

On the other hand, the state disturbance could be viewed as predominantly a consequence of a positional or a velocity signal associated with broadcast ephemeris, which implies that the uncompensated accelerations are negligible, but due to some reason, there is a systematic deviation in position or velocity which can be associated with the broadcast ephemeris as a stochastic process.

47

In this investigation four different types of signals have been studied by computing their statistics, and one type of signal has actually been used to study its effect in local orbit refinement.

The theoretical stochastic process of the signal is denoted as $\xi(t)$, while the practical outcomes of this process are denoted as $s(t)$ where t denotes time. The autocovariance of $\xi(t)$ is denoted as $R(u)$, while the sample autocovariance obtained from data is denoted as $C(u)$, where the lag parameter u represents the separation in t. The subscripts clarify the specific signal intended. The signals and their statistics, as obtained in this study, are described in this chapter, and their applications are discussed in Chapter 5.

4.2 Computation of the Signal Outcomes

The ephemerides provide position and velocity components in the earth-fixed systems. As indicated in the previous chapter, these components are more correlated than the in-track, cross-track, and radial components which are obtainable by transforming the state vectors into a spherical system. As explained in Section 4.1, keeping precise exhemeris as the standard, realizations of the following four signals were computed for Data Sets D and S which are in the current WGS 72 system:

(i) Acceleration signal $\xi_{\ddot{X}}(t)$, $\xi_{\ddot{Y}}(t)$, $\xi_{\ddot{Z}}(t)$ in the Cartesian system

(ii) Acceleration signal $\xi_{\ddot{\lambda}}(t)$, $\xi_{\ddot{\varphi}}(t)$, $\xi_{\ddot{r}}(t)$ in the polar system

(iii) Velocity signal $\xi_{\dot{\lambda}}(t)$, $\xi_{\dot{\varphi}}(t)$, $\xi_{\dot{r}}(t)$ in the polar system

(iv) Position signal $\xi_{\lambda}(t)$, $\xi_{\varphi}(t)$, $\xi_{r}(t)$ in the polar system

All signal outcomes were computed by first transforming the precise ephemeris state vectors to the WGS 72 system of the broadcast ephemeris. However, it has been found both analytically and numerically that the transformation has a negligible effect on the acceleration signal. This is shown in Appendix A.

The actual mechanics for the realizations of the above signals will now be described, followed by the procedure used to obtain the statistics.

4.2.1 Acceleration Signal

If $\dot{X}_p(t_i)$ and $\dot{X}_p(t_{i+2})$ are the X components of a satellite velocity in m/s according to the precise ephemeris after transformation to the WGS 72 system, and $\dot{X}_n(t_i)$ and $\dot{X}_n(t_{i+2})$ are their corresponding values according to the broadcast ephemeris at even-minute epochs t_i and t_{i+2}, then

$$\ddot{X}_p(t_{i+1}) \;=\; \frac{\dot{X}_p(t_{i+2}) \,-\, \dot{X}_p(t_i)}{120} \qquad \text{in m/s}^2 \tag{4.3}$$

and

$$\ddot{X}_n(t_{i+1}) \;=\; \frac{\dot{X}_n(t_{i+2}) \,-\, \dot{X}_n(t_i)}{120} \qquad \text{in m/s}^2 \tag{4.4}$$

The realization $s_{\ddot{X}}(t_{i+1})$ of the acceleration signal $\xi_{\ddot{X}}(t_{i+1})$ will be given by

$$s_{\ddot{X}}(t_{i+1}) \;=\; \ddot{X}_p(t_{i+1}) \,-\, \ddot{X}_n(t_{i+1}) \tag{4.5}$$

Similar computations yield the realizations $s_{\ddot{Y}}(t)$ and $s_{\ddot{Z}}(t)$ of the signals $\xi_{\ddot{Y}}(t)$ and $\xi_{\ddot{Z}}(t)$.

To obtain the outcomes of the signal $\xi_{\ddot{\lambda}}(t)$, $\xi_{\ddot{\varphi}}(t)$, $\xi_{\ddot{r}}(t)$, a similar procedure was used by first transforming the precise and broadcast ephemeris state vectors from the Cartesian system to the spherical system as explained in Section 3.5.1.

4.2.2 Velocity Signal

Similarly, if $\dot{\lambda}_p(t_i)$ and $\dot{\lambda}_n(t_i)$ are the components of a satellite velocity in "/s according to the precise and broadcast ephemeris, respectively, at the same even-minute epoch (t_i), the outcome $s_{\dot{\lambda}}(t_i)$ of the velocity signal $\xi_{\dot{\lambda}}(t_i)$ will be given by

$$s_{\dot{\lambda}}(t_i) \;=\; \dot{\lambda}_p(t_i) \,-\, \dot{\lambda}_n(t_i) \tag{4.6}$$

Similar computations yielded

$$s_{\dot{\varphi}}(t_i), \; s_{\dot{r}}(t_i) \qquad \text{the realizations of the velocity signals}$$
$$\xi_{\dot{\varphi}}(t_i), \; \xi_{\dot{r}}(t_i) \qquad \text{in the spherical system.}$$

49

4.2.3 Position Signals

Following the same procedure, the realizations $s_\lambda(t_i)$ of the signal $\xi_\lambda(t_i)$ were obtained from the relation

$$s_\lambda(t_i) = \lambda_p(t_i) - \lambda_n(t_i)$$

where $\lambda_p(t_i)$ and $\lambda_n(t_i)$ are the λ position components of the satellite at even-minute epoch t_i in the precise and broadcast ephemeris, respectively. Similarly, the realizations $s_\varphi(t_i)$, $s_r(t_i)$ of the signals $\xi_\varphi(t_i)$ and $\xi_r(t_i)$ were obtained.

4.3 Computation of the Signal Statistics

Considering each of the signals $\xi(t)$ above as a stochastic process, the computations of Section 4.2 yield the discrete observations $s(t_i)$ or outcomes of the continuous time series at equal intervals of two minutes over the available data spans.

For computing further statistics, the following assumptions were made:

(i) The process $\xi(t)$ has reached a steady state in the sense that the statistical properties of the series are independent of absolute time. This implies that the probability density function of each signal is independent of time, has a constant mean μ and constant variance σ^2. That is, it forms a stationary time series.

(ii) The process exhibits the property of ergodicity, which enables the computation of a time average over a record to represent an ensemble average.

With these assumptions the outcomes $s(t)$ can be used to form the sample autocovariance function, the sample cross-covariance function, and the sample autocorrelation functions.

For example, considering $\xi_X(t)$, its autocovariance function is defined as

$$R_{XX}(t_1, t_2) \quad E\left[(\xi_X(t_1) - \mu_X(t_1)) (\xi_X(t_2) - \mu_X(t_2)) \right] \qquad (4.6)$$

where E is the expectation operator, and $\mu_{\ddot{X}}(t) = E[\xi_{\ddot{X}}(t)]$. Because of the stationarity assumption, $R_{\ddot{X}\ddot{X}}(t_1, t_2)$ immediately becomes a function of the time lag $u = t_2 - t_1$ only, and

$$R_{\ddot{X}\ddot{X}}(u) = E[(\xi_{\ddot{X}}(t) - \mu_{\ddot{X}})(\xi_{\ddot{X}}(t+u) - \mu_{\ddot{X}})] \qquad (4.7)$$

Sample autocovariance $C_{\ddot{X}\ddot{X}}(u)$, its estimate from data is computed from the outcomes $s_{\ddot{X}}(t_i)$ using the relation

$$C_{\ddot{X}\ddot{X}}(u) = \frac{1}{N}\sum_{i=1}^{N-u}(s_{\ddot{X}}(t_i) - \bar{s}_{\ddot{X}})(s_{\ddot{X}}(t_{i+u}) - \bar{s}_{\ddot{X}}) \qquad (4.8)$$

where

$$\bar{s}_{\ddot{X}} = \frac{1}{N}\sum_{i=1}^{N} s_{\ddot{X}}(t_i)$$

    i represents the epoch of each data point taken at two-minute

    intervals in an ordered set

   N is the total number of data points   [Jenkins and Watts, 1968]

The sample autocorrelation function $r_{\ddot{X}\ddot{X}}(u)$ is given by

$$r_{\ddot{X}\ddot{X}}(u) = \frac{C_{\ddot{X}\ddot{X}}(u)}{C_{\ddot{X}\ddot{X}}(0)}$$

Similarly, if we consider two signals $\xi_{\ddot{X}}(t)$ and $\xi_{\ddot{Y}}(t)$, the cross-covariance function for lag u becomes

$$R_{\ddot{X}\ddot{Y}}(u) = E[(\xi_{\ddot{X}}(t) - \mu_{\ddot{X}})(\xi_{\ddot{Y}}(t+u) - \mu_{\ddot{Y}})]$$

for which the sample cross-covariance function is

$$C_{\ddot{X}\ddot{Y}}(u) = \frac{1}{N}\sum_{i=1}^{N-u}(s_{\ddot{X}}(t_i) - \bar{s}_{\ddot{X}})(s_{\ddot{Y}}(t_{i+u}) - \bar{s}_{\ddot{Y}}) \qquad (4.9)$$

where

$$\bar{s}_{\ddot{Y}} = \frac{1}{N}\sum_{i=1}^{N} s_{\ddot{Y}}(t_i)$$

51

For equations (4.8) and (4.9), an alternate formulation is also available in the literature [Anderson, 1971] according to which the divisor (N-u) is used instead of N for computing the estimates. Divisor N has been used in this investigation as estimators with divisor N usually have smaller mean square error and are positive definite [Jenkins and Watts, 1968 p. 184]. For lag o, the sample cross-correlation matrix for signals $\xi_{\ddot{X}}(t)$, $\xi_{\ddot{Y}}(t)$, $\xi_{\ddot{Z}}(t)$ is formed by unities along the diagonal and factors like

$$\frac{C_{\ddot{X}\ddot{Y}}(o)}{\sqrt{(C_{\ddot{X}\ddot{X}}(o)\ C_{\ddot{Y}\ddot{Y}}(o))}} \qquad \text{as off-diagonal terms.}$$

Similar statistics for all signals have been obtained and are shown in various figures as follows:

Fig. 4.2	$C_{\ddot{X}\ddot{X}}(u)$	for Data Sets D and S
Fig. 4.3	$r_{\ddot{X}\ddot{X}}(u)$	for Data Sets D and S
Fig. 4.4	$C_{\ddot{Y}\ddot{Y}}(u)$	for Data Sets D and S
Fig. 4.5	$r_{\ddot{Y}\ddot{Y}}(u)$	for Data Sets D and S
Fig. 4.6	$C_{\ddot{Z}\ddot{Z}}(u)$	for Data Sets D and S
Fig. 4.7	$r_{\ddot{Z}\ddot{Z}}(u)$	for Data Sets D and S
Fig. 4.8	$C_{\lambda\lambda}(u)$	for Data Sets D and S
Fig. 4.9	$r_{\lambda\lambda}(u)$	for Data Sets D and S
Fig. 4.10	$C_{\varphi\varphi}(u)$	for Data Sets D and S
Fig. 4.11	$r_{\varphi\varphi}(u)$	for Data Sets D and S
Fig. 4.12	$C_{rr}(u)$	for Data Sets D and S
Fig. 4.13	$r_{rr}(u)$	for Data Sets D and S
Fig. 4.14	$C_{\ddot{\lambda}\ddot{\lambda}}(u)$	for Data Sets D and S
Fig. 4.15	$r_{\ddot{\lambda}\ddot{\lambda}}(u)$	for Data Sets D and S
Fig. 4.16	$C_{\ddot{\varphi}\ddot{\varphi}}(u)$	for Data Sets D and S
Fig. 4.17	$r_{\ddot{\varphi}\ddot{\varphi}}(u)$	for Data Sets D and S
Fig. 4.18	$C_{\ddot{r}\ddot{r}}(u)$	for Data Sets D and S
Fig. 4.19	$r_{\ddot{r}\ddot{r}}(u)$	for Data Sets D and S
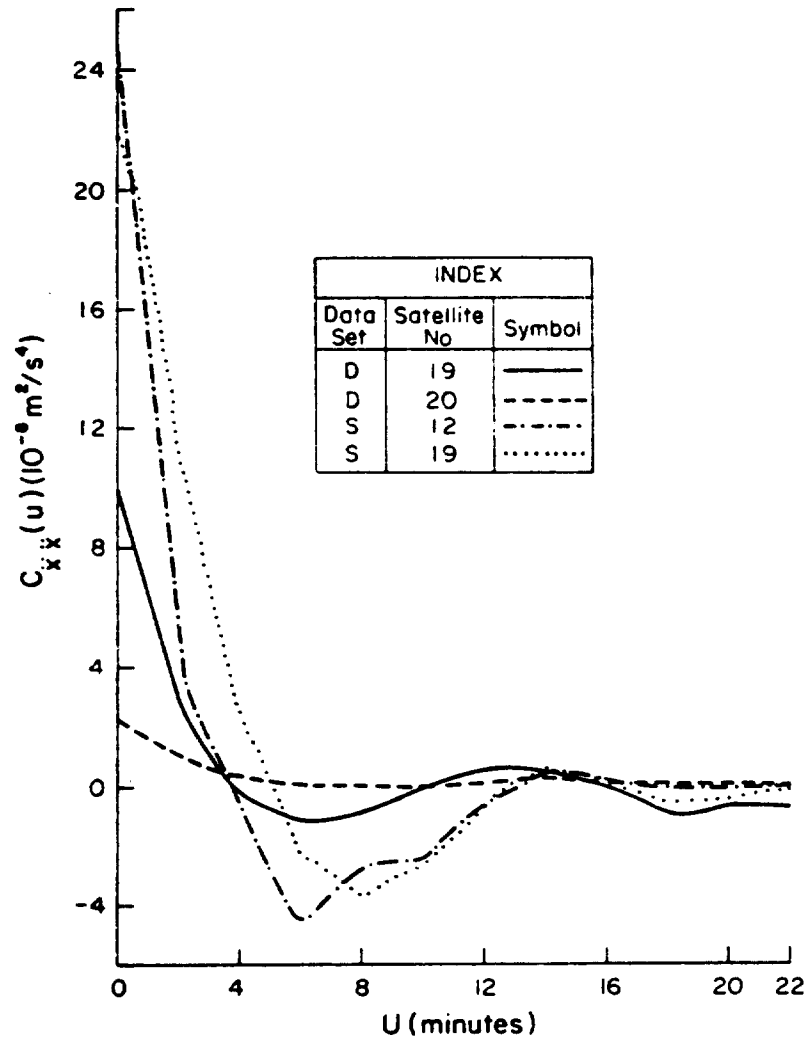
Figure 4.2   Sample Autocovariance $C_{\ddot{X}\ddot{X}}(u)$
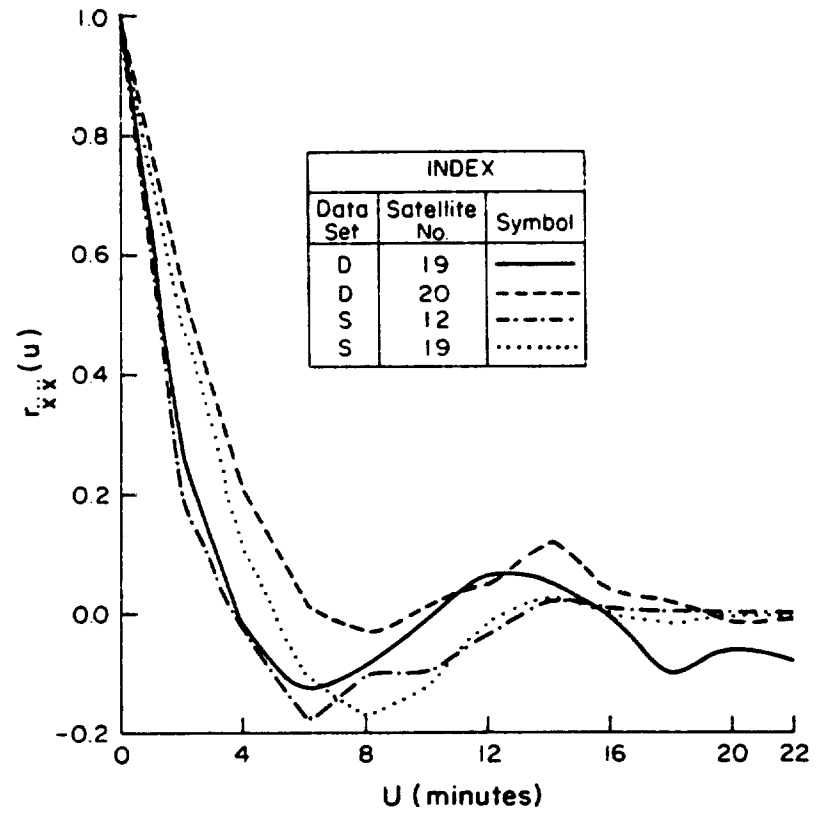
Figure 4.3   Sample Autocorrelation $r_{\ddot{X}\ddot{X}}(u)$
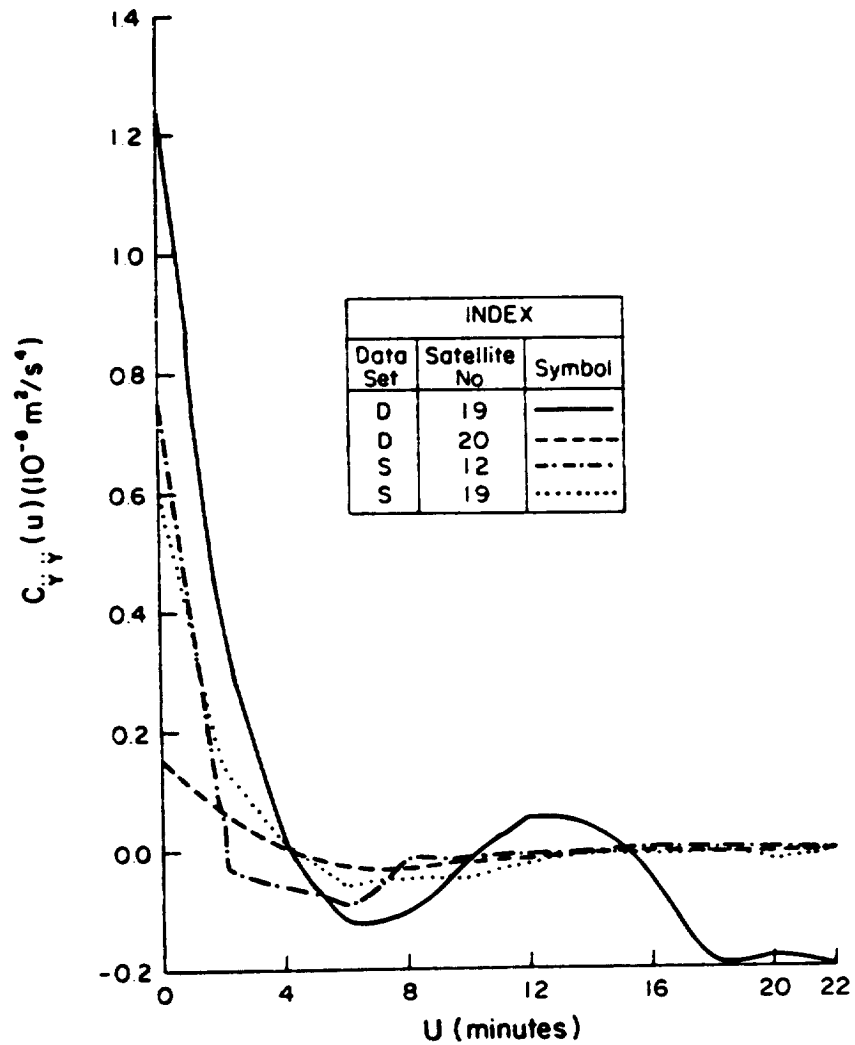
Figure 4.4 Sample Autocovariance $C_{\tilde{Y}\tilde{Y}}(u)$
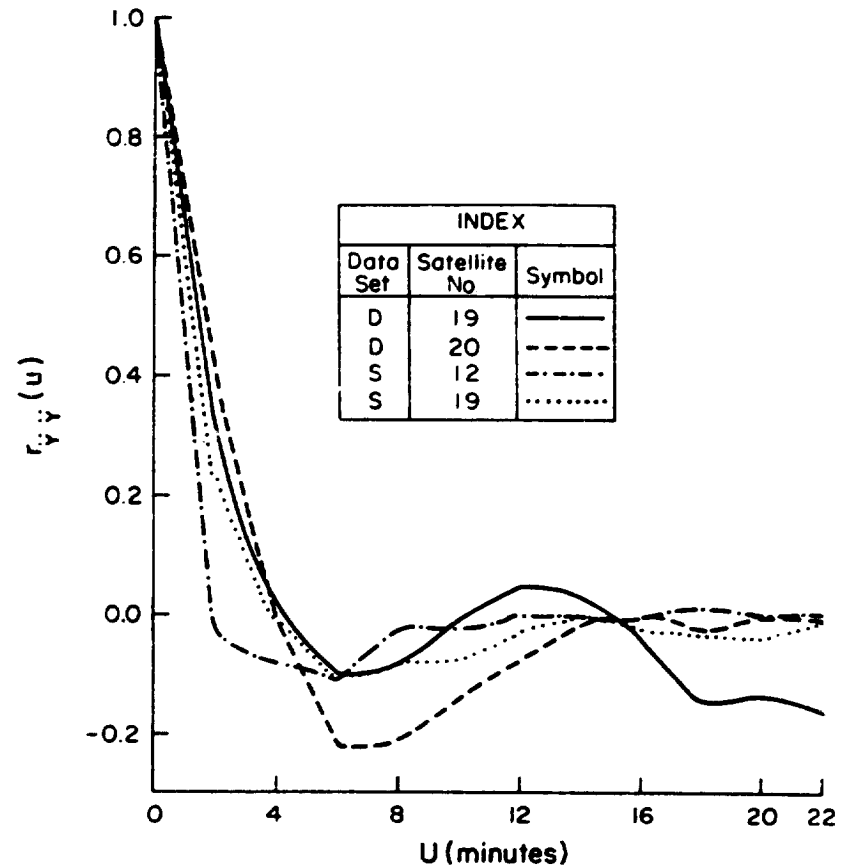
Figure 4.5 Sample Autocorrelation $r_{\tilde{Y}\tilde{Y}}(u)$

54
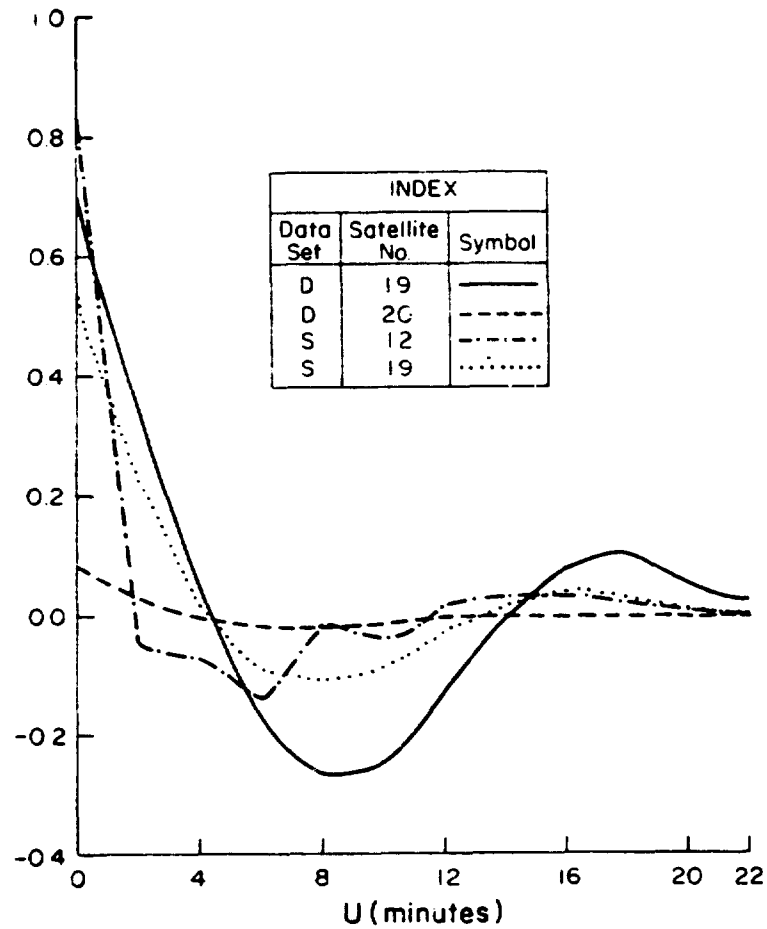
Figure 4.6   Sample Autocovariance $C_{\ddot{Z}\ddot{Z}}(u)$
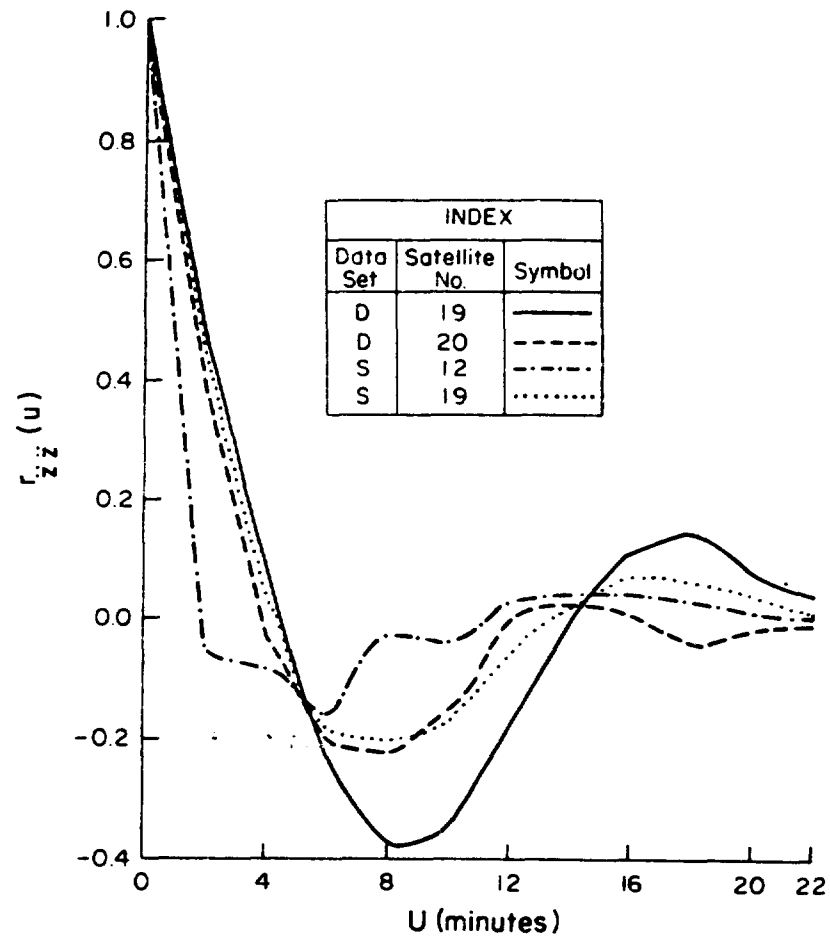
Figure 4.7   Sample Autocorrelation $r_{\ddot{Z}\ddot{Z}}(u)$

Figure 4.6 (left plot)

Y-axis: $C_{\ddot{Z}\ddot{Z}}(u)$ $(10.^{-8}\,m^2/s^4)$

X-axis: U (minutes)

	INDEX	
Data Set	Satellite No.	Symbol
D	19	
D	2C	
S	12	
S	19	

Figure 4.7 (right plot)

Y-axis: $r_{\ddot{Z}\ddot{Z}}(u)$

X-axis: U (minutes)

	INDEX	
Data Set	Satellite No.	Symbol
D	19	
D	20	
S	12	
S	19	
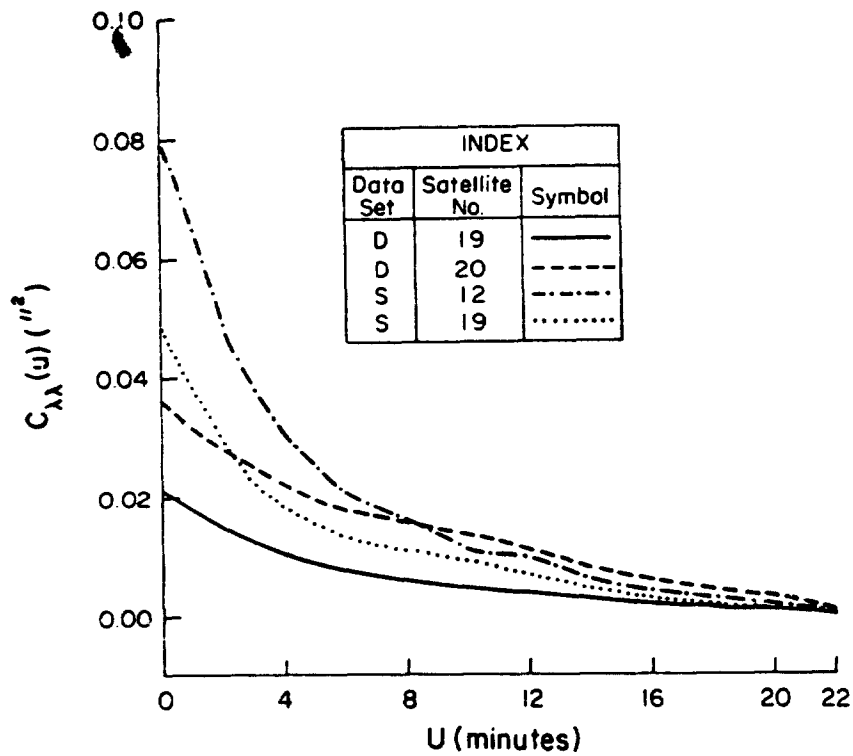
Figure 4.8   Sample Autocovariance $C_{\lambda\lambda}(u)$
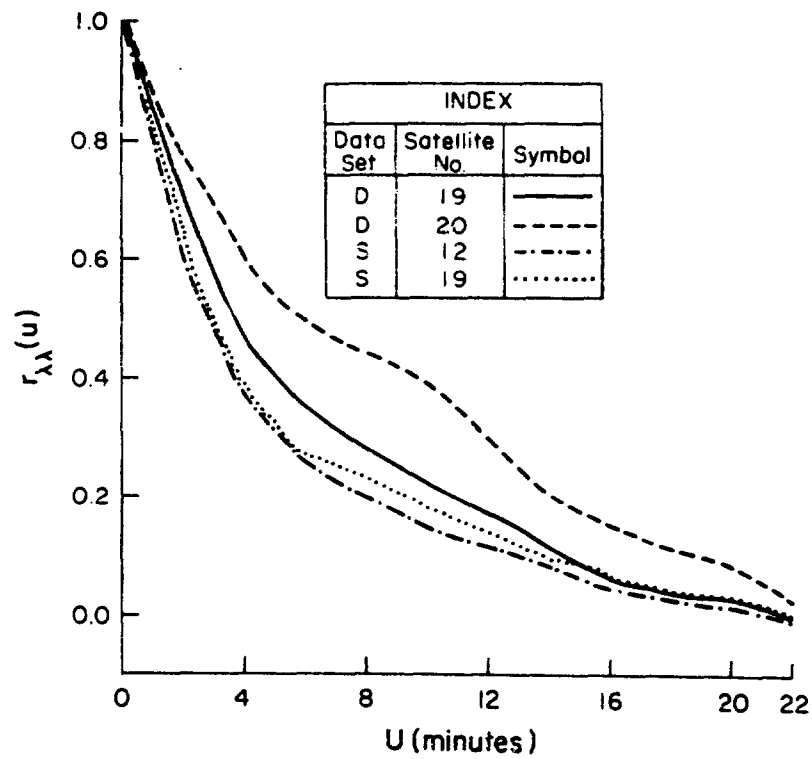
Figure 4.9   Sample Autocorrelation $r_{\lambda\lambda}(u)$
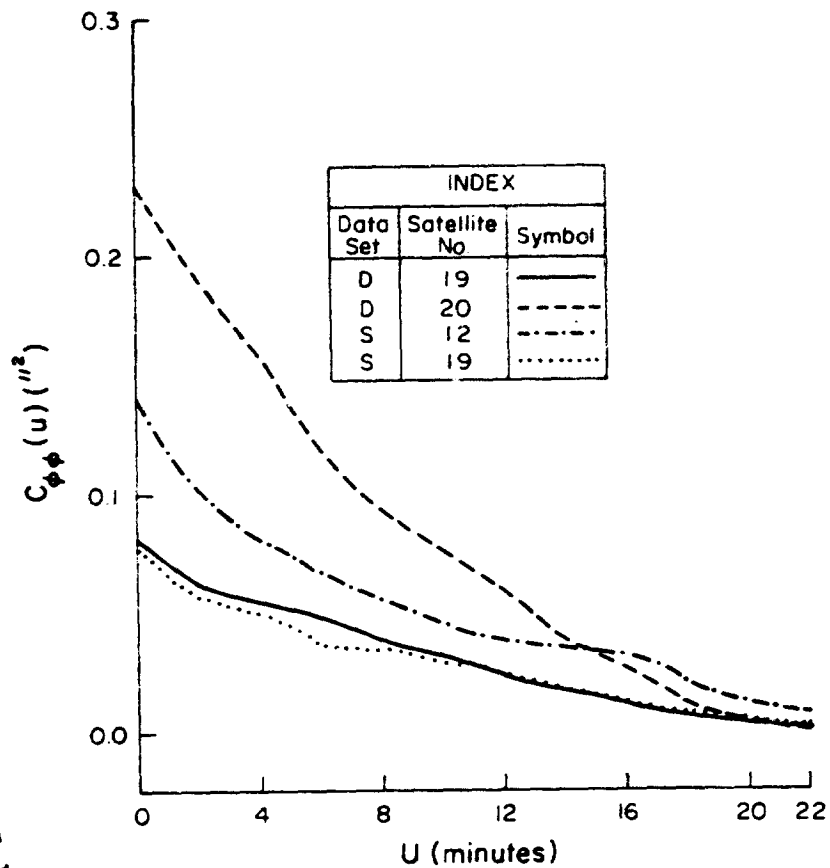
Figure 4.10   Sample Autocovariance $C_{\varphi\varphi}(u)$
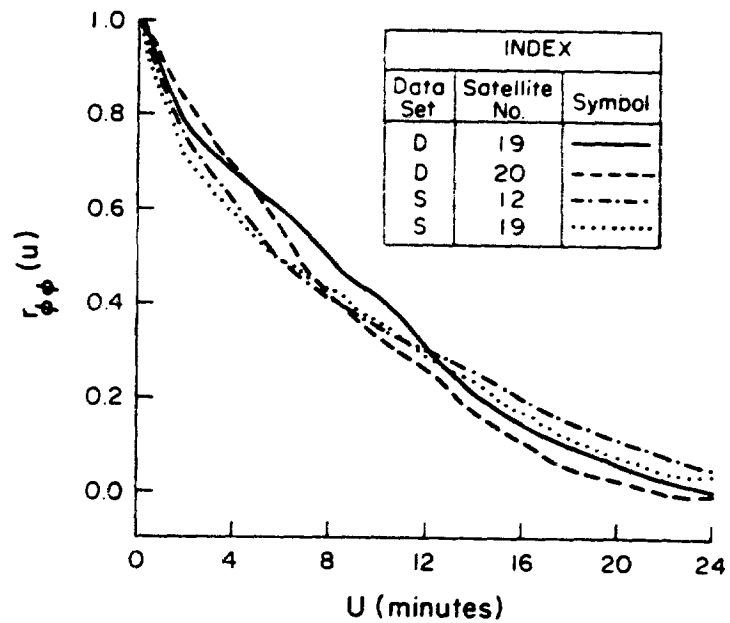
Figure 4.11   Sample Autocorrelation $r_{\varphi\varphi}(u)$

57
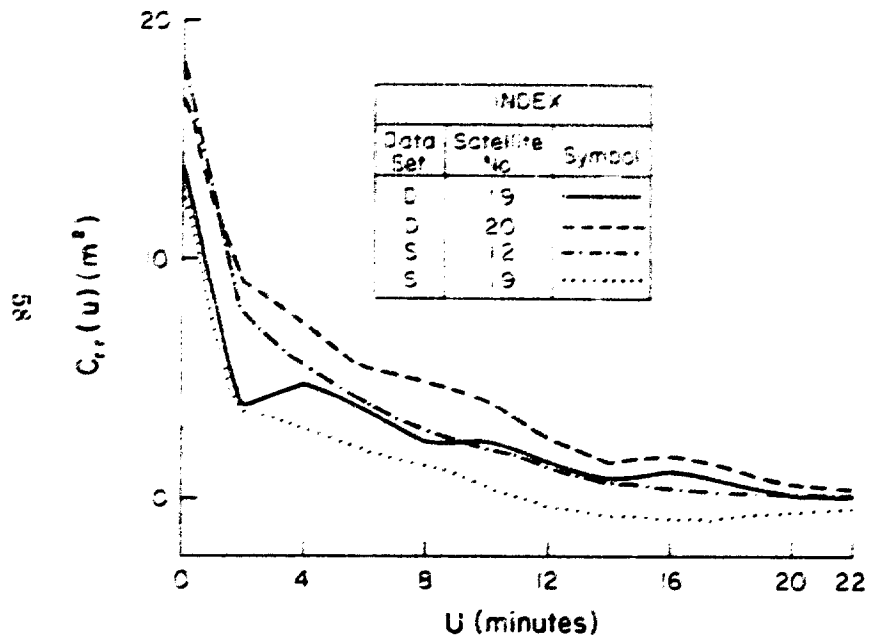
Figure 4.12 Sample Autocovariance $C_{rr}(u)$
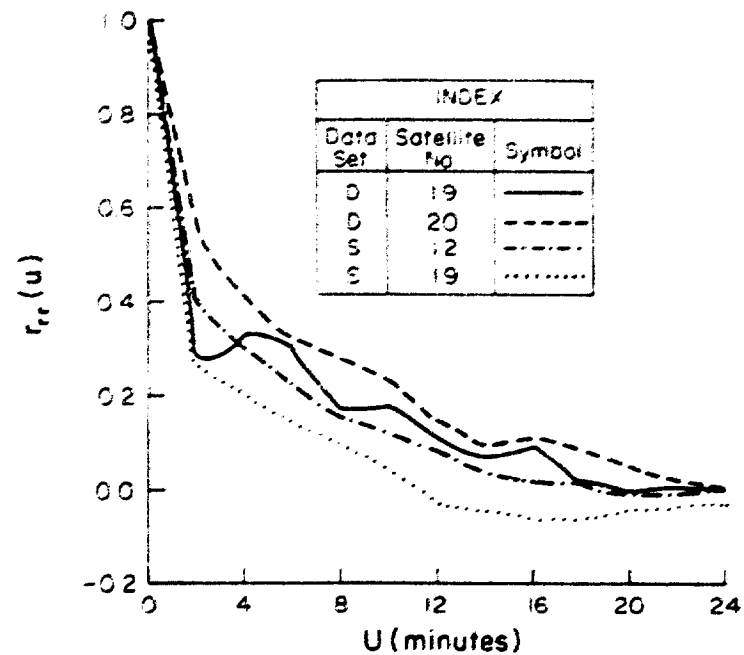
Figure 4.13 Sample Autocorrelation $r_{rr}(u)$
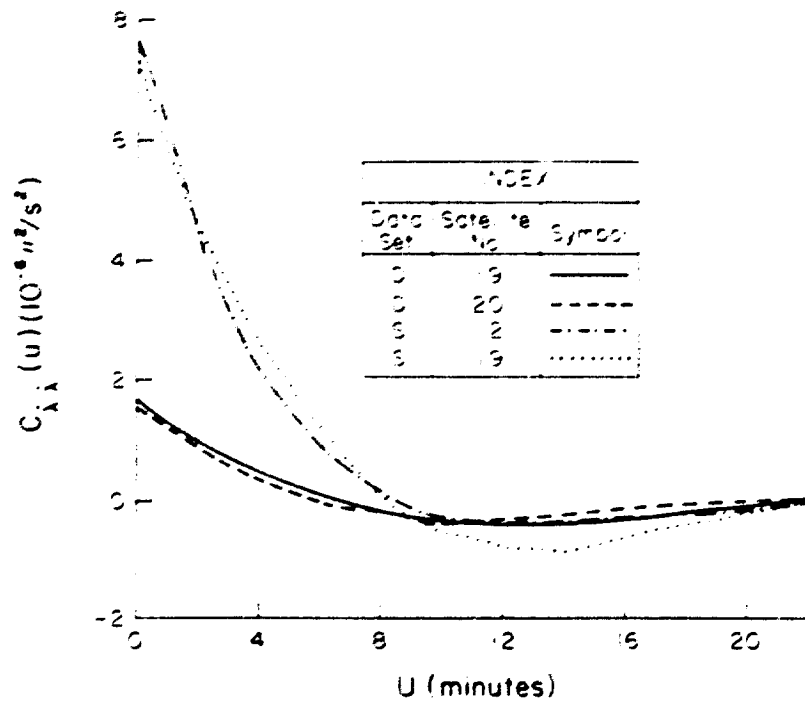
Figure 4.14   Sample Autocovariance $C_{\lambda\lambda}(u)$
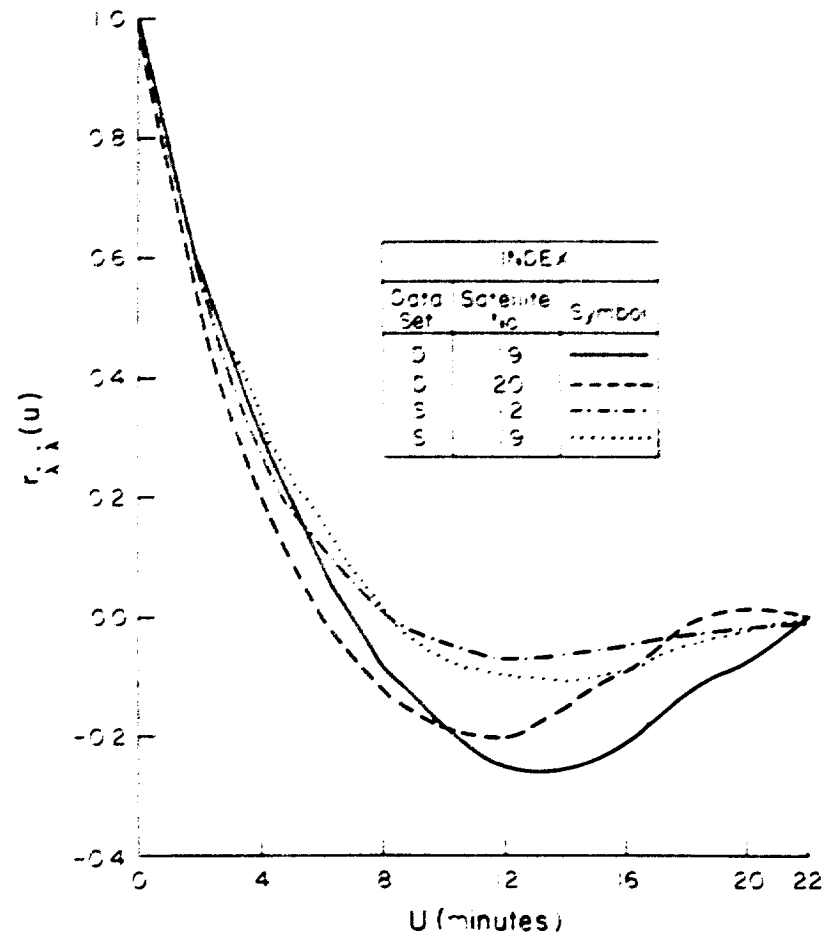
Figure 4.15   Sample Autocorrelation $r_{\lambda\lambda}(u)$
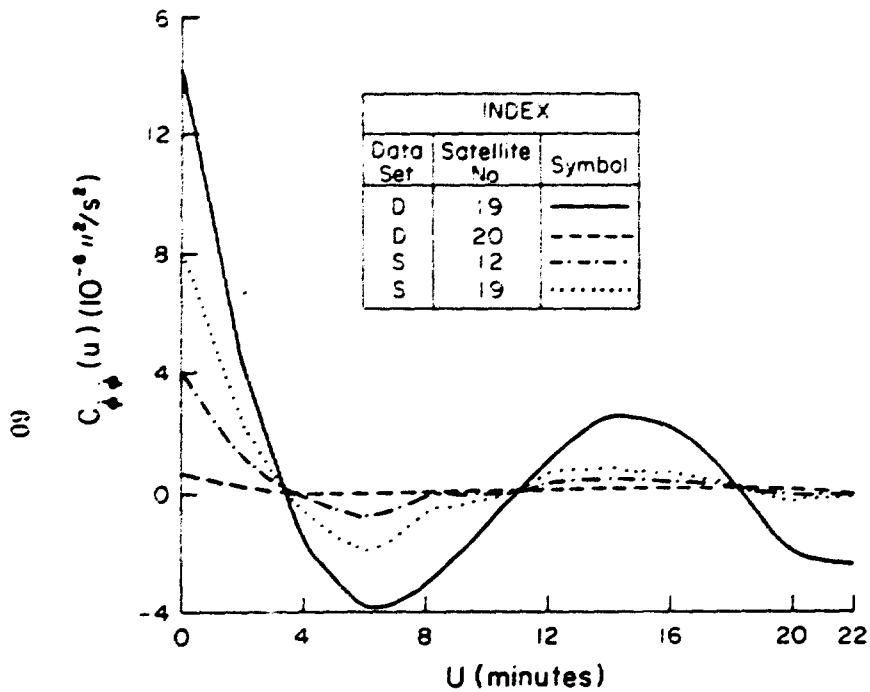
Figure 4.16   Sample Autocovariance $C_{\dot{\varphi}\dot{\varphi}}(u)$
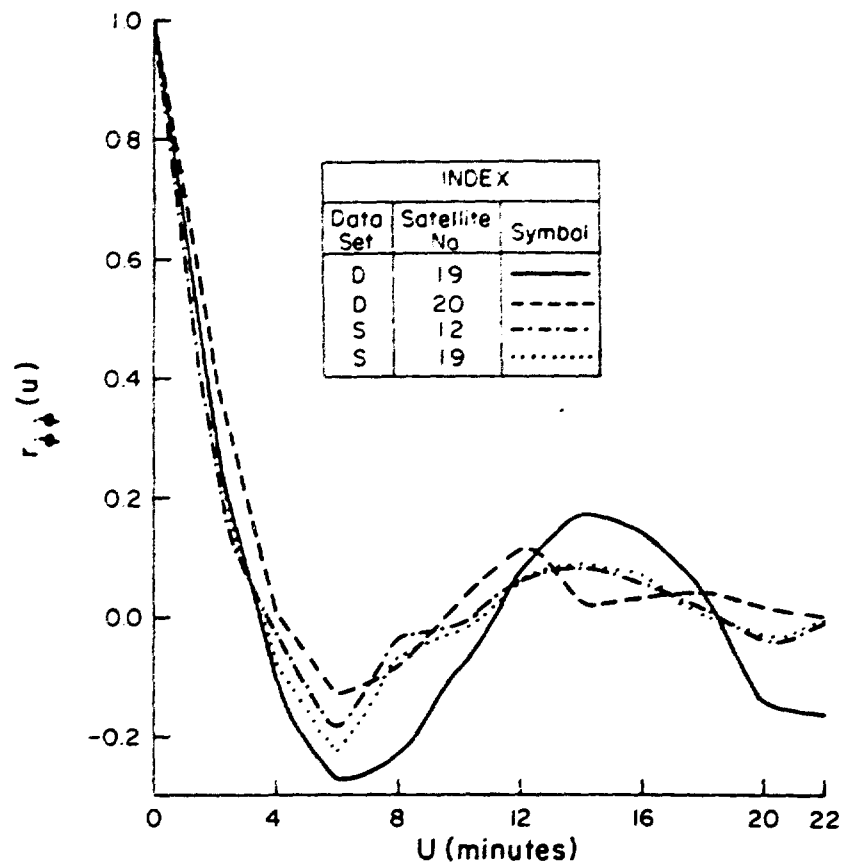
Figure 4.17   Sample Autocorrelation $r_{\dot{\varphi}\dot{\varphi}}(u)$

INDEX		
Data Set	Satellite No	Symbol
D	19	———
D	20	– – –
S	12	–·–·–
S	19	·····

$C_{\dot{r}\dot{r}}(u)\,(10^{-2}\,m^2/s^2)$

U (minutes)
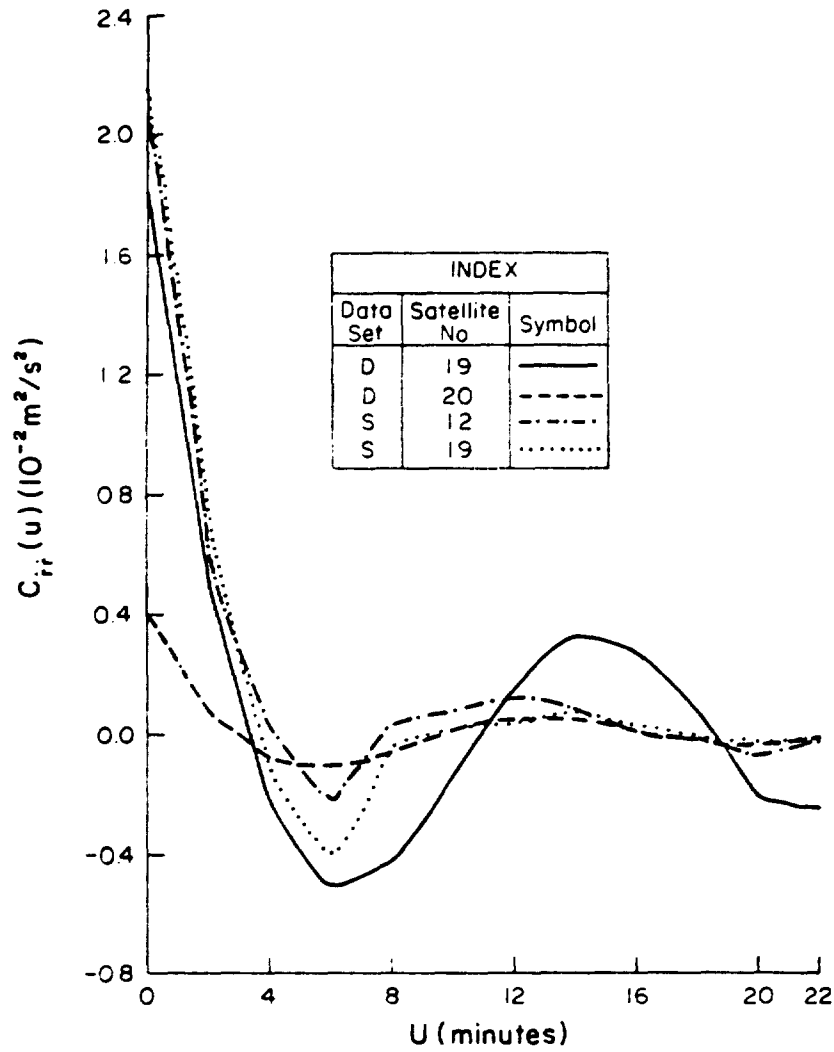
Figure 4.18   Sample Autocovariance $C_{\dot{r}\dot{r}}(u)$

INDEX		
Data Set	Satellite No.	Symbol
D	19	———
D	20	– – –
S	12	–·–·–
S	19	·····

$r_{\dot{r}\dot{r}}(u)$

U (minutes)
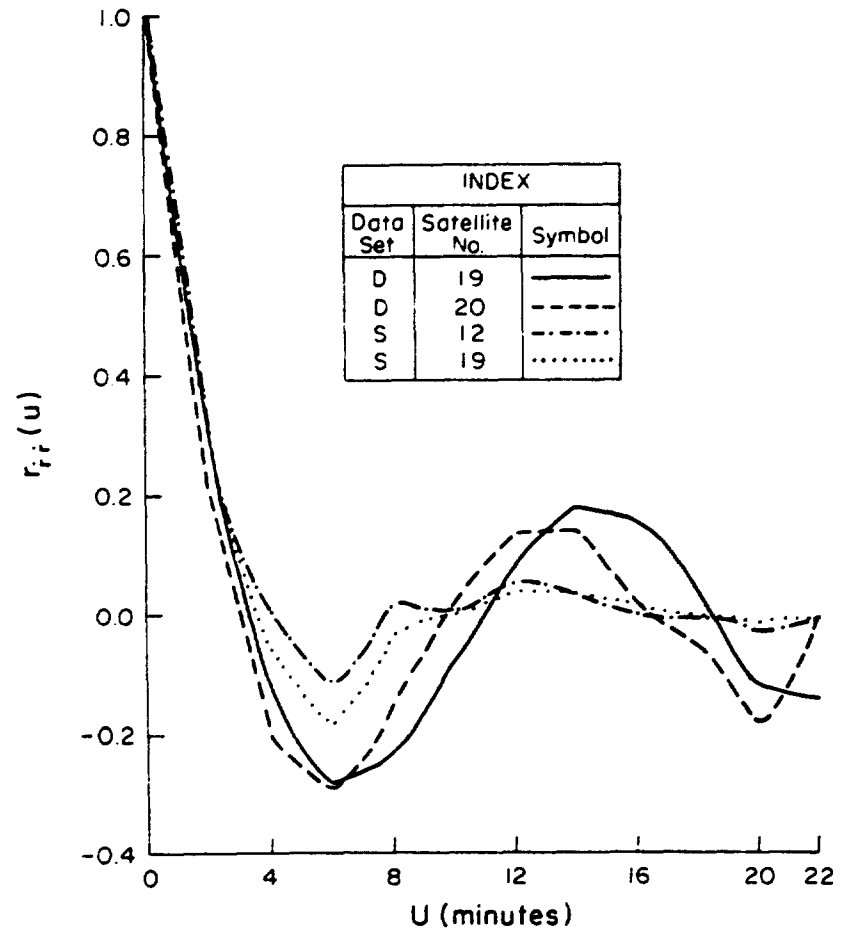
Figure 4.19   Sample Autocorrelation $r_{\dot{r}\dot{r}}(u)$

The sample cross-correlation matrix for the signals has been worked out for a typical case of satellite 19 for the lag u = 0 for Data Set S. The matrices obtained are as follows:

Sample Cross-Correlation Matrix for $\xi_{\ddot{X}}(0)$, $\xi_{\ddot{Y}}(0)$, $\xi_{\ddot{Z}}(0)$
Satellite 19

$$
\begin{array}{ccc}
\xi_{\ddot{X}} & \xi_{\ddot{Y}} & \xi_{\ddot{Z}} \\
\end{array}
$$
$$
\begin{bmatrix}
1 & 0.589 & -0.073 \\
 & 1 & -0.234 \\
 & & 1
\end{bmatrix}
$$

Sample Cross-Correlation Matrix for $\xi_{\lambda}(0)$, $\xi_{\varphi}(0)$, $\xi_{r}(0)$
Satellite 19

$$
\begin{array}{ccc}
\xi_{\lambda} & \xi_{\varphi} & \xi_{r} \\
\end{array}
$$
$$
\begin{bmatrix}
1 & -0.018 & -0.168 \\
 & 1 & -0.135 \\
 & & 1
\end{bmatrix}
$$

Sample Cross-Correlation Matrix for $\xi_{\dot{\lambda}}(0)$, $\xi_{\dot{\varphi}}(0)$, $\xi_{\dot{r}}(0)$
Satellite 19

$$
\begin{array}{ccc}
\xi_{\dot{\lambda}} & \xi_{\dot{\varphi}} & \xi_{\dot{r}} \\
\end{array}
$$
$$
\begin{bmatrix}
1 & -0.011 & 0.029 \\
 & 1 & -0.003 \\
 & & 1
\end{bmatrix}
$$

62

Figure 4.20 Sample Autocovariance $C_{\bar{\lambda}\bar{\lambda}}(u)$
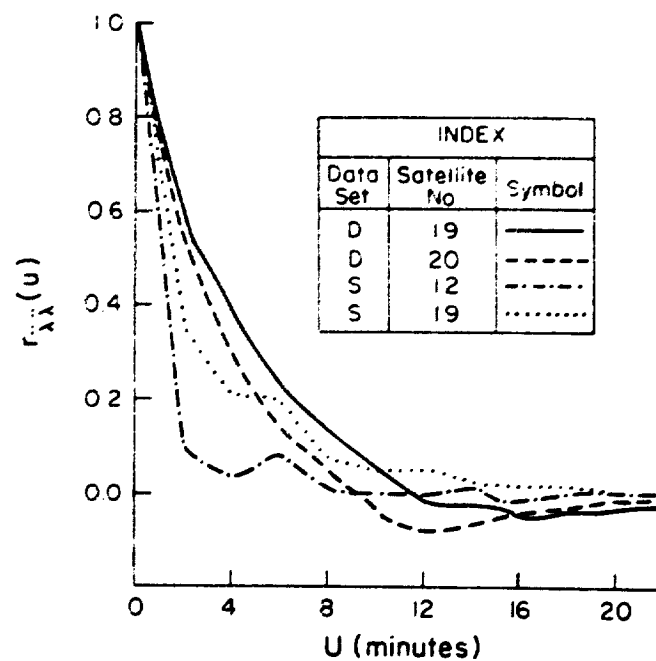
Figure 4.21 Sample Autocorrelation $r_{\bar{\lambda}\bar{\lambda}}(u)$
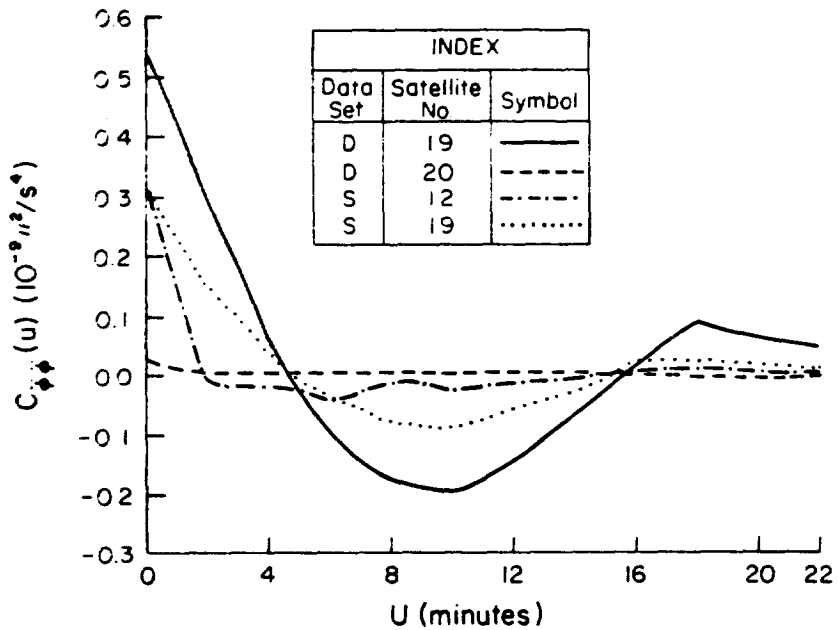
Figure 4.22   Sample Autocovariance $C_{\tilde{\phi}\tilde{\phi}}(u)$
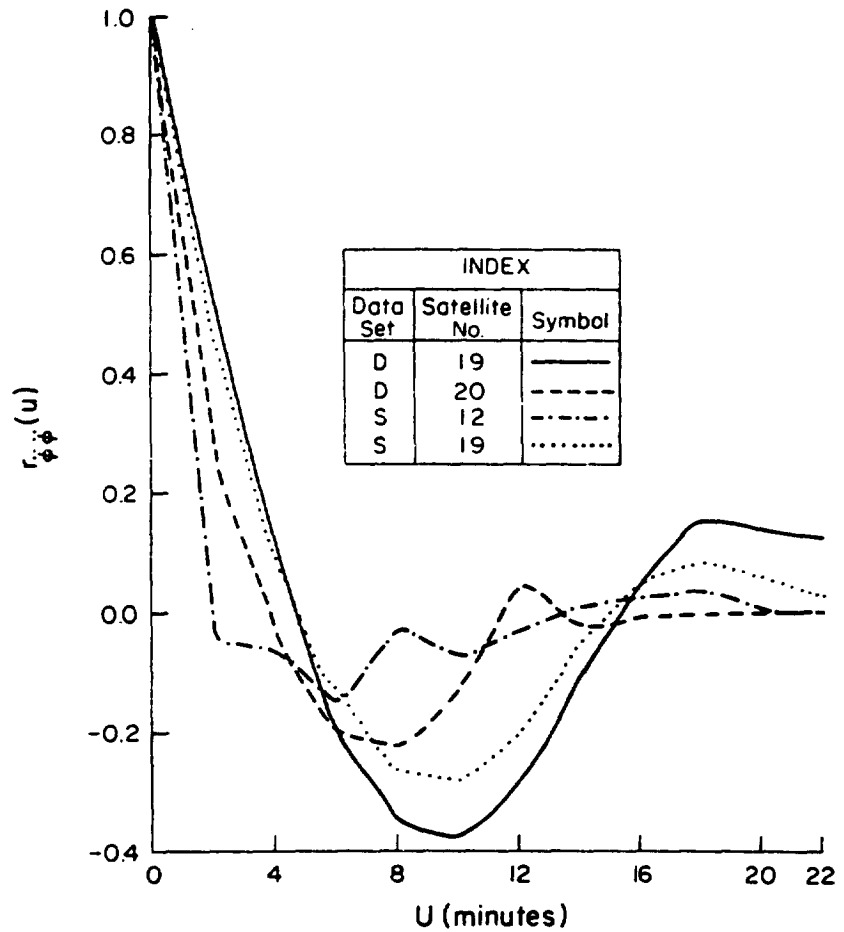
Figure 4.23   Sample Autocorrelation $r_{\tilde{\phi}\tilde{\phi}}(u)$

Left figure axes: $C_{\tilde{\phi}\tilde{\phi}}(u)$ $(10^{-6} \cdot s^2/s^4)$, U (minutes)

INDEX

Data Set	Satellite No.	Symbol
D	19	——
D	20	- - -
S	12	-·-·-
S	19	······

Right figure axes: $r_{\tilde{\phi}\tilde{\phi}}(u)$, U (minutes)

INDEX

Data Set	Satellite No.	Symbol
D	19	——
D	20	- - -
S	12	-·-·-
S	19	······
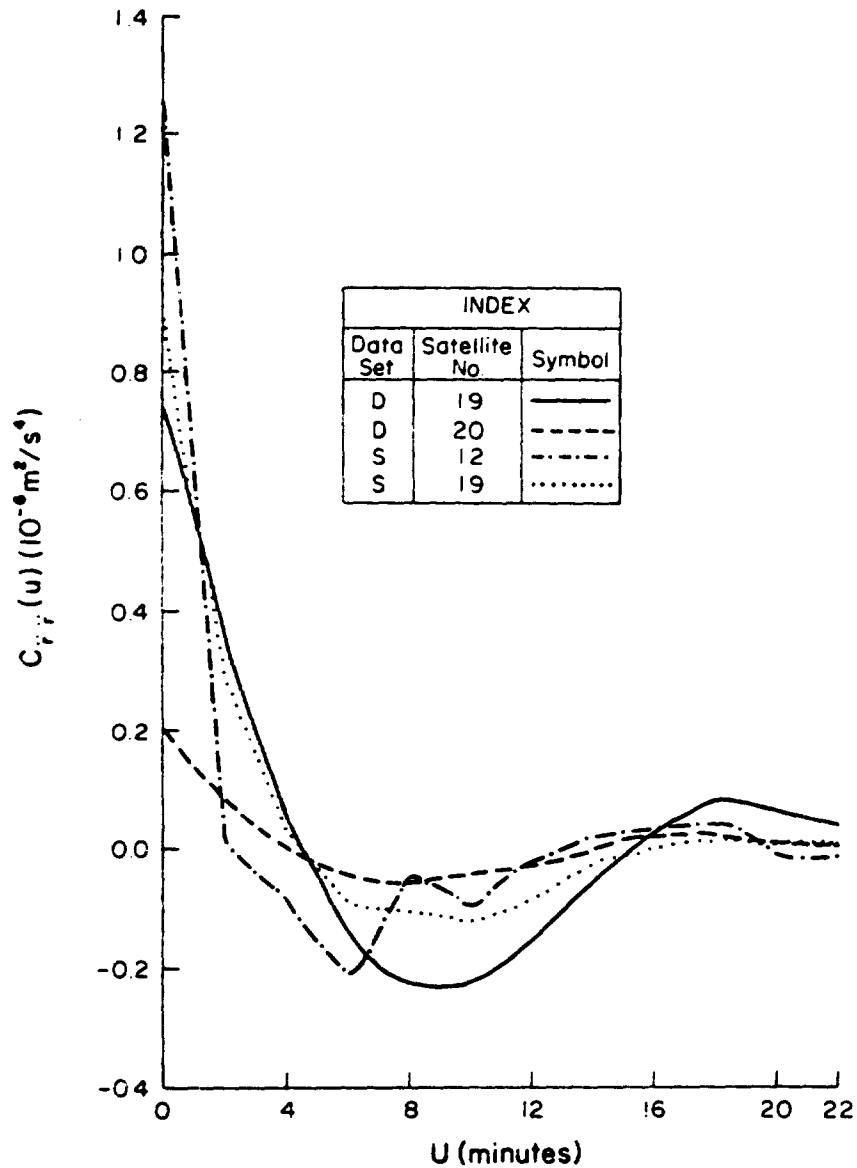
Figure 4.24   Sample Autocovariance $C_{\ddot{r}\ddot{r}}(u)$
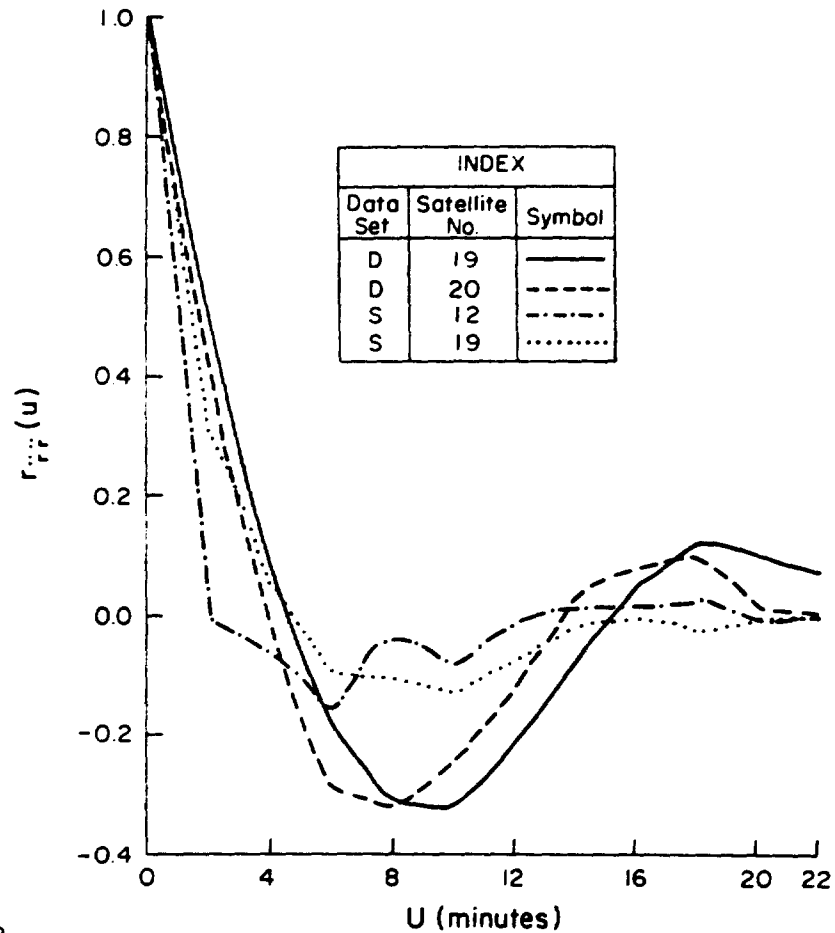
Figure 4.25   Sample Autocorrelation $r_{\ddot{r}\ddot{r}}(u)$

65

Sample Cross-Correlation Matrix for $\xi_{\ddot{\lambda}}(0)$, $\xi_{\ddot{\varphi}}(0)$, $\xi_{\ddot{r}}(0)$
Satellite 19

$$
\begin{array}{ccc}
\xi_{\ddot{\lambda}} & \xi_{\ddot{\varphi}} & \xi_{\ddot{r}} \\
\begin{bmatrix} 1 & 0.041 & 0.005 \\ & 1 & -0.042 \\ & & 1 \end{bmatrix}
\end{array}
$$

Table 4-1 gives a summary of the data analyzed in obtaining the statistics. It may be noticed that satellite 19 is common to Data Sets D and S. The number of data points shown refer to the number of realizations of the acceleration signal. The realizations for other signals are larger than this number.

Table 4-1

Summary of Data Analyzed
for Signal Statistics

Data Set	Satellite	Minimum No. of Data Points
D	19	182
	20	118
S	12	1674
	19	1502

4.4 Observations

The purpose of obtaining sample autocovariance functions and related quantities is to determine a model for the underlying stochastic process, in this case, the various signals. The following observations can be made based on the values obtained taking the various types of signals in turn.

66

4.4.1 Acceleration Signals $\xi_{\ddot{X}}(u)$, $\xi_{\ddot{Y}}(u)$, $\xi_{\ddot{Z}}(u)$

(i) The signal with the smallest autocovariance has a magnitude of over 2.0×10^{-8} m^2/s^4. Acceleration of 1.0×10^{-4} m/s^2 can cause a positional deviation of 1.8 m after ten minutes which can be taken as the observation period of a pass. So the signal is not insignificant where submeter accuracies are sought. The largest covariance is over 1.0×10^{-6} m^2/s^4.

(ii) Except for satellite 12 of Data Set S, the autocovariances are positive for a lag up to four minutes. For $\xi_{\ddot{Y}}(u)$ and $\xi_{\ddot{Z}}(u)$ of satellite 12, the autocovariance is positive up to a lag of two minutes.

When dealing with Doppler observations with a JMR-1 receiver as in Data Set D, the Doppler counts are available at every 4.6 seconds approximately, and if three stations coobserve a pass, data is acquired at a rapid pace of about 78 observations for every two minutes observed in common. So this signal is worth attempting to model in an effort to refine the orbit.

It will be seen in Chapter 5 that a simple and mathematically tractable model is sought for the stochastic process. A simple and convenient model for the autocovariance is an exponential form without any periodic term which gives rise only to nonnegative values. The lag up to which the sample autocovariance is positive is therefore very relevant.

(iii) The sample cross-correlation matrix of component signals indicates correlation of about -0.53 between $\xi_{\ddot{Y}}$ and $\xi_{\ddot{Z}}$ and a correlation of about 0.59 between $\xi_{\ddot{X}}$ and $\xi_{\ddot{Y}}$. So this is not the ideal set of signals to attempt to model in any procedure where an assumption of noncorrelation of the component signals simplifies covariance propagation. However, it is not too high either to leave this procedure completely out of consideration.

4.4.2 Acceleration Signals $\xi_{\ddot{\lambda}}(u)$, $\xi_{\ddot{\varphi}}(u)$, $\xi_{\ddot{r}}(u)$

(i) The signal with the smallest autocovariance has a magnitude of over 0.2×10^{-10} ("/s^2) which can cause a positional deviation of one meter after ten minutes. The largest autocovariance has a magnitude of over 1.2×10^{-6} m/s^4.

(ii) Regarding the lags up to which the autocovariance is positive, the same remarks as for $\xi_{\ddot{X}}(u)$, $\xi_{\ddot{Y}}(u)$, $\xi_{\ddot{Z}}(u)$ above apply in the case of $\xi_{\ddot{\varphi}}(u)$ and $\xi_{\ddot{r}}(u)$. For the signal $\xi_{\ddot{\lambda}}(u)$, the positive autocovariance persists even after eight minutes.

(iii) The sample cross-correlation matrix shows the largest correlation as low as 0.04 making this set of signals a good candidate to model.

4.4.3 Velocity Signals $\xi_{\dot{\lambda}}(u)$, $\xi_{\dot{\varphi}}(u)$, $\xi_{\dot{r}}(u)$

(i) The signal with the smallest autocovariance is over 0.4×10^{-6} ("/s)^2. A velocity of 0.1×10^{-3} "/s implies a positional deviation of over 2 m after ten minutes. The maximum autocovariance is in the order of 14.0×10^{-6} ("/s)^2.

(ii) Regarding the duration of positive covariance, the same remarks as above apply for signals $\xi_{\dot{\varphi}}(u)$ and $\xi_{\dot{r}}(u)$. In the case of the signal $\xi_{\dot{\lambda}}(u)$, the positive correlation continues to six minutes.

(iii) The largest correlation is only 0.03 as seen from the sample cross-correlation matrix making this another good candidate for an attempt to model the signal.

4.4.4 Position Signals $\xi_{\lambda}(u)$, $\xi_{\varphi}(u)$, $\xi_{r}(u)$

(i) In this case the smallest autocovariance is over 0.02 (")^2. 0!'1 implies a deviation of 3.6 m at the altitude of the satellite. The largest autocovariance is over 0.2 (")^2.

68

(ii) The duration of positive correlation is much larger than in the cases of all previous signals. It persists at least up to eight minutes in case $\xi_r(u)$ for satellite 19 in Data Set S and extends over 18 minutes in other cases, making this a good candidate for an effort to model.

(iii) The maximum correlation indicated in the cross-correlation matrix is 0.17 which is fairly low making this signal worthwhile being modeled.

(iv) Another interesting observation in the case of these autocovariances is the value of the mean of the signal realizations obtained in forming sample autocovariances $C_{rr}(u)$. The mean in all cases was a negative value varying in magnitude from -3.3 to -7.8 m. The effect of treating this as a bias in a point positioning experiment has been described in Chapter 5.

4.5 Application in Present Study

The computations of the realizations of the signals and their sample statistics have been described above. Some general observations about the statistics obtained have also been made.

It can be noticed that satellite 19 is common to Data Sets D and S, and Data Set S is over five times larger than Data Set D. So satellite 19 was a good candidate for experimentation, giving a greater weight to the statistics obtained from Data Set S.

In each of the figures 4.2 to 4.25 there are two curves with respect to satellite 19, one pertaining to the period January, 1976, and the other to the period October, 1976. It is comforting to see that these two curves are close to each other in most figures indicating a nearly stabilized situation.

It will be seen in Chapter 5 that the model chosen for the stochastic process of the signal $\xi(t)$ is of the form

$$\dot{\xi}(t) = -\beta\,\xi(t) + \sigma\beta\,w(t)$$

where

w(t)　　　is the Gaussian noise with the properties $E[w(t)] = 0$,

　　　　　$E[w(t) w(s)] = \delta(t - s)$

σ　　　is the variance parameter

$\delta(t-s)$　is the Dirac delta func'ion

β　　　is the time correlation coefficient

This choice arises from the fact that if it is further assumed that $\xi(o) \sim$ $N(o, \sigma^2 \beta /2)$, independent of $\{w(t)\}$ in the above model, then

$$R_{\xi \xi}(u) = \sigma^2 (\beta/2) e^{-\beta(u)} \qquad \text{[Jazwinsky, 1970]}$$

which is the analog of the first-order autoregressive process or first-order Gauss-Markov process. In this situation, the curves obtained in this study can directly give the initial estimates of the parameters of the autocovariance function in procedures to be described in Chapter 5.

It is evident that with the material available many different experiments and approaches are possible, depending on which signal is proposed to be chosen to represent the state disturbance. In this study, however, the constraints on time available to the author and the form of software available have made only some types of experiments possible. These have been discussed in the next chapter.

70

5. EXPERIMENTS FOR IMPROVED POSITIONING

5.1 Introductory Remarks

With the statistical information obtained in Chapters 3 and 4, a couple of experiments were undertaken in which this information was utilized. These experiments and their results have been described in this chapter.

At this stage it is appropriate to indicate the overall philosophy adopted in designing these experiments, for the ultimate aim of gaining improved station positions with broadcast ephemeris and Doppler data.

The Doppler observational data available and used pertains to Data Set D in which three stations have coobserved several passes. As discussed in Chapters 2 and 4, it is possible to carry out a solution in a short arc mode and obtain values for both the orbit unknowns and the station unknowns. But as indicated in Chapter 2, such solutions may have a problem which is precisely stated by Mueller [1976]:

> The results are being scrutinized by theoreticians who regard the results as "meaningless" in view of the fact that the dynamic solutions are rank deficient and as such the problem (of simultaneously determining geocentric station and satellite parameters) is theoretically unsolvable, e.g., the system of reference defined by such solutions would depend entirely on the a priorily selected values of parameters (e.g., station coordinates).

In this study, the knowledge of the satellite positions is available in the form of broadcast ephemeris. The broadcast ephemeris gives a set of values in a consistent coordinate system with uncertainties which have been assessed in the study and described in Chapter 3.

Doppler observational data from three coobserving stations (Data Set D) has been used with broadcast ephemeris to obtain the best values for the

ORIGINAL PAGE IS
OF POOR QUALITY

station coordinates which could be held fixed in a subsequent filtering program for orbit refinement. Under this situation, and keeping in view the rank deficiency problem described earlier, a decision was to be taken about the specific constraints to be used in this study in the solution for station positions.

As described by Pope [1971], the rank deficiency of the normal matrix can be obviated by use of either (a) weighted constraints or (b) absolute constraints on parameters. Method (a) becomes (b) as weights on the parameters are increased to infinity.

As regards the number of constraints, they can be either the minimal set of constraints, or they can be more than minimal. Among minimal constraints, there is the attractive possibility of using an inner constraint solution [Blaha, 1971] which leads to the "free network adjustment" without explicitly forming a pseudo-inverse matrix.

Although inner constraints yield an optimum coordinate system with a minimum trace for the variance-covariance matrix of the parameter estimates, the solution and the coordinate system itself is optimized with respect to the initial values of the parameters used in the adjustment. While this may be advantageous in a larger network adjustment where the coordinate system also needs to be optimized, in a local adjustment like the one used in this study where a coordinate system in unambiguously accessible (viz., the WGS 72 system through the broadcase ephemeris), it is best to adopt it and to ensure that the values obtained in the adjustment are in the chosen coordinate system.

Since the ground station positions are the main unknowns, this could be achieved by absolutely constraining the satellite orbits by introducing very large weights. Thus it was decided to hold the satellite orbit fixed in the solution for station positions with SAGA.

Adopting and maintaining the WGS 72 coordinate system as described above, the problem is tackled in the following three stages:

(i)   Determination of station positions with observational data, holding the orbits fixed,

(ii)   Improving the orbits keeping the station positions unchanged,

(iii) Redetermination of station positions holding the improved orbits fixed.

Within the time available, only two experiments could be completed, and only these two experiments have been described. In the first experiment the radial bias noticed vide Section 3.5 has been taken into account, and the effect of removing this suspected bias in the broadcast ephemeris on station position recovery has been determined. This experiment was aimed only to study the radial bias identified in Chapter 3. Similar studies must be carried out with respect to other biases, but for reasons explained in Section 3.2, these have not been pursued in this investigation. As a follow up of this experiment, the reason for the radial bias has also been investigated.

In the second experiment, the first steps have been taken to judge the feasibility of utilizing the statistical information obtained in Chapter 4 in an adaptive filtering procedure for orbit improvement. In this experiment, the station positions have been held fixed at values obtained in stage (i). Statistical information obtained earlier was utilized, but simulated range rate observations available from existing software were utilized to judge the performance of the filtering procedure.

Simulated range rate observations have been used in this study only as a first step to judge the feasibility of using the adaptive filtering approach in practice, so that the available software could be used with minimum modifications. In position determination with Doppler data, range differences would have been the appropriate observations.

Range difference observations have a more direct influence than range rates on the position of a satellite. So in using simulated range rates to judge the feasibility of the filtering procedure, an observational mode less optimum than that obtained in reality is being adopted. The next steps in this study would have been to first try the procedure with simulated range differences

73

and then to use real data. It is best to undertake these steps after first deciding the optimum model for the state disturbance. For example, the formulations for viewing the state disturbance as an acceleration signal in the Cartesian coordinate system would differ considerably from the formulation for state disturbance viewed as a position signal in the spherical coordinate system. Unfortunately, in the time frame available to the author, it was not possible to complete these further steps.

The presence of state disturbance and its role in the evolution of the state characterizes the main distinguishing feature of the filtering procedure in this study. But the method of estimation from observations is similar to the least squares techniques. Thus it was felt appropriate to review the mathematical formulations leading to the conventional sequential filter algorithm (also called the first order filtering technique) as a background to the adaptive filtering procedure in the second experiment. These are included in Appendix B.

5.2 Experiment for Radial Bias

5.2.1 Determination of Station Positions

Station positions for three stations in the Florida area were obtained with the help of the Short Arc Geodetic Program (SAGA) [Brown and Trotter, 1969] available at The Ohio State University. The formulation used in the program is documented both in the above-referred publication [Kumar, 1976] and in [Brown, 1976].

With the version of SAGA available at OSU, the following main steps were required to obtain a solution:

(i)   modification of the available subroutine for Geoceiver raw data to make it compatible with JMR raw data,

(ii)   majority vote of the ephemeris message to obtain state vectors of satellites at two-minute intervals,

(iii)   computation of mid arc state vectors for each pass for input to SAGA with the program SAMVAP.

The meteorological data acquired at the stations formed part of the input.

The solution was obtained from 12 passes holding the orbits fixed and allowing the station positions to remain free in the adjustment.

5.2.2 Determination of Radial Bias

As mentioned in Section 4.5, a negative radial bias was noticed while computing the sample autocovariance $C_{rr}(u)$ for both Data Sets S and D. To assess a more reliable value of the suspected bias, Data Sets S and D for the four satellites were combined with the following results:

$$
\begin{array}{ll}
\text{degrees of freedom} & 4313 \\
\text{bias} = \overline{\Delta r} = & -5.3 \text{ m} \\
\sigma_{\Delta r} = & 4.5 \text{ m}
\end{array}
$$

A t-test is not strictly valid because of the fact that adjacent outcomes of Δr are correlated. However, in view of the large degree of freedom available, a t-test was carried out to test the hypothesis H_0: $\mu = 0$ against H_1: $\mu \neq 0$ at $\alpha = 0.05$.

$$
t \text{ (computed)} = \frac{-5.257}{4.507/\sqrt{4314}} = -76.61
$$

$$
t \text{ (tabular)} = 1.960
$$

Therefore the hypothesis that $\mu = 0$ is rejected.

5.2.3 Correction of the State Vectors for Bias

The mid arc state vectors used in Section 5.2.1 were corrected for a radial bias of -5.3 m. As shown in Section 4.2.3, the radial signal $s_r = r_p - r_n = \Delta r$. The bias is the mean value of s_r. The corrected radial distance $r_c = r_n + \overline{\Delta r}$.

For each pass used in the solution in 5.2.1, the mid arc state vector was first transformed from the Cartesian components (X, Y, Z) to the polar components (λ, φ, r). The radial component was corrected to r_c. The corrected

components (λ, φ, r_c) were transformed back to the Cartesian components (X_c, Y_c, Z_c), and the solution of Section 5.2.1 was repeated.

5.2.4 Redetermination of Station Positions After Removal of Bias

Table 5-1 gives the results of station position determination obtained before and after removal of radial bias. Table 5-2 shows the weight coefficient matrix which remained unchanged to the number of digits shown.

5.2.5 Observations

(i) The a posteriori variance of unit weight was reduced by a very small amount (.0003) after removal of bias. The weight coefficient matrix is unchanged to four decimal places. The station coordinates changed by very small amounts (< 0.1 m).

(ii) The bias was absorbed by small changes in the values of station coordinates and other pass parameters such as frequency bias, frequency drift, and refraction scaling factor.

(iii) One external check was available. The distance between stations 1 and 3, according to terrestrial survey, was 29 360.880 m, as given in [Brown, 1976]. In the above determinations, the distance was 29 361.003 m before correction for bias and 29 360.928 m after removal of bias.

The large standard deviation of the chord recovered (8.7 m) precludes a more positive statement. However, the removal of bias has made the solution for chord length closer to the terrestrial value.

5.2.6 Explanation for Radial Bias

As a follow up of the above experiment, an effort was made to understand the reason for the existence of the radial bias by carrying out the following adjustment.

It was assumed that the transformation parameters given by Anderle [1976] between the NWL 9D of precise ephemeris and the WGS 72 of broadcast

76

Table 5-1

Results of Station Position Determination

State Vectors As Broadcast :

A priori Standard Deviation of Observation = σr = 20 cm

Degrees of Freedom = 1311

Final Station Coordinates

Station No.	X (m)	Y (m)	Z (m)
1	920731.202	-5578835.827	2941252.526
3	892362.893	-5579450.679	2948797.691
4	885656.500	-5573826.292	2961347.463

$\hat{\sigma}_0$ = 1.07703

State Vectors As Corrected for Bias :

A priori Standard Deviation of Observations = σr = 20 cm

Degrees of Freedom = 1311

Final Station Coordinates

Station No.	X (m)	Y (m)	Z (m)
1	920731.111	-5578835.925	2941252.572
3	892362.866	-5579450.681	2948797.692
4	885656.456	-5573826.278	2961347.440

$\hat{\sigma}_0$ = 1.07671

Table 5-2

Weight Coefficient Matrix for Station Coordinates
(m^2)

X_1	Y_1	Z_1	X_3	Y_3	Z_3	X_4	Y_4	Z_4
0.51870+02								
0.47040+02	0.76740+02							
-0.16310+02	-0.20550+02	0.19610+02						
0.15040-06	0.56190-07	-0.16690-05	0.24070+02					
0.11070-07	0.24000-06	0.51980-06	-0.95700+01	0.21520+02				
-0.47810-07	0.11600-06	0.23980-06	0.15000+02	-0.16670+02	0.23090+02			
0.23070-06	-0.22670-07	-0.17630-07	0.15080-06	-0.85740-07	-0.12280-06	0.21140+02		
-0.68660-07	0.26230-06	0.36720-06	-0.78690-07	0.60200-06	0.31010-06	-0.59110+01	0.18430+02	
0.10500-06	-0.13520-07	0.35340-06	-0.33270-07	0.16240-06	0.93090-07	0.76820+01	-0.10540+02	0.11720+02

ephemeris take care of the rotations completely but not scale and origin shift. With this assumption, a four-parameter transformation was carried out between the precise ephemeris, transformed to WGS 72 as per parameters given by Anderle [1976] and broadcast ephemeris. Points were selected at intervals of over 72 hours to break possible correlation existing between adjacent data points. From Data Sets D and S, 26 points were available for satellites 12, 19 and 20, thus giving 78 observations in an observation equation model.

Adjustment was carried out with the following mathematical model in which ΔX, ΔY, ΔZ and ΔL were considered as the translation and scale parameters

$$\begin{bmatrix} X \\ Y \\ Z \end{bmatrix}_N = \begin{bmatrix} \Delta X \\ \Delta Y \\ \Delta Z \end{bmatrix} + \begin{bmatrix} 1 + \Delta L & 0 & 0 \\ 0 & 1 + \Delta L & 0 \\ 0 & 0 & 1 + \Delta L \end{bmatrix} \begin{bmatrix} X \\ Y \\ Z \end{bmatrix}_P \qquad (5.1)$$

where

    N   denotes the NAG broadcast ephemeris

    P   denotes the precise ephemeris transformed to WGS 72 as per given

        transformation parameters [Anderle, 1976]

The results obtained were: The correlation matrix was:

$\hat{\sigma}_0^2 = 0.913$

	ΔX	ΔY	ΔZ	ΔL
	1	0.252	-0.160	0.337
		1	-0.355	0.748
			1	-0.475
				1

$\hat{\Delta} X = -2.3$ $\hat{\sigma}_{\hat{\Delta} X} = 1.4 \text{ m}$

$\hat{\Delta} Y = 9.8$ $\hat{\sigma}_{\hat{\Delta} Y} = 2.0 \text{ m}$

$\hat{\Delta} Z = -2.0$ $\hat{\sigma}_{\hat{\Delta} Z} = 2.6 \text{ m}$

$\hat{\Delta} L = 1.43$ $\hat{\sigma}_{\hat{\Delta} L} = 0.34 \text{ ppm}$

A t-test was carried out at $\alpha = 0.05$ to test if the parameters could be considered as 0. The test failed with respect to ΔY and ΔL. So there are strong indications that there is an origin shift of about 9.8 m in the Y-axis direction and a scale correction of about 1.4 ppm between the two coordinate systems considered above. These two parameters can be explained as follows:

If the origin of the precise ephemeris coordinate system is assumed to coincide with the geocenter, the origin of the broadcast ephemeris system gets an offset of about 9.8 m in the direction of 90° W longitude, which is understandable as all the four stations generating the broadcast ephemeris are located in continental United States.

As regards the scale parameter, it is conjectured that this scale factor consists of two components. One component of about 0.9 ppm is due to the scale difference always noticed between the Doppler system and terrestrial surveys for some unknown reasons. As seen in Chapter 2, the scale in a Doppler system is derived from λ, the wave length of transmission. The second part of about 0.5 ppm is the inherent scale difference between the precise and broadcast ephemerides. A similar scale factor of about 0.4 ppm had been detected by White [1975] when he carried out the transformations in his study. During that time, the coordinate system of both the ephemerides was assumed to be the same (NWL 9D).

5.3 Experiment in Adaptive Filtering

The aim of this experiment was to assess the feasibility of utilizing the statistics collected in Chapter 4 in an adaptive filtering procedure described in [Myers, 1973] for orbit improvement. The mathematical formulation of adaptive filtering and the description of the software which motivated the present experiment will first be given before describing the experiment and the results.

5.3.1 Adaptive Filtering

In the classical sequential estimation procedure, as described in Appendix B, the state disturbance is viewed as white noise and is compensated for. An alternate method of handling state disturbance is to treat it as a signal considering its correlated character. Its expectation is still considered to be zero, but its autocovariance, considering the signal as a stochastic process, is associated with an assumed model.

If the parameters of the autocovariance model are assumed to be known, then the signal and the state can be estimated as per normal least squares collocation procedures [Moritz, 1972]. For example, consider the procedures in gravimetry. The parameters of normal gravity may be considered as constituting the state. The gravity anomalies may be considered as the state disturbance or signal with known autocovariance function depending on the separation in distance instead of separation in time as in the case of this study. Further, the state would be considered time independent unlike the state in this study whose evolution in time is governed by the differential equations of motion.

But if the parameters of the autocovariance function are not well known, it is possible to include them in an augmented state vector in the adaptive filtering technique or the dynamic model compensation technique, as described in [Myers, 1973].

The detailed procedures depend on how it is proposed to model the state disturbance. For example, in this study, referring to the statistics collected in Chapter 4, the state disturbance could be considered to be constituted mainly of position signal, velocity signal, or acceleration signal. Further, the acceleration signal could be either in the Cartesian coordinate system or in the spherical system.

The computer software available was based on formulations for an acceleration signal in the Cartesian coordinate system. So, to judge the feasibility of using this procedure in the present problem, it was decided to attempt the procedure of adaptive filtering with the acceleration signal in the Cartesian coordinate system. The formulation for this based on [Myers, 1973] and

ORIGINAL PAGE IS OF POOR QUALITY

[Tapley, 1972] is given below. Formulations for other signals will need suitable modifications.

The true equations of motion can be expressed as a system of first-order differential equations.

$$\begin{aligned}\dot{\overline{r}} &= \overline{v} \\ \dot{\overline{v}} &= \overline{a}\ (\overline{r},\ \overline{v},\ t) + \overline{\xi}\,(t)\end{aligned} \tag{5.2}$$

where $\overline{r}$ and $\overline{v}$ are three-vectors which describe true position and velocity in an inertial frame as a function of time, $\overline{a}$ is a three-vector function of acceleration components in the nominal dynamical model, and $\overline{\xi}\,(t)$ is a three-vector acceleration signal.

If $\overline{\xi}\,(t)$ is considered as white noise, the procedure of classical sequential estimation could be applied as stated earlier. But from the study in Chapter 4, it is indicated that the realizations of $\xi_{\overline{X}}(t)$, $\xi_{\overline{Y}}(t)$, $\xi_{\overline{Z}}(t)$, which are the components of $\overline{\xi}\,(t)$, are correlated, and so a white noise model is not adequate. Therefore, $\overline{\xi}\,(t)$ is approximated by a vector stochastic process $\overline{\epsilon}(t) = [\epsilon_X(t) \quad \epsilon_Y(t) \quad \epsilon_Z(t)]^{\mathsf{T}}$, and a simple model is assumed for this process by considering the components of $\overline{\epsilon}(t)$ as a time-correlated first-order Gauss-Markov process satisfying the stochastic differential equation

$$\dot{\overline{\epsilon}}\,(t) = -B(t)\ \overline{\epsilon}(t) + \overline{W}_\epsilon\,(t) \tag{5.3}$$

Here, $\overline{W}_\epsilon\,(t)$ is a three vector of Gaussian noise with the properties

$$E\,\{\,\overline{W}_\epsilon(t)\,\} = 0 \qquad E\,\{\,\overline{W}_\epsilon(t)\,\overline{W}_\epsilon^{\mathsf{T}}(s)\,\} = q_\epsilon\,(t)\ \delta(t-s) \tag{5.4}$$

where

$$q_\epsilon(t) = \begin{bmatrix} q_{\epsilon_X} & 0 & 0 \\ 0 & q_{\epsilon_Y} & 0 \\ 0 & 0 & q_{\epsilon_Z} \end{bmatrix} \tag{5.5}$$

is the matrix of variance parameters associated with $\overline{\epsilon}\,(t)$, and $B(t)$ is a 3×3 diagonal matrix of time correlation coefficients

$$B(t) = \begin{bmatrix} \beta_X & 0 & 0 \\ 0 & \beta_Y & 0 \\ 0 & 0 & \beta_Z \end{bmatrix} \tag{5.6}$$

Further, for reasons explained overleaf, the evolution of

$$\bar{\beta}(t) = \begin{bmatrix} \beta_X \\ \beta_Y \\ \beta_Z \end{bmatrix}$$

is assumed to be governed by the differential equation

$$\dot{\bar{\beta}}(t) = 0 \tag{5.7}$$

Considering the above additional parametrization, the model in (5.2) is augmented to become

$$
\begin{aligned}
\dot{\bar{r}} &= \bar{v} \\
\dot{\bar{v}} &= \bar{a}(\bar{r}, \bar{v}, t) + \bar{\epsilon}(t) \\
\dot{\bar{\epsilon}} &= -B\bar{\epsilon} + \overline{W}_\epsilon(t) \\
\dot{\bar{\beta}} &= 0
\end{aligned} \tag{5.8}
$$

The new state vector is a 12-vector,

$$\overline{X}^\tau(t) = [\bar{r}^\tau : \bar{v}^\tau : \bar{\epsilon}^\tau : \bar{\beta}^\tau] \tag{5.9}$$

and the functional form of (5.8) is

$$\dot{\overline{X}} = F(\overline{X}, \overline{W}, t); \qquad \overline{X}(t_0) = \overline{X}_0 \tag{5.10}$$

With this augmentation the algorithm is similar to that of the first-order filter given in Appendix B.

The advantage of the model of the form (considering one component),

$$\dot{\epsilon}_X(t) = -\beta_X \epsilon_X(t) + W_{\epsilon_X}(t), \qquad \epsilon_X(0) \sim N\left(0, \frac{q_{\epsilon_X}}{2\beta}\right) \tag{5.11}$$

is that it gives rise to a stationary, exponentially correlated Gaussian process or colored noise if the variance parameter and the time correlation coefficient

83

are constant [Jazwinsky, 1970]. It may be recollected that an assumption of stationarity had been made for computing sample autocovariance of signals in Chapter 4. In this algorithm, the process is reinitialized at every step, and the parameters are treated as constant for that step. This explains why $\dot{\overline{\beta}}(t) = 0$ in equation (5.7).

From the above formulations, it is easy to understand the interrelations between some of the estimation procedures used in geodesy. In the adaptive filtering procedure used in this study, the state is time dependent. The state disturbance is viewed as a signal. The parameters of the autocovariance model of the signal are assumed not to be perfectly known and are included in the sequential estimation procedure along with the signals. The state to be estimated would be given by equation (5.9).

If the parameters of the autocovariance model of the signal are assumed to be perfectly known, these can be excluded from the estimation procedure, and the state to be estimated would be

$$\overline{X}^{\tau}(t) = [\,\overline{r}^{\tau} : \overline{v}^{\tau} : \overline{\epsilon}^{\tau}\,]$$

This would be the familiar least squares collocation procedure extended to a dynamic situation.

If the state disturbance is viewed only as a "noise " in this dynamic situation, the state to be estimated would be

$$\overline{X}^{\tau}(t) = [\,\overline{r}^{\tau} : \overline{v}^{\tau}\,]$$

as there is no signal to be computed, and this leads to the Kalman filtering procedure or the first-order filtering procedure described in Appendix B.

Further, if the state is assumed to be time independent in the above, the familiar least squares sequential adjustment procedure with weighted parameters is obtained.

84

5.3.2 Estimation of Initial Values of Parameters

The sample autocovariances $C_{\tilde{X}\tilde{X}}(u)$, $C_{\tilde{Y}\tilde{Y}}(u)$, $C_{\tilde{Z}\tilde{Z}}(u)$ and sample autocorrelations $r_{\tilde{X}\tilde{X}}(u)$, $r_{\tilde{Y}\tilde{Y}}(u)$, $r_{\tilde{Z}\tilde{Z}}(u)$ are helpful to determine good initial values of parameters for use in the algorithm to improve the orbit represented by the broadcast ephemeris.

The stochastic process considered above is the same as the first-order autoregressive process or the first-order Markov process [Jenkins, 1968]. Consider the component process $\epsilon_X(t)$ from above. It is assumed to satisfy a differential equation of the form

$$\dot{\epsilon}_X = -\beta_X \, \epsilon_X(t) + W_{\epsilon_X}(t) \tag{5.12}$$

Considering the Gaussian white noise $W_{\epsilon_X}(t)$ as input and $\epsilon_X(t)$ as output, the autocorrelation function of the output process, $\epsilon_X(t)$, is

$$\rho_{XX}(u) = e^{-|u|\beta_X} \tag{5.13}$$

[Jenkins and Watts, 1968, p. 162]

where u is the time lag. This is an analog of the following discrete first-order autoregressive process

$$\epsilon_{X_{t_n}} - \mu_{t_n} = \alpha_1 \left(\epsilon_{X_{t_{n-1}}} - \mu_{t_{n-1}} \right) + W_{t_n} \tag{5.14}$$

where $\mu_{t_1} = E\{\epsilon_{X_{t_1}}\}$. In this study $\mu = 0$, and so

$$\epsilon_{X_{t_n}} = \alpha_1 \epsilon_{X_{t_{n-1}}} + W_{t_n} \tag{5.15}$$

The autocorrelation function of this discrete process is given by

$$\rho_{XX}(k) = \alpha_1^{|k|} \tag{5.16}$$

where α_1 is the autoregression coefficient and $k = 0, \pm 1, \pm 2$ are the lags. In this study $k \geq 0$. The correspondence between (5.13) and (5.16) is readily seen, which helps in computing β_X from α_1.

Further, assuming a Gaussian distribution for W_{t_n}, the estimate $\hat{\alpha}_1$ of α_1 is given by

$$\hat{\alpha}_1 = r_{\ddot{X}\ddot{X}}(1) \tag{5.17}$$

<center>[Jenkins and Watts, 1968]</center>

the autocorrelation at first lag (in this case, the lag of two minutes).

It is clear that with $\hat{\alpha}_1$ taken from the $r_{\ddot{X}\ddot{X}}(u)$ curve in Chapter 4, the initial value of β_X parameter in the algorithm is easily computed. Similarly, the variance parameter of W_{t_m} is estimated by

$$S_w^2 \approx C_{\ddot{X}\ddot{X}}(0) - \hat{\alpha}_1 C_{\ddot{X}\ddot{X}}(1)$$

for a large sample size. Parameters for other component processes ϵ_Y and ϵ_Z are similarly obtained.

5.3.3 Simulation Program - EARTHOD

The experiment in adaptive filtering has been carried out with the station positioning results of the experiment in Section 5.2, the statistical analysis shown in Chapter 4, and the simulation program, EARTHOD, obtained from the Department of Aerospace Engineering and Engineering Mechanics at the University of Texas at Austin, duly modified.

The program provides the capability for simulation studies of an earth satellite observed by up to twelve ground-based tracking stations making as many as twelve simultaneous range, range-rate, elevation, and azimuth measurements.

Observations are generated from a set of true equations of motion operated on a true state of the satellite and are corrupted by Gaussian white noise. The program has an option for estimating the state of the satellite as well as the acceleration signal components and the parameters of autocovariance, based on the simulated observations, in an adaptive manner.

Since both the true state and the estimated state based on the observations and the nominal state are available in the simulation, actual estimation errors are easily determined for the judgment of the filter performance. The equations of motion are expressed in an earth-centered inertial (ECI) coordinate system and are numerically integrated with an

<center>86</center>

efficient Runge-Kutta-Fehlberg algorithm [Fehlberg, 1968].

For use in this study, the program written in Fortran IV in overlay form for the CDC 6600 operating system has been modified to run on the IBM 370/168 operating system at The Ohio State University.

State vectors derived from the precise and broadcast ephemerides have been used in lieu of the initial true and nominal states, respectively, as inputs, after transforming them from the earth-fixed system to the inertial system. The propagation of state is carried out with an eighth-order Runge-Kutta algorithm. The station coordinates are assumed to be known.

Results from EARTHOD simulations are available in terms of Root Sum Square (RSS) errors and covariance norms defined as follows: The RSS errors in position and velocity are, respectively:

$$\Delta R = [e_X^2 + e_Y^2 + e_Z^2]^{\frac{1}{2}} \tag{5.18}$$

$$\Delta V = [e_{\dot{X}}^2 + e_{\dot{Y}}^2 + e_{\dot{Z}}^2]^{\frac{1}{2}} \tag{5.19}$$

where $e_X = X - \hat{X}$ represents the true error component in the state position estimate $\hat{X}$. Similar definitions apply to other components. $e_{\dot{X}} = \dot{X} - \hat{\dot{X}}$ represents the true error component in the state velocity estimate $\hat{\dot{X}}$.

In this study, $\overline{X}$ represents the vector of state components based on precise ephemeris and $\hat{\overline{X}}$ represents the vector of their estimates based on observations and the nominal state component. The nominal state was derived from the broadcast ephemeris.

The position covariance norm is defined

$$NP = [p_{11} + p_{22} + p_{33}]^{\frac{1}{2}} \tag{5.20}$$

the square root of trace of the covariance elements associated with the position estimate and is obtained from the diagonal of $\hat{P}$ matrix in the algorithm, vide equation (B 58).

The velocity covariance norm is defined by

$$NV \quad [p_{44} + p_{55} + p_{66}]^{\frac{1}{2}} \tag{5.21}$$

which is likewise the square root trace of the covariance elements associated with the velocity estimate.

5.3.4 Description of the Experiment and Results

An experiment in adaptive filtering was carried out for one pass of satellite 19 in Data Set D. The station coordinates for the three stations, as obtained in the experiment (before removal of radial bias), were taken as known. Within the capability of the software, range-rate observations were the closest to Doppler observations, and so for further reasons explained in Section 5.1 the mode of simulated range rates was chosen, giving a three-vector observation at each step.

A fixed integration step of 0.075 minutes was chosen which is close to the rate of data acquisition with a JMR 1 receiver. The common two-minute epoch at the commencement of the observations from the three stations was chosen as the initial time t_0 for commencing the algorithm. The precise state vector (transformed to WGS 72 system) and broadcast ephemeris state vector at t_0 were transformed from the earth-fixed system to the inertial system. The values for polar motion components were taken as published by Bureau International de l'Heure, and the value for the Greenwich apparent sidereal time at t_0 was obtained from the American Ephemeris and Nautical Almanac 1976. The Jet Propulsion Laboratory ephemeris tape provided the inertial state vectors for sun and moon.

In the experiment for obtaining station positions, the range observation standard deviation was taken as 0.20 m. So a range-rate standard deviation of 0.002 m/s appears reasonable. Based on the study in Chapter 3, the uncertainties in the position and velocity components of the broadcast state vector were taken as [14.0 15.0 22.0 0.20 0.25 0.30] in units of meters and seconds for initial values in $\hat{P}_0$ in the first six diagonal locations. The values for the next three diagonal elements in $\hat{P}_0$, which referred to the autocovariance of the acceleration signal at lag 0, were taken from the curves $C_{\ddot{X}\ddot{X}}(u)$, $C_{\ddot{Y}\ddot{Y}}(u)$,

88

and $C_{\ddot{Z}\ddot{Z}}(u)$. The last three elements of $\hat{P}_0$ refer to the uncertainties of the time correlation coefficients. The values for these were taken either as five times the coefficients (as used in past investigations of Myers [1973]) or derived from the difference between the two values for the coefficients from the two sets of the curves $C_{\ddot{X}\ddot{X}}(u)$, $C_{\ddot{Y}\ddot{Y}}(u)$, and $C_{\ddot{Z}\ddot{Z}}(u)$ for satellite 19, one from Data Set D and the other from Data Set S.

Four trials were taken, varying slightly the standard deviation of observation and the initial values for the state noise parameters, from the analysis in Chapter 4.

In trial 1, the standard deviation of observations was kept as 0.002 m/s, but the initial parameter values were based on the information collected for satellite 19 from Data Set D. Uncertainties of β_X, β_Y, β_Z for $\hat{P}_0$ matrix were taken as five times their values.

In trial 2, the standard deviation of observations was kept as 0.002 m/s for the R matrix in the algorithm, but the initial parameter values for state noise referred to Data Set S. Uncertainties of β_X, β_Y, and β_Z for $\hat{P}_0$ matrix were taken as five times the initial values of the coefficients.

In trial 3, the standard deviation of observations was increased to 0.005 m/s, and the initial parameters were the same as in trial 2.

Trial 4 was similar to trial 2 in all respects except that the uncertainties of β_X, β_Y, β_Z in the $\hat{P}_0$ matrix were based on the difference between the two sample values for β_X, β_Y, β_Z for satellite 19 obtainable from Data Sets D and S.

The structures of the A and H matrices required in the algorithm are given in detail in [Ingram, 1971] and [Myers, 1973] and incorporated in the software used.

The sample autocovariance curves from the data analyzed in Chapter 4 were used directly for the trial values with the procedures given above. No least squares adjustments were made for estimates of parameters since it was the intention of this experiment to judge the adaptive property of the filter.

Figs. 5.1 and 5.2 show the values of ΔR, NR and ΔV, NV, respectively, against i, the number of integration steps of 0.075 minute, for trial 1. Figs. 5.3 to 5.8 give the same information for trials 2, 3, and 4.

Table 5-3 gives the components of state vector pertaining to the state disturbance (i.e., acceleration signal and time correlation coefficients) and their values at various integration steps, i. Tables 5-4 to 5-6 give the same information for trials 2, 3, and 4.

5.3.5 Observations

From the results of the trials, the following observations can be made:

(i) The initial deviation of 12.91 m in the position of the satellite as given by precise and broadcast ephemerides narrows down by about 0.6 m in about 20 integration steps but later diverges.

(ii) The uncertainty in position of the satellite as given by broadcast ephemeris reduces by about 4.2 m in about ten integration steps and later diverges.

(iii) The rate of change of improvement is the largest during the first five integration steps.

(iv) The optimum situation for position uncertainty arises fairly close to the optimum situation for position and the ΔR curve is flatter than the NR curve. This is of particular significance from the point of view of users who have no access to precise ephemeris. When this procedure is used with real observations and the broadcast ephemeris, only the NR curves are available. The curves in this study indicate that the state vector at optimum positional uncertainty, given by the NR curve, also yields a near optimum value for the position of the state vector.

(v) Velocity uncertainty decreases by about 0.2 m/s in the first five integration steps. This is followed by further improvement at a very slow rate.

(vi) Velocity error reduces by about 0.011 m/s in the first step. Later the error increases steadily to about 0.033 m/s in about thirty integration steps. This is followed by further steady improvement.

90
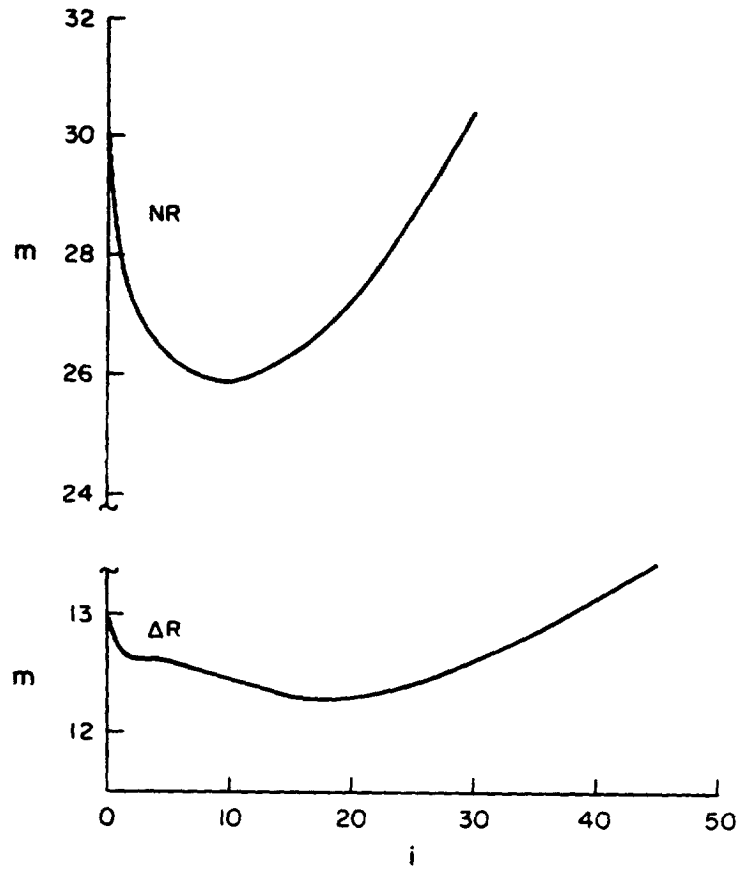
Figure 5.1

Position Error and Covariance Norm in Trial 1
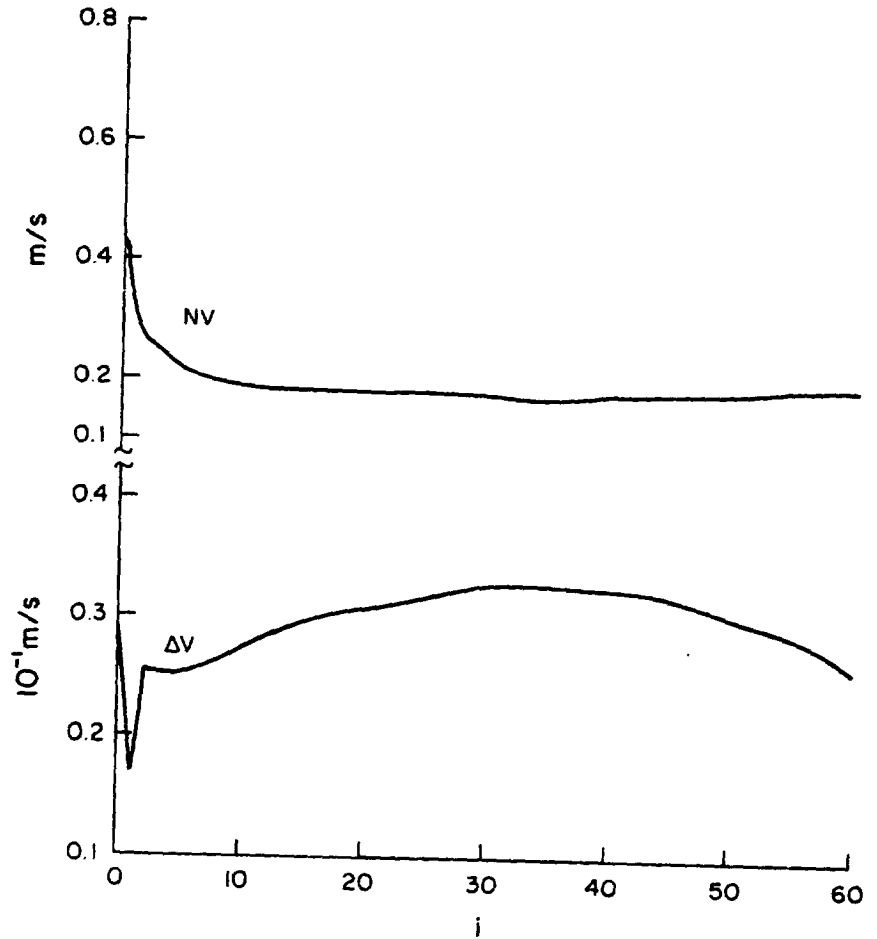
Figure 5.2

Velocity Error and Covariance Norm in Trial 1
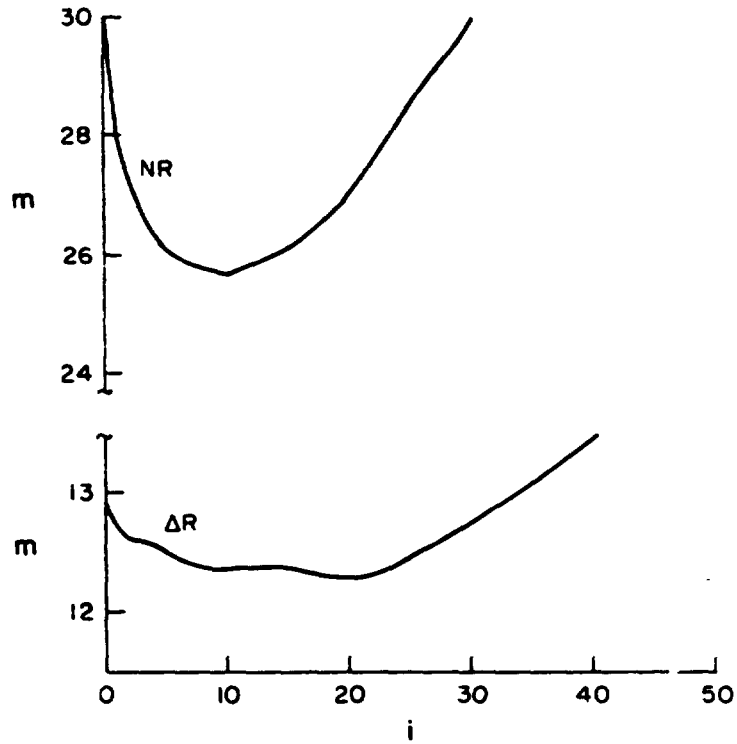
Figure 5.3

Position Error and Covariance Norm in Trial 2
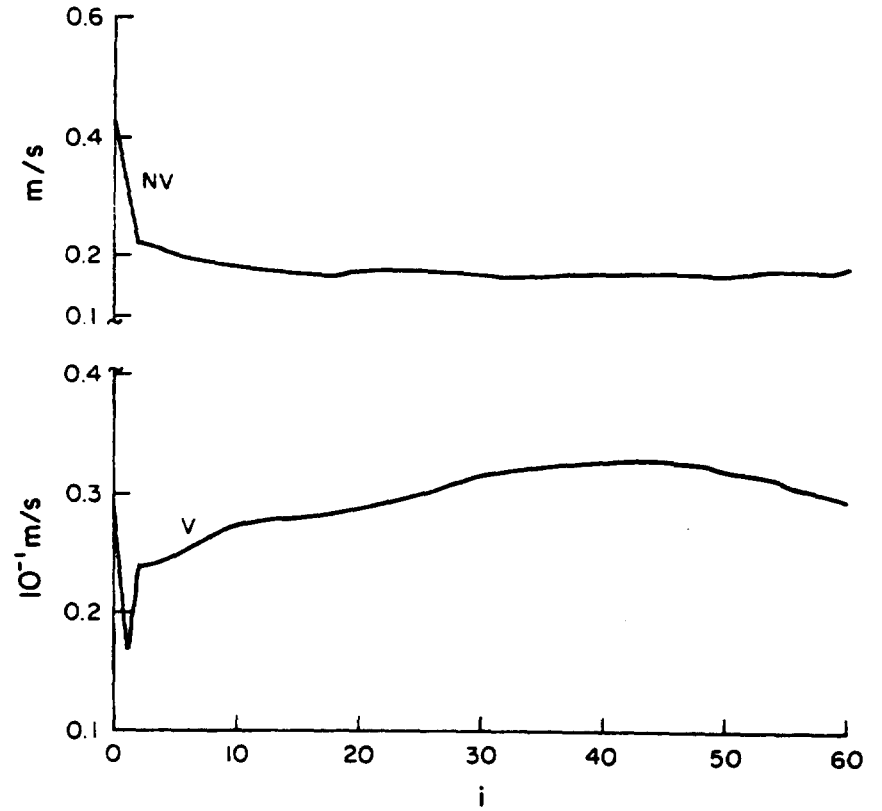
Figure 5.4

Velocity Error and Covariance Norm in Trial 2
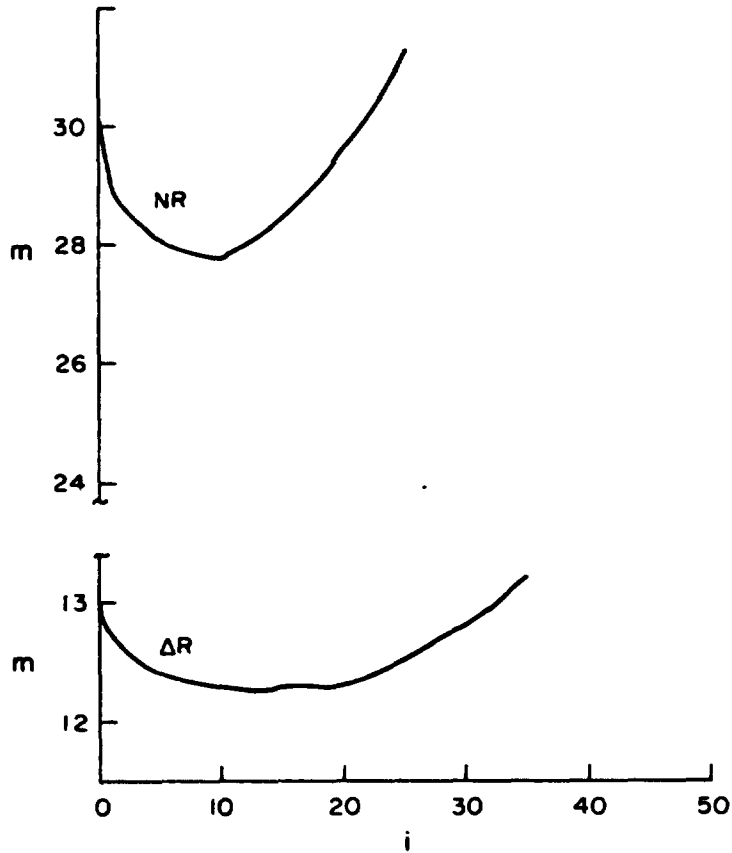
Figure 5.5

Position Error and Covariance Norm in Trial 3
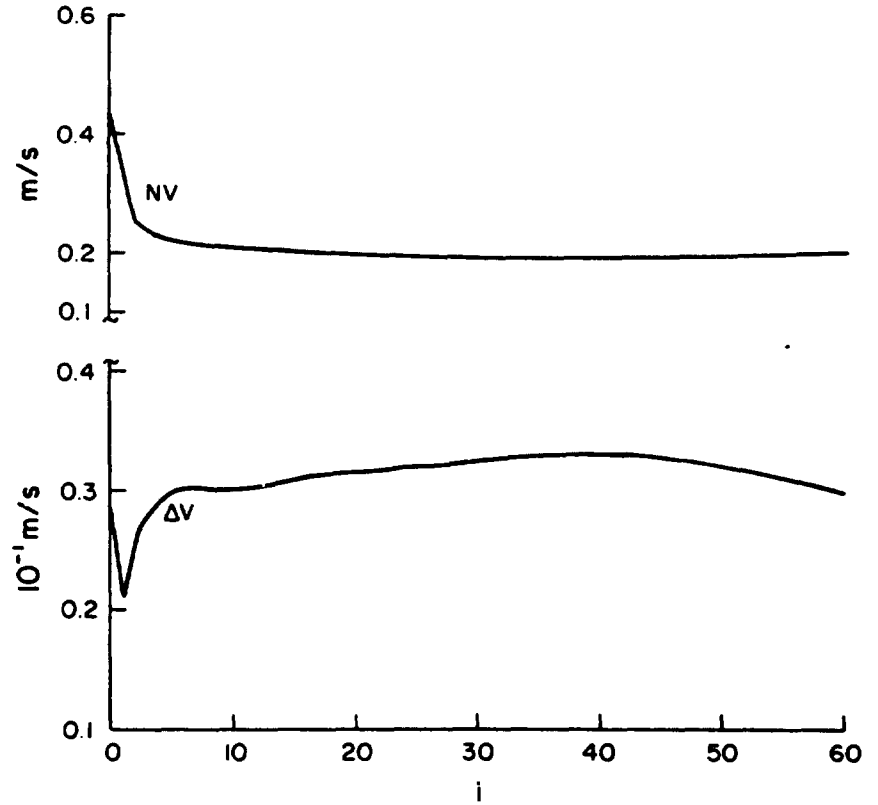
Figure 5.6

Velocity Error and Covariance Norm in Trial 3
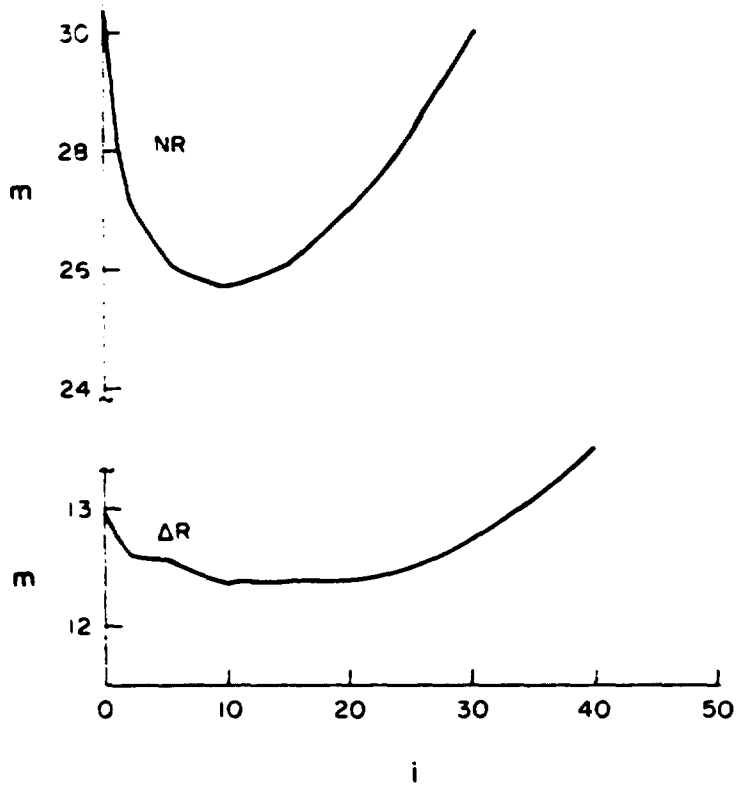
Figure 5.7

Position Error and Covariance Norm in Trial 4
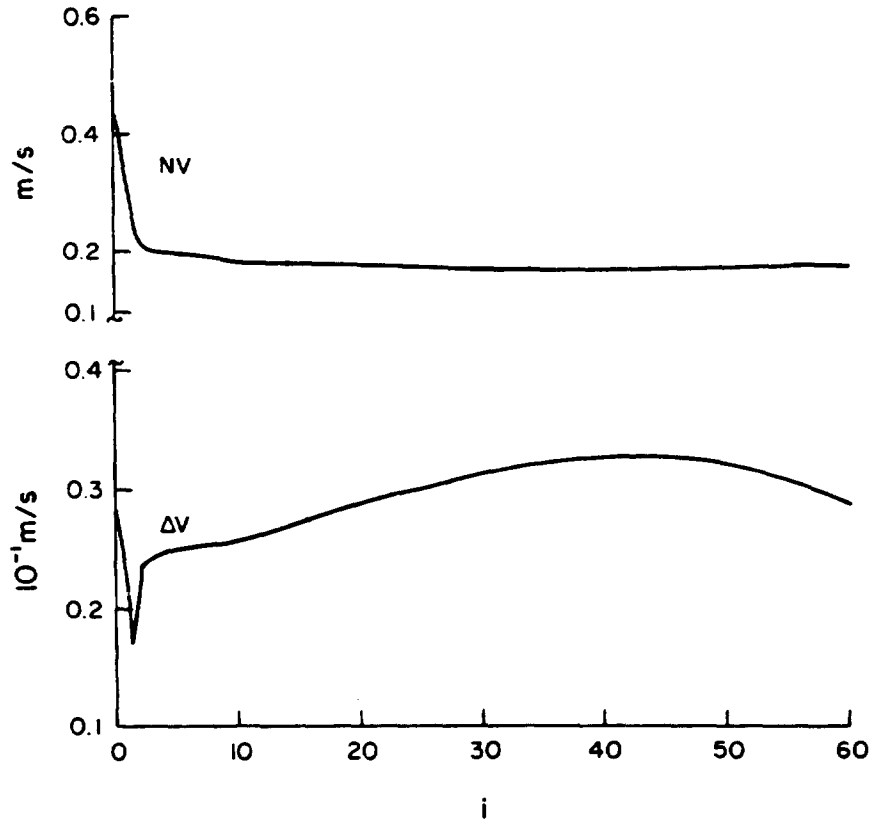
Figure 5.8

Velocity Error and Covariance Norm in Trial 4

Table 5-3

State Disturbance Components in Trial 1

Integration step i	ϵ_x 10^{-4} m/s²	ϵ_y 10^{-4} m/s²	ϵ_z 10^{-4} m/s²	$1/\beta_x$ sec	$1/\beta_y$ sec	$1/\beta_z$ sec
0	0.00	0.00	0.00	86.56	96.94	163.50
5	0.00	-0.04	0.03	86.56	96.91	163.50
10	0.00	-0.26	-0.02	86.56	97.00	163.49
15	0.01	-0.43	-0.01	86.56	98.07	163.47
20	0.01	-0.57	-0.07	86.58	100.39	163.48
25	0.02	-0.67	-0.14	86.61	103.58	163.72
30	0.03	-0.73	-0.23	86.68	106.80	164.44
35	0.03	-0.73	-0.32	86.78	109.10	165.93
40	0.04	-0.68	-0.42	86.91	109.90	168.33
45	0.04	-0.58	-0.51	87.03	109.16	171.40
50	0.04	-0.45	-0.56	87.13	107.27	174.67

Table 5-4

State Disturbance Components in Trial 2

Integration step i	ϵ_x 10^6 m/s²	ϵ_y 10^{-4} m/s²	ϵ_z 10^6 m/s²	$1/\beta_x$ sec	$1/\beta_y$ sec	$1/\beta_z$ sec
0	0.00	0.00	0.00	168.20	81.60	134.59
5	0.00	-0.03	0.02	168.20	81.61	134.59
10	0.01	-0.16	-0.01	168.19	81.65	134.59
15	0.04	-0.26	-0.02	168.21	82.43	134.56
20	0.08	-0.34	-0.07	168.30	84.10	134.60
25	0.11	-0.39	-0.13	168.56	86.34	134.89
30	0.15	-0.42	-0.19	169.06	88.52	135.62
35	0.18	-0.41	-0.26	169.79	90.03	136.90
40	0.20	-0.37	-0.32	170.65	90.50	138.67
45	0.20	-0.30	-0.37	171.46	89.93	140.71
50	0.20	-0.23	-0.40	172.05	88.58	142.71

Table 5-5

State Disturbance Components in Trial 3

Integration step i	ϵ_x 10^{-4} m/s^2	ϵ_y 10^{-4} m/s^2	ϵ_z 10^{-4} m/s^2	β_x sec	β_y sec	β_z sec
0	0.00	0.00	0.00	168.20	81.60	134.59
5	-0.01	0.10	0.02	168.20	81.63	134.59
10	0.00	0.03	-0.00	168.20	81.48	134.58
15	0.02	-0.03	-0.07	168.20	81.40	134.58
20	0.04	-0.07	-0.13	168.22	81.65	134.70
25	0.06	-0.11	-0.20	168.31	82.19	135.18
30	0.09	-0.13	-0.27	168.49	82.82	136.22
35	0.10	-0.14	-0.34	168.80	83.34	137.95
40	0.12	-0.13	-0.40	169.20	83.60	140.28
45	0.13	-0.11	-0.44	169.63	83.52	142.97
50	0.13	-0.08	-0.48	170.04	83.16	145.67

Table 5-6

State Disturbance Components in Trial 4

Integration step i	ϵ_x 10^{-4} m/s^2	ϵ_y 10^{-4} m/s^2	ϵ_z 10^{-4} m/s^2	β_x sec	β_y sec	β_z sec
0	0.00	0.00	0.00	168.20	81.60	134.59
5	0.00	-0.03	0.02	168.20	81.60	134.59
10	0.01	-0.16	-0.02	168.20	81.60	134.59
15	0.04	-0.26	-0.02	168.20	81.60	134.59
20	0.08	-0.34	-0.07	168.20	81.60	134.59
25	0.11	-0.38	-0.13	168.20	81.61	134.59
30	0.15	-0.41	-0.19	168.21	81.62	134.59
35	0.18	-0.40	-0.26	168.22	81.62	134.59
40	0.20	-0.36	-0.31	168.22	81.62	134.60
45	0.20	-0.29	-0.36	168.23	81.62	134.60
50	0.20	-0.22	-0.39	168.24	81.62	134.61

(vii) From the observations at (i) to (vi), it appears that from the point of
view of a user, the value of the state vector at optimum uncertainty of
position could be taken as the best outcome of this filtering procedure.
Specifically, in this experiment the results of the tenth integration step
would be the optimum.

(viii) From Tables 5-3 to 5-6 it can be seen that the values of β_X, β_Y, β_Z
are relatively insensitive to the filtering procedure. So it is best to
use as realistic values as possible for this procedure. On the other
hand, changes in values of β_X, β_Y, β_Z in trials 1 and 2 have not given
significantly different results.

This indicates that while it is advisable to repeat studies of this nature
occasionally to ascertain the autocovariances for all satellites, since
the autocovariance curves of the three satellites in this study are fairly
close to each other, the values based on the data analysis in Chapter 4
could be applied to other satellites as well, until studies for
other satellites are completed.

(ix) It is clear that some improvement in position and velocity is possible
with this procedure though the gain in reducing the uncertainty of position
and velocity is greater. It is, therefore, conceivable that if the software
is suitably modified the optimum state vectors for the 12 passes in experi-
ment 1 can be obtained using broadcast ephemeris and observational data.
With these optimized state vectors held fixed, the solution in experiment 1
could be repeated for improved station position recovery.

(x) It is noticed that the filter diverges within a very short time of about 20
integration steps. However, from Chapter 4 it is known that this filtering
procedure is being used with acceleration signal in Cartesian coordinate
system from consideration of available software. This signal has a posi-
tive autocovariance for only two to four minutes, and the signal compo-
nents are mutually correlated to some extent. Much better results can
be expected if the positional signal in spherical system is used, which
has a positive autocovariance up to about 20 minutes. However, the

97

feasibility of this procedure has been demonstrated. The divergence is also partly due to the weak geometry represented by three nearby stations (only about 30 km apart), coobserving a satellite at a height of about 1100 km.

(xi) As expected, the results of trial 3 with a larger observational standard deviation show a smaller improvement compared to the other trials.

(xii) Results of trial 4 are the best among the four trials.

(xiii) The signals ϵ_X, ϵ_Y, ϵ_Z can be viewed as acceleration biases associated with the specific pass of the satellite used in the experiment. It can be easily seen that if a filtering procedure as above is carried out with formulations for positional signals in a spherical system, the signals obtained would be the in-track, out-of-plane, and radial pass biases referred to in Section 3.5.2.

5.3.6 Limitations of the Filter World

For computing ΔR, the positional deviation between the estimated state and the true state of the satellite, the latter is obtained by integrating the state derived from the precise ephemeris at t_0. Ideally, the force model for this integration should be the one adopted by DMA with all its elaborations. Similarly, the nominal state should use the force model of the NAG computations.

However, due to the limitations of the software and the nonavailability of the values of the gravity field in current use by DMA and NAG in open literature, there is an inescapable mismatch between the force model in the filter world and reality.

The force model in the filter in this experiment includes the gravitational field of the earth (GEM 7 geopotential model [Lerch et al., 1975] with coefficients up to degree and order four and additional zonals up to degree six), two-body perturbations of the sun and the moon, and atmospheric drag, for both the true and the nominal state.

98

So in order to obtain realistic results, it has to be assumed that the optimum results of the filter are obtained before they are vitiated by the mismatch in the force models.

For checking the validity of this assumption, trial 4 was repeated with an integration interval of 0.05 minutes, and the positional deviation of the estimate was computed directly with respect to the corresponding precise ephemeris state vectors at integral minutes. Fig. 5.9 shows this deviation ΔR_p against the time t in intervals of one minute after t_0.
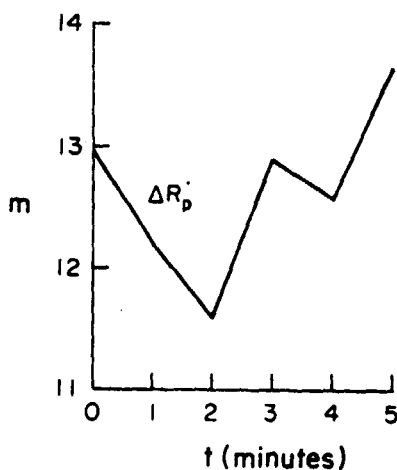
Figure 5.9

Position Error with respect to Precise Ephemeris in Trial 4

Comparing this curve with Fig. 5.7, it can be seen that there has been no adverse effect of the mismatch during the first minute in which the optimum results of the filter have been realized. The three-minute mark in Fig. 5.9 corresponds to the 40th integration step in Fig. 5.7.

99

6. CONCLUSIONS AND RECOMMENDATIONS

The objective of this study has been to investigate the possibility of locally optimizing the Navy Navigation Satellite broadcast ephemeris for improved recovery of station positions with Doppler observations.

The rank deficiency problem which is intimately connected with Doppler surveys has been studied, and it has been shown that the minimum rank deficiency in a short arc mode of survey is six and the scale information is derived from the wavelength of transmission. Coordinate differences are estimable quantities if the stations coobserve the same pass of the satellite whose motion is governed by an assumed force model.

Accuracy estimates of broadcast ephemeris have been formed from the study of sampled data. It is concluded that, depending on the location of the epoch of observation in the interinjection period, the positional uncertainty of broadcast ephemeris may vary between 19 m to 26 m in-track, 15 m to 20 m cross-track, and 9 m to 10 m in radial directions.

The broadcast ephemeris indicated a radial bias of about -5 m when compared with the precise ephemeris transformed to WGS 72 system according to the currently known transformation parameters.

The experiment in removal of radial bias along with recovery of station positions holding the orbit fixed showed that the removal of bias has a negligible effect on the uncertainties of the station coordinates. But the values of the coordinates as well as the values of other pass parameters change slightly. Removal of bias brought a chord distance in better agreement with terrestrial survey. This radial bias appears to be the consequence of the following two factors brought to light in this study:

(i) The origin of the broadcast ephemeris coordinate system appears to have an offset of about 10 m in the direction of 90°W longitude, with

100

respect to the geocenter.

(ii) The broadcast ephemeris appears to need a scale correction of -1.4 ppm to make it compatible with a terrestrial system obtainable from a scale-corrected precise ephemeris.

It is recommended that experiments be carried out with more data sets in the future to identify in-track and out-of-plane biases also. These could not be included in this study for lack of adequate evidence with the available data sets.

Sample autocovariance and autocorrelation functions of acceleration, velocity, and position signals have been computed by comparing precise and broadcast ephemerides. The curves indicate an exponential form which has been assumed for the signal stochastic process.

Satellites decay with time. So it is recommended that studies similar to this study be repeated occasionally so that the statistical characteristics of the broadcast ephemeris of all the satellites are available as they evolve with time. It is difficult to suggest the time interval at which such studies are to be repeated. In this study two data sets of the same satellite (satellite 19) were available at an interval of ten months. But the earlier data set had only about 180 values against about 1500 in the second. The same autocovariance functions derived from the two data sets do show variations which are partly due to the unequal size of the data sets. Keeping this in view, an interval of one year for repeating such studies appears reasonable.

The experiment in adaptive filtering for one pass of satellite 19, with station coordinates obtained in the earlier experiment, parameters of the auto-covariance model of acceleration signal in the Cartesian coordinate system obtained from sampled data, and simulated range rate observations, leads to the conclusion that adaptive filtering is a feasible approach from a practical point of view. The experiment indicated an orbit improvement of about 4 m in the positional uncertainty and 0.6 in position within the first 20 sequential co-observations from three-stations at intervals of 0.75 minutes. But the filter

101

diverges after giving this improvement. Positional signals in the polar system which have autocovariances which are larger and remain positive for up to about 20-minute lag are expected to give better results with this procedure. It is recommended that further studies in this respect be made.

Any satellite ephemeris derived from satellite transmission is of necessity predictive and less accurate than that of an ephemeris computed after the fact and possibly with more data (e.g., the satellites of the NAVSTAR Global Positioning System). In all such situations where sample statistics of state disturbance can be predetermined from comparison of predicted and post-fitted ephemeris, filtering procedures could be applied in conjunction with broadcast ephemeris and current observational data for local improvement of orbit.

Further studies are also recommended to study the performance of the adaptive filter with real data and a better geometry of tracking stations than three stations about 30 km apart as in this study.

As a result of this study, the following steps can be recommended for improved positioning with broadcast ephemeris and Doppler data:

(i) Correction of broadcast ephemeris for the biases identified. In this study the radial .as identified was traced to an origin shift and a scale correction.

(ii) Position determination with broadcast ephemeris and coobserved tracking data from at least three stations, holding the orbit fixed.

(iii) Local improvement of the satellite orbits for all the passes used in (ii), in an adaptive filtering procedure, using the sample autocovariance function derived from comparisons of precise and broadcast ephemerides in the recent past and the observational data.

(iv) Redetermination of positions as in (ii) with the improved orbits.

The improvement that can be achieved by this procedure can only be estimated after studying a test case with real data for steps (iii) and (iv) which is recommended as a follow-up of this study. However, this study has succeeded in indicating the feasibility of this approach.

APPENDIX A

INFLUENCE OF TRANSFORMATION PARAMETERS
ON ACCELERATION SIGNAL

The broadcast ephemeris and the precise ephemeris are in coordinate systems which differ from each other by small amounts. The following analytical study was carried out to find out to what extent the transformation parameters are likely to influence the values of acceleration signals obtained in Chapter 4.

Consider the following system of first-order differential equations for governing the true state of the satellite in the WGS 72 system of the broadcast ephemeris.

$$\dot{\overline{X}}_N = \overline{V}_N \tag{A1}$$

$$\dot{\overline{V}}_N = \overline{a}_N + \overline{\xi}_N \tag{A2}$$

where $\overline{X}_N$, $\overline{V}_N$, $\overline{a}_N$, $\overline{\xi}_N$ are the three-vectors for position, velocity, acceleration, and acceleration signal, respectively.

Similarly, consider the following system of equations for governing the state of the satellite in the NWL 9D system of the precise ephemeris, which for the purpose of this study is considered errorless:

$$\dot{\overline{X}}_p = \overline{V}_p \tag{A3}$$

$$\dot{\overline{V}}_p = \overline{a}_p \tag{A4}$$

where $\dot{\overline{X}}_p$, $\dot{\overline{V}}_p$, $\overline{a}_p$ denote the three-vectors for position, velocity and acceleration as per precise ephemeris.

It is assumed that the state vectors based on the precise and broadcast ephemeris represent a set of consistent values in their respective coordinate systems, which makes the following similarity transformation relation possible for the ith point

103

$$
\begin{bmatrix} X_N \\ Y_N \\ Z_N \end{bmatrix}_i = \begin{bmatrix} X_p \\ Y_p \\ Z_p \end{bmatrix}_i + \begin{bmatrix} \Delta X_p \\ \Delta Y_p \\ \Delta Z_p \end{bmatrix} + \begin{bmatrix} 0 & W & -\Psi \\ -W & 0 & \epsilon \\ \Psi & -\epsilon & 0 \end{bmatrix} \begin{bmatrix} X_p \\ Y_p \\ Z_p \end{bmatrix}_i + \Delta L \begin{bmatrix} X_p \\ Y_p \\ Z_p \end{bmatrix}_i
$$

$$
= \begin{bmatrix} \Delta X_p \\ \Delta Y_p \\ \Delta Z_p \end{bmatrix} + \begin{bmatrix} 1+\Delta L & W & -\Psi \\ -W & 1+\Delta L & \epsilon \\ \Psi & -\epsilon & 1+\Delta L \end{bmatrix} \begin{bmatrix} X_p \\ Y_p \\ Z_p \end{bmatrix}_i \qquad \text{(A5)}
$$

Here

$$
[X_p \quad Y_p \quad Z_p]^T = \overline{X}_p
$$

$$
[X_N \quad Y_N \quad Z_N]^T = \overline{X}_N
$$

$$
[\Delta X_p \quad \Delta Y_p \quad \Delta Z_p]^T = \overline{T}_p, \text{ the vector of translation parameters.}
$$

ΔL is the scale parameter

W, ϵ, and Ψ are the rotation parameters.

If R is the 3×3 rotation cum scale matrix, equation (A5) can be rewritten as

$$
\overline{X}_N = \overline{T}_p + R\overline{X}_p \qquad \text{(A6)}
$$

The transformation parameters are time independent, so time derivatives of (A6) yield

$$
\dot{\overline{X}}_N = R\dot{\overline{X}}_p + \dot{R}\overline{X}_p = R\dot{\overline{X}}_p \qquad \text{as } \dot{R} = 0 \qquad \text{(A7)}
$$

Therefore,

$$
\overline{V}_N = R\overline{V}_p \qquad \text{(A8)}
$$

$$
\dot{\overline{V}}_N = R\dot{\overline{V}}_p + \dot{R}\overline{V}_p = R\dot{\overline{V}}_p \qquad \text{(A9)}
$$

$$
\overline{a}_N + \overline{\xi}_N = R[\overline{a}_p] \qquad \text{(A10)}
$$

To seek the influence of transformation parameters on $\overline{\xi}_N$ signal, consider a vector

$$
\overline{U} = [\Delta L, \ W, \ \Psi, \ \epsilon]^T
$$

and differentiate (A10) with respect to the variables of interest. The left member yields, on differentiation,

104

$$\frac{\partial \overline{a}_N}{\partial \overline{\xi}_N} \, d\overline{\xi}_N + \frac{\partial \overline{a}_N}{\partial \overline{U}} \, d\overline{U} + d\overline{\xi}_N$$

considering R matrix in the element notation, the right member of (A 10) may be written

$$R[\,\overline{a}_p\,] = \begin{bmatrix} r_{11} & r_{12} & r_{13} \\ r_{21} & r_{22} & r_{23} \\ r_{31} & r_{32} & r_{33} \end{bmatrix} \overline{a}_p = \begin{bmatrix} r_{11}\,a_{p1} \\ r_{21}\,a_{p1} \\ r_{31}\,a_{p1} \end{bmatrix} + \begin{bmatrix} r_{12}\,a_{p2} \\ r_{22}\,a_{p2} \\ r_{32}\,a_{p2} \end{bmatrix} + \begin{bmatrix} r_{13}\,a_{p3} \\ r_{23}\,a_{p3} \\ r_{33}\,a_{p3} \end{bmatrix}$$

$$\equiv \overline{R}_1 + \overline{R}_2 + \overline{R}_3$$

where $\overline{R}_1$, $\overline{R}_2$, $\overline{R}_3$ stand for the corresponding vectors above. Differentiation of the right member therefore yields

$$\frac{\partial \overline{R}_1}{\partial \overline{\xi}_N} \, d\overline{\xi}_N + \frac{\partial \overline{R}_1}{\partial \overline{U}} \, d\overline{U} + \frac{\partial \overline{R}_2}{\partial \overline{\xi}_N} \, d\overline{\xi}_N + \frac{\partial \overline{R}_2}{\partial \overline{U}} \, d\overline{y} + \frac{\partial \overline{R}_3}{\partial \overline{\xi}_N} \, d\overline{\xi}_N + \frac{\partial \overline{R}_3}{\partial \overline{U}} \, d\overline{U}$$

The modeled acceleration $\overline{a}_N$ does not depend on the acceleration signal or on the transformation parameters. Therefore

$$\frac{\partial \overline{a}_N}{\partial \overline{\xi}_N} = 0 \qquad \frac{\partial \overline{a}_N}{\partial \overline{y}} = 0$$

Similarly,

$$\frac{\partial \overline{R}_1}{\partial \overline{\xi}_N} = \frac{\partial \overline{R}_2}{\partial \overline{\xi}_N} = \frac{\partial \overline{R}_3}{\partial \overline{\xi}_N} = 0$$

Therefore, differentiation of right member of (A 10) yields

$$\frac{\partial \overline{R}_1}{\partial \overline{U}} \, d\overline{U} + \frac{\partial \overline{R}_2}{\partial \overline{U}} \, d\overline{U} + \frac{\partial \overline{R}_3}{\partial \overline{U}} \, d\overline{U} =$$

$$
= \begin{bmatrix} \dfrac{\partial r_{11}}{\partial \Delta L} & \dfrac{\partial r_{11}}{\partial W} & \dfrac{\partial r_{11}}{\partial \Psi} & \dfrac{\partial r_{11}}{\partial \epsilon} \\[2mm] \dfrac{\partial r_{21}}{\partial \Delta L} & \dfrac{\partial r_{21}}{\partial W} & \dfrac{\partial r_{21}}{\partial \Psi} & \dfrac{\partial_{21}}{\partial \epsilon} \\[2mm] \dfrac{\partial r_{31}}{\partial \Delta L} & \dfrac{\partial r_{31}}{\partial W} & \dfrac{\partial r_{31}}{\partial \Psi} & \dfrac{\partial r_{31}}{\partial \epsilon} \end{bmatrix} a_{p1}\, d\overline{U} \;+
$$

$$
\begin{bmatrix} \dfrac{\partial r_{12}}{\partial \Delta L} & \dfrac{\partial r_{12}}{\partial W} & \dfrac{\partial r_{12}}{\partial \Psi} & \dfrac{\partial r_{12}}{\partial \epsilon} \\[2mm] \dfrac{\partial r_{22}}{\partial \Delta L} & \dfrac{\partial r_{22}}{\partial W} & \dfrac{\partial r_{22}}{\partial \Psi} & \dfrac{\partial r_{22}}{\partial \epsilon} \\[2mm] \dfrac{\partial r_{32}}{\partial \Delta L} & \dfrac{\partial r_{32}}{\partial W} & \dfrac{\partial r_{32}}{\partial \Psi} & \dfrac{\partial r_{32}}{\partial \epsilon} \end{bmatrix} a_{p2}\, d\overline{U} \;+
$$

$$
\begin{bmatrix} \dfrac{\partial r_{13}}{\partial \Delta L} & \dfrac{\partial r_{13}}{\partial W} & \dfrac{\partial r_{13}}{\partial \Psi} & \dfrac{\partial r_{13}}{\partial \epsilon} \\[2mm] \dfrac{\partial r_{23}}{\partial \Delta L} & \dfrac{\partial r_{23}}{\partial W} & \dfrac{\partial r_{23}}{\partial \Psi} & \dfrac{\partial r_{23}}{\partial \epsilon} \\[2mm] \dfrac{\partial r_{33}}{\partial \Delta L} & \dfrac{\partial r_{33}}{\partial W} & \dfrac{\partial r_{33}}{\partial \Psi} & \dfrac{\partial r_{33}}{\partial \epsilon} \end{bmatrix} a_{p3}\, d\overline{U}
$$

$$
= \begin{bmatrix} 1 & 0 & 0 & 0 \\ 0 & -1 & 0 & 0 \\ 0 & 0 & 1 & 0 \end{bmatrix} a_{p1}\, d\overline{U} \;+\; \begin{bmatrix} 0 & 1 & 0 & 0 \\ 1 & 0 & 0 & 0 \\ 0 & 0 & 0 & -1 \end{bmatrix} a_{p2}\, d\overline{U} \;+
$$

$$
+\; \begin{bmatrix} 0 & 0 & -1 & 0 \\ 0 & 0 & 0 & 1 \\ 1 & 0 & 0 & 0 \end{bmatrix} a_{p3}\, d\overline{U}
$$

Therefore,

$$
d\overline{\xi}_N \quad \begin{bmatrix} a_{p1} & a_{p2} & -a_{p3} & 0 \\ a_{p2} & -a_{p1} & 0 & a_{p3} \\ a_{p3} & 0 & a_{p1} & -a_{p2} \end{bmatrix} d\overline{U} \tag{A 11}
$$

In this study, the $\overline{U}$ vector has the following values for the components

$$\Delta L \quad = \quad -0.826 \ 3 \ ppm$$

$$W \quad = \quad -0.000 \ 001 \ 260 \ 5 \ radian$$

$$\Psi \quad = \quad 0$$

$$\epsilon \quad = \quad 0$$

At the satellite altitude of about 1000 km, the approximate value of normal gravity is 743.4 gals. Considering this value and even the full values of the $\overline{U}$ vector, the maximum component of $d\xi_N$ is of the order $0.15 \times 10^{-6} \ m/s^2$, which is negligible compared to the signals of the order of $0.3 \times 10^{-3} \ m/s^2$ obtained in the study.

It may, therefore, be concluded that the transformation parameters have had an insignificant role in causing the acceleration signals.

This was also verified numerically by obtaining acceleration signals in two models in a test case:

(i) by comparing broadcast and precise ephemeris without transformation,

(ii) by comparing broadcast and precise ephemeris after transformation.

Considering acceleration in units of m/s^2, the RMS values of the signals in (i) and (ii) are generally in agreement up to the fifth decimal place of a meter.

APPENDIX B

FIRST ORDER FILTERING TECHNIQUE

1. Systems Equation

The true equations of motion for the satellite are expressed in the earth-centered inertial coordinate system. The equations take the functional form of a system of first-order deterministic differential equations (i.e., without the inclusion of state noise):

$$\dot{\bar{r}} = \bar{v}$$
$$\dot{\bar{v}} = \bar{a}(\bar{r}, \bar{v}, t) \tag{B1}$$

where $\bar{r}$ with components (X, Y, Z) and $\bar{v}$ with components $(\dot{X}, \dot{Y}, \dot{Z})$ are three vectors used in defining the true state $\bar{X}$, an n-vector which is to be estimated. For example, if the state vector were to consist of only position and velocity components, then $n = 6$, and

$$\bar{X}^T = [X \ Y \ Z \ \dot{X} \ \dot{Y} \ \dot{Z}]^T = [\bar{r}^T \ \bar{v}^T]$$

$\bar{a}$ is the true acceleration vector. Equation (B1) can also be written in a functional form as

$$\dot{\bar{X}} = F(\bar{X}, t) \tag{B2}$$

where F represents the n-dimensional functional form of the right side of the equations (B1).

Now, if a state noise n-vector $\overline{W}(t)$ is also included in the equation, the differential equation will take the form

$$\dot{\overline{X}} = F(\overline{X}, \overline{W}, t) \tag{B3}$$

For seeking a solution, a nominal state $\overline{X}^*(t)$ is first assumed, and a differential state deviation is considered in the form:

$$\overline{x}(t) = \overline{X}(t) - \overline{X}^*(t) \tag{B4}$$

$$\dot{\overline{x}}(t) = \dot{\overline{X}}(t) - \dot{\overline{X}}^*(t) \tag{B5}$$

State relation (B3) can now be expanded by a Taylor series around $\overline{X}^*(t)$ giving the linearized first-order differential equation

$$\dot{\overline{x}}(t) = A(t)\,\overline{x}(t) + G(t)\,\overline{W}(t) \tag{B6}$$

which corresponds to the equation given in (4.1) [Ingram, 1971; Tapley et al., 1972]. Here

$$A = \left[\frac{\partial F}{\partial \overline{X}}\right]^* \qquad G = \left[\frac{\partial F}{\partial \overline{W}}\right]^*$$

are the $n \times n$ matrices of partial derivatives evaluated at the nominal values $\overline{X}^*(t)$.

Equation (B6) represents the state of the system (in this case the parameters associated with the satellite orbit) for $t > t_o$, where the initial time t_o is fixed and the initial state $\overline{X}(t_o)$ is assumed known.

2. Concept of the State Transition Matrix

In many problems a representation in terms of the so-called state transition matrix helps to obtain an explicit expression for the solution of equation (B6). Since the system in (B6) is linear, its complete solution

consists of a linear combination of its homogeneous (or force-free solution) and a particular (or forced) solution.

Consider first the homogeneous solution of the system

$$\dot{\overline{x}}(t) = A(t)\,\overline{x}(t) \tag{B7}$$

for $t \geq t_0$ with $\overline{x}(t_0)$ arbitrary. Substitute into (B7) a trial solution of the form

$$\overline{x}(t) = M(t)\,\overline{x}(t_0)$$

where $M(t)$ is an unknown $n \times n$ matrix. This yields

$$[\dot{M} - A(t)\,M]\,\overline{x}(t_0) = 0 \tag{B8}$$

which must hold for all $t \geq t_0$. Since $\overline{x}(t_0)$ is arbitrary, this relation is satisfied if and only if $M(t)$ satisfies the system of $n \times n$ differential equations

$$\dot{M} = A(t)\,M \tag{B9}$$

for all $t \geq t_0$. Further, at $t = t_0$, $\overline{x}(t_0) = M(t_0)\,\overline{x}(t_0)$ which implies that $M(t_0) = I$ is the initial condition for (B9). The homogeneous solution of equation (B6) can then be written as

$$\overline{x}(t) = M(t)\,\overline{x}(t_0) \tag{B10}$$

where

$$\dot{M} = A(t)\,M \qquad \text{and} \qquad M(t_0) = I$$

The particular solution for (B6) is next obtained by using the Lagrange variation of parameter technique. Assume a solution of the form

$$\overline{x}(t) = M(t)\,\overline{l}(t) \tag{B11}$$

where $M(t)$ is as above, and $\overline{l}(t)$ is an unknown n vector. Substituting this result in (B6)

$$\dot{M}(t)\,\overline{l}(t) + M(t)\,\dot{\overline{l}}(t) = A(t)\,M(t)\,\overline{l}(t) + G(t)\,\overline{W}(t) \tag{B12}$$

However, since $\dot{M}(t) = A(t)\,M(t)$, (B12) reduces to

$$M(t)\,\dot{\overline{l}}(t) = G(t)\,\overline{W}(t) \tag{B13}$$

110

It can be verified that M(t) is nonsingular for all $t \geq t_0$ [Meditch, 1969].
Therefore,

$$\dot{\bar{I}}(t) = M^{-1}(t) \, G(t) \, \overline{W}(t) \tag{B14}$$

Integrating (B14),

$$\overline{I}(t) = \int_{t_0}^{t} M^{-1}(\tau) \, G(\tau) \, \overline{W}(\tau) \, d\tau \tag{B15}$$

Therefore, the particular solution of (B6) can be taken as

$$\overline{x}(t) = M(t) \int_{t_0}^{t} M^{-1}(\tau) \, G(\tau) \, \overline{W}(\tau) \, d\tau \tag{B16}$$

Combining (B10) and (B16), the complete solution of (B6) will have the form

$$\overline{x}(t) = M(t) \, \overline{x}(t_0) + M(t) \int_{t_0}^{t} M^{-1}(\tau) \, G(\tau) \, \overline{W}(\tau) \, d\tau \tag{B17}$$

where the second part of the right member can be viewed as the contribution of the state noise to the state.

M(t) is called the fundamental matrix of the system in (B6). Now define

$$\Phi(t, \tau) = M(t) \, M^{-1}(\tau) \tag{B18}$$

the $n \times n$ transition matrix for the system in (B6). It is noted that

$$\Phi(t, t_0) = M(t) \, M^{-1}(t_0) = M(t)$$

since $M^{-1}(t_0) = I$. Thus the complete solution (B17) can be written in transition matrix form as

$$\overline{x}(t) = \Phi(t, t_0) \, \overline{x}(t_0) + \int_{t_0}^{t} \Phi(t, \tau) \, G(\tau) \, \overline{W}(\tau) \, d\tau \tag{B19}$$

where $t \geq t_0$. (B18) is differentiated with respect to t

111

$$\frac{\partial \Phi(t, \tau)}{\partial t} = \dot{M}(t) M^{-1}(\tau) = A(t) M(t) M^{-1}(\tau)$$

Therefore,

$$\dot{\Phi}(t, \tau) = A(t) \Phi(t, \tau) \tag{B 20}$$

where differentiation with respect to t is implied. From (B 18)

$$\Phi(t, t) = I, \qquad \text{for } t \geq t_0.$$

So, to obtain $\Phi(t, \tau)$ required in the computation of x (t) in (B 19), the differential equation

$$\dot{\Phi}(t, t_0) = A(t) \Phi(t, t_0)$$

is solved subject to initial condition $\Phi(t_0, t_0) = I$ and t_0 is replaced by τ to obtain $\Phi(t, \tau)$.

3. Observation – State Relation

The equation relating observations and the state in a linearized observation equation form can be expressed as

$$\overline{y}(t) = H(t) \overline{x}(t) + \overline{V}(t) \tag{B 21}$$

where $\overline{y}(t)$ is the p vector of observations in the differential form (observed – computed). H is the p $\times$ n design matrix of the conventional observation equation model [Uotila, 1967]. $\overline{x}(t)$, the deviation of the state from the nominal, can also be viewed as the unknown corrections to the assumed values of the state. $\overline{V}(t)$ is the p vector of observational errors.

Substituting the expression for $\dot{\overline{x}}(t)$ from (B 19),

$$\overline{y}(t) = H(t) \left[\Phi(t, t_0) \overline{x}(t_0) + \int_{t_0}^{t} \Phi(t, \tau) G(\tau) \overline{W}(\tau) d\tau \right] + \overline{V}(t)$$

$$= H(t) \Phi(t, t_0) \overline{x}(t_0) + \int_{t_0}^{t} H(t) \Phi(t, \tau) G(\tau) \overline{W}(\tau) d\tau + \overline{V}(t)$$

Defining

$$D(t, \tau) = H(t) \Phi(t, \tau) G(\tau),$$

$$\bar{y}(t) = H(t) \Phi(t, t_0) \bar{x}(t_0) + \int_{t_0}^{t} D(t, \tau) \overline{W}(\tau) \, d\tau + \overline{V}(t) \qquad (B\,22)$$

Often the noise vector $\overline{W}(t)$ is considered as input, the observable $\bar{y}(t)$ as output, and the matrix $D(t, \tau)$ as a system weighting function, in the literature.

4. Sampled Data Model

Although the evolution of state is continuous in time, observations are generally available only at discrete times. The study of the effect of noise is also facilitated if the system is discretized and the continuous relations in a system are treated as limiting cases of discrete forms.

Assuming that the disturbance or "noise" vector in equation (B 6) is a piece-wise constant function of time which changes values at time points at which measurements are also made, a time interval $t_k \le t \le t_{k+1}$ is considered for some $k = 0, 1, \ldots$. If $\bar{x}(t_k)$ is given and $\overline{W}(t) = \overline{W}(k)$ — constant, in the interval $t_k \le t \le t_{k+1}$, from (B 19):

$$\bar{x}(t_{k+1}) = \Phi(t_{k+1}, t_k) \bar{x}(t_k) + \left[\int_{t_k}^{t_{k+1}} \Phi(t_{k+1}, \tau) G(\tau) \, d\tau \right] \overline{W}(k) \qquad (B\,23)$$

Defining

$$\int_{t_k}^{t_{k+1}} \Phi(t_{k+1}, \tau) G(\tau) \, d\tau = \Gamma(k+1, k)$$

as the disturbance transition matrix, and denoting

$$\bar{x}(t_{k+1}) \qquad \bar{x}(k+1)$$

$$\bar{x}(t_k) \qquad \bar{x}(k)$$

$$\Phi(t_{k+1}, t_k) \qquad \Phi(k+1, k)$$

113

(B 23) can be written as

$$\overline{x}(k+1) = \Phi(k+1, k)\, \overline{x}(k) + \Gamma(k+1, k)\, \overline{W}(k) \qquad (B24)$$

for $k = 0, 1, \ldots$.

The observation state relation (B 21) can also be written in the discretized form as

$$\overline{y}(t_{k+1}) = H(t_{k+1})\, \overline{x}(t_{k+1}) + \overline{V}(t_{k+1})$$

or

$$\overline{y}(k+1) = H(k+1)\, \overline{x}(k+1) + \overline{V}(k+1) \qquad (B25)$$

It is easy to see that the continuous case can be considered as a limiting case of the above discrete model by denoting discrete time (k) and (k+1) as (t) and (t+Δt) and letting $\Delta t \to 0$.

5. Nature of Gaussian White Process

The nature of Gaussian white process in system dynamics will be first considered. Let $\{\overline{W}(t),\ t \geq t_0 \}$ be an n-dimensional independent Gaussian process with mean

$$E[\overline{W}(t)] = \overline{W}_m(t)$$

and covariance kernel

$$E\{[\overline{W}(t) - \overline{W}_m(t)][\overline{W}(\tau) - \overline{W}_m(\tau)]^T\} = Q(t)\, \delta(t-\tau)$$

where t_0 is an initial time, $t, \tau \geq t_0$, $Q(t)$ is a continuous positive semi-definite n × n matrix, and $\delta(t-\tau)$ the Dirac delta function.

The above equation implies the limiting behavior of a piece-wise constant Gaussian white sequence in which the frequency of event points is made arbitrarily large within a given time interval.

Consider sequences $\{\overline{W}(k), k = 0, 1, \ldots \}$ to be zero mean Gaussian white with covariance

$$E[\overline{W}(j)\, \overline{W}^T(k)] = Q(k)\, \delta_{jk}, \quad k = 0, 1, \ldots$$

114

and successive time points separated by $\Delta t > 0$. If t denotes continuous time, t_0 corresponds to $k = 0$, and t_1 corresponds to $k = n$,

$$t_1 = t_0 + n \Delta t$$

For given value of n, let $\{ \overline{W}^{(n)}(t), \ t_0 \leq t \leq t_1 \}$ denote a piece-wise constant Gaussian white sequence. Keeping t_1 fixed while increasing n such that $n \Delta t = t_1 - t_0$ is constant, the nature of $\{ W^{(n)}(t), \ t_0 \leq t \leq t_1 \}$ as $n \to \infty$ and $\Delta t \to 0$ is considered.

As proved in [Meditch, 1969], the Gaussian white process

$$\{ \overline{W}(t), \ t_0 \leq t \leq t_1 \} = \lim_{n \to \infty} \{ \overline{W}^{(n)}(t), \ t_0 \leq t \leq t_1 \}$$

as described above, where the covariance matrix $Q(t_0 + i \Delta t) = Q(i)$, $i = 0, 1, \ldots, n-1$, is to be replaced by $Q(t)/\Delta t$ in taking limits where t corresponds to the time point i and $Q(t) = Q(i)$. Then $\lim_{\Delta t \to 0} \dfrac{Q(t)}{\Delta t}$ is understood in the sense that the quantity dealt with is defined over an interval of width Δt, and in the limit as $\Delta t \to 0$, the function which is $1/\Delta t$ over the interval Δt and zero elsewhere becomes the dirac delta function, giving

$$E \{ [\overline{W}(t) - \overline{W}_m(t)] [\overline{W}(\tau) - \overline{W}_m(\tau)]^{\tau} \} = Q(t) \delta(t - \tau)$$

for all $t, \tau \geq t_0$.

6. Probabilistic Description of System Dynamics

The probabilistic nature of state noise and its constribution to the evolution of the state makes the study of probabilistic description of the state model imperative.

6.1 Evolution of State in Presence of White Noise

As indicated earlier, equation (B.24) can be rewritten in the form

$$\overline{x}(t+\Delta t) \;=\; \Phi(t+\Delta t,\, t)\,\overline{x}(t) + \int_{t}^{t+\Delta t} \Phi(t+\Delta t,\, \tau)\, G(\tau)\, \overline{W}(\tau)\, d\tau \;=\;$$

$$=\; \Phi(t+\Delta t,\, t)\,\overline{x}(t) + \Gamma(t+\Delta t,\, t)\,\overline{W}(t) \tag{B 26}$$

under the assumption that $\overline{W}(\tau) = \overline{W}(t) = $ constant for $t \le \tau < t+\Delta t$. Treating the noise process $\{\overline{W}(\tau),\ t \le \tau \le t + \Delta t\}$ to be the limit of a sequence, as described above, $\overline{W}(t)$ in (B 26) can be replaced by a member of the sequence $\overline{W}^{(n)}(t)$. Further, $\Phi(t+\Delta t,\, t)$ expanded around t in a Taylor series up to linear terms yields

$$\Phi(t+\Delta t,\, t) \;=\; \Phi(t,\, t) + \dot{\Phi}(t,\, t)\,\Delta t \;=\; I + A(t)\,\Delta t \tag{B 27}$$

Also,

$$\Gamma(t+\Delta t,\, t) \;=\; \int_{t}^{t+\Delta t} \Phi(t+\Delta t,\, \tau)\, G(\tau)\, d\tau \;=\; G(t)\,\Delta t \tag{B 28}$$

With these simplifications, equation (B 26) can be written as

$$\overline{x}(t+\Delta t) \;=\; [\,I + A(t)\,\Delta t\,]\,\overline{x}(t) + G(t)\,\overline{W}^{(n)}(t)\,\Delta t$$

This can further be written in the form of a difference equation as

$$\overline{x}(t+\Delta t) - \overline{x}(t) \;=\; A(t)\,\overline{x}(t)\,\Delta t + G(t)\,\overline{W}^{(n)}(t)\,\Delta t \tag{B 29}$$

Now let $\overline{W}(t)$ be a Gaussian white process with the mean $E\{\overline{W}(t)\} = \overline{W}_m(t)$ and covariance kernel

$$E\left\{ [\,\overline{W}(t) - \overline{W}_m(t)\,]\,[\,\overline{W}(\tau) - \overline{W}_m(\tau)\,]^{\tau} \right\} \;=\; Q(t)\,\delta(t-\tau) \tag{B 30}$$

where $Q(t)$ is a continuous semidefinite $n \times n$ matrix, and $\delta(t - \tau)$ the dirac delta function. Now dividing (B 29) by Δt, and taking the limit $\Delta t \to 0$, leads to the continuous linear system

$$\dot{\overline{x}} \;=\; A(t)\,\overline{x} + G(t)\,\overline{W}(t) \tag{B 31}$$

Now let $\overline{x}(t_0)$ be a Gaussian random n vector which is independent of $\{\overline{W}(t),\ t \ge t_0\}$ and has mean $\overline{x}_m(t_0)$ and positive semidefinite $n \times n$ covariance matrix

$$E\left\{\left[\,\overline{x}(t_0) - \overline{x}_m(t_0)\right]\left[\,\overline{x}(t_0) - \overline{x}_m(t_0)\right]^\top\right\} = P(t_0) \tag{B 32}$$

As a consequence of the assumption of independence,

$$E\left\{\left[\,\overline{x}(t_0) - \overline{x}_m(t_0)\right]\left[\,\overline{W}(t) - \overline{W}_m(t)\right]^\top\right\} = 0 \tag{B 33}$$
$$\text{for all } t \geq t_0.$$

To examine the nature of $\{\overline{x}(t),\ t \geq t_0\}$, the solution of (B 31) can be written as

$$\overline{x}(t_m) = \Phi(t_m, t_{m-1})\,\overline{x}(t_{m-1}) + \int_{t_{m-1}}^{t_m} \Phi(t_m, \tau)\,G(\tau)\,\overline{W}(\tau)\,d\tau \tag{B 34}$$

Thus, for $t_m > t_{m-1} \geq t_0$, the probability law describing the process $\overline{x}(t)$ in the future (i.e., at time t_m) depends only on the present value the process assumes (i.e., at t_{m-1}) and is completely independent of the behavior of the process in the past. Therefore, the process $\overline{x}(t)$ is a Markov process.

Further, if $\overline{x}(t_0)$ is a Gaussian random n vector, then it can be deduced that

$$\overline{x}^{(n)}(t), \qquad n = 1, 2, \ldots$$

is also a Gaussian random vector [Meditch, 1969]. Thus $\overline{x}(t)$ is a Gauss-Markov process. Taking expectations of (B 31),

$$\dot{\overline{x}}_m = E\{\dot{\overline{x}}\} = A(t)\,\overline{x}_m + G(t)\,\overline{W}_m(t) \tag{B 35}$$

for $t \geq t_0$ and subject to initial condition $\overline{x}(t_0)$.

6.2 Evolution of State Covariance Matrix in Presence of White Noise

An expression is now obtained for

$$P(t) \quad E\left\{\left[\,\overline{x}(t) - \overline{x}_m(t)\right]\left[\,\overline{x}(t) - \overline{x}_m(t)\right]^\top\right\}$$

From (B 26)

$$\overline{x}(k+1) \quad \Phi(k+1, k)\,\overline{x}(k) + \Gamma(k+1, k)\,\overline{W}(k) \tag{B 23}$$

from which it is clear that

$$\overline{x}(j+1) \quad \Phi(j+1, j)\,\overline{x}(j) + \Gamma(j+1, j)\,\overline{W}(j) \tag{B 36}$$

117

and

$$\overline{x}(j+2) = \Phi(j+2, j+1) \overline{x}(j+1) + \Gamma(j+2, j+1) \overline{W}(j+1)$$

Therefore,

$$\overline{x}(j+2) = \Phi(j+2, j+1) [\Phi(j+1, j) \overline{x}(j) + \Gamma(j+1, j) \overline{W}(j)] +$$
$$+ \Gamma(j+2, j+1) \overline{W}(j+1)$$
$$= \Phi(j+2, j) \overline{x}(j) + \sum_{i=j+1}^{j+2} \Phi(j+2, i) \Gamma(i, i-1) \overline{W}(i-1) \tag{B 37}$$

Following the above recursive relation,

$$\overline{x}(k) = \Phi(k, j) \overline{x}(j) + \sum_{i=j+1}^{k} \Phi(k, i) \Gamma(i, i-1) W(i-1) \tag{B 38}$$

It is clear that for $\overline{W}(i-1)$, $i = 1, \ldots, k$, Gaussian, $\overline{x}(k)$ is Gauss-Markov. From (B 26), taking expectations,

$$\overline{x}_m(k+1) = \Phi(k+1, k) \overline{x}_m(k) + \Gamma(k+1), k) \overline{W}_m(k) \tag{B 39}$$

for $k \in I$, the set of integers. If $\overline{x}_m(0)$ and $\overline{W}_m(k)$, $k \in I$ are given, (B 39) becomes a recursive relation for the mean of the sequence. Now

$$P(k+1) = E \{ [\overline{x}(k+1) - \overline{x}_m(k+1)] [\overline{x}(k+1) - \overline{x}_m(k+1)]^T \}$$
$$= E (\{ \Phi(k+1, k) [\overline{x}(k) - \overline{x}_m(k)] + \Gamma(k+1, k) [\overline{W}(k) - \overline{W}_m(k)] \}$$
$$\{ \Phi(k+1, k) [\overline{x}(k) - \overline{x}_m(k)] + \Gamma(k+1, k) [\overline{W}(k) - \overline{W}_m(k)] \}^T)$$
$$= \Phi(k+1, k) P(k) \Phi^T(k+1, k) + \Phi(k+1, k) E \{ [\overline{x}(k) - \overline{x}_m(k)]$$
$$[\overline{W}(k) - \overline{W}_m(k)]^T \} \Gamma^T(k+1, k) + \Gamma(k+1, k) E \{ [\overline{W}(k) - \overline{W}_m(k)]$$
$$[\overline{x}(k) - \overline{x}_m(k)]^T \} \Phi^T(k+1, k) + \Gamma(k+1, k) Q(k) \Gamma^T(k+1, k) \tag{B 41}$$

To evaluate the middle terms in the above, (B 39) is subtracted from (B 26) to give

$$\overline{x}(k+1) - \overline{x}_m(k+1) = \Phi(k+1, k) [\overline{x}(k) - \overline{x}_m(k)] +$$
$$+ \Gamma(k+1, k) [\overline{W}(k) - \overline{W}_m(k)] \tag{B 42}$$

118

Let

$$\widetilde{x}(k) = \overline{x}(k) - \overline{x}_a(k) \qquad \text{and} \qquad \widetilde{W}(k) = \overline{W}(k) - \overline{W}_a(k)$$

Then

$$\widetilde{x}(k+1) = \Phi(k+1, k)\,\widetilde{x}(k) + \Gamma(k+1, k)\,\widetilde{W}(k) \quad \text{for } k = 0, 1, \ldots$$

Setting $j = 0$ in equation (B 38),

$$\overline{x}(k) = \Phi(k, 0)\,\overline{x}(0) + \sum_{i=1}^{k} \Phi(k, i)\,\Gamma(i, i-1)\,\overline{W}(i-1) \qquad \text{(B 43)}$$

In analogy to (B 43)

$$\widetilde{x}(k) = \Phi(k, 0)\,\widetilde{x}(0) + \sum_{i=1}^{k} \Phi(k, i)\,\Gamma(i, i-1)\,\widetilde{W}(i-1)$$

and, therefore,

$$E[\widetilde{x}(k)\,\widetilde{W}^{\mathsf{T}}(k)] = \Phi(k, 0)\,E[\widetilde{x}(0)\,\widetilde{W}^{\mathsf{T}}(k)] +$$

$$+ \sum_{i=1}^{k} \Phi(k, i)\,\Gamma(i, i-1)\,E[\widetilde{W}(i-1)\,\widetilde{W}^{\mathsf{T}}(k)]$$

$\widetilde{W}(k)$, $k = 0, 1, \ldots$ is a zero mean Gaussian white sequence independent of the zero mean Gaussian random n vector $\widetilde{x}(0)$, i.e.,

$$E[\widetilde{x}(k)\,\widetilde{W}^{\mathsf{T}}(k)] = 0$$

and

$$E[\widetilde{W}(i-1)\,\widetilde{W}^{\mathsf{T}}(k)] = 0, \qquad i-1 \neq k$$

Therefore, reverting to (B 41)

$$P(k+1) = \Phi(k+1, k)\,P(k)\,\Phi^{\mathsf{T}}(k+1, k) +$$

$$+ \Gamma(k+1, k)\,Q(k)\,\Gamma^{\mathsf{T}}(k+1, k) \qquad \text{for } k = 0, 1, \ldots$$
$$\text{(B 44)}$$

This equation gives the evolution of the covariance matrix for the discrete version of the stochastic process.

If t corresponds to time point k and $t+\Delta t$ to $k+1$ with $\Delta t > 0$, and considering that the analog of Q(k) for the continuous case needs to be obtained as $Q(t)/\Delta t$ [Meditch, 1969], we have

$$P(t+\Delta t) = \Phi(t+\Delta t,\ t)\ P(t)\ \Phi^\tau(t+\Delta t,\ t) +$$
$$+ \Gamma(t+\Delta t,\ t)\ \frac{Q(t)}{\Delta t}\ \Gamma^\tau(t+\Delta t,\ t)$$

Substituting for $\Phi(t+\Delta t,\ t)$ and $\Gamma(t+\Delta t,\ t)$ and expanding as in equations (b 27) and (B 28),

$$P(t+\Delta t) = [I+A(t)\Delta t]\ P(t)\ [I+A(t)\Delta t]^\tau + [G(t)\Delta t]\ \frac{Q(t)}{\Delta t}\ [G(t)\Delta t]^\tau =$$
$$= P(t) + A(t)\ P(t)\Delta t + P(t)\ A^\tau(t)\Delta t$$
$$+ G(t)\ Q(t)\ G^\tau(t)\ \Delta t$$

Transposing P(t) to the left and taking the limit as $\Delta t \to 0$ gives the matrix differential equation

$$\dot{P} = A(t)P + PA^\tau(t) + G(t)\ Q(t)\ G^\tau(t) \qquad \text{for} \quad t \geq t_0 \qquad (B\,45)$$

with the initial condition $P(t_0)$. This equation describes how uncertainty propagates in the system dynamics. The solution of this is of the form

$$P(t) = \Phi(t,\ t_0)\ P(t_0)\ \Phi^\tau(t,\ t_0) + \int_{t_0}^{t} \Phi(t,\ \tau)\ G(\tau)\ Q(\tau)\ G^\tau(\tau)\ \Phi^\tau(t,\ \tau)\,d\tau$$
$$(B\,46)$$

Equation (B 46) is not of much use in the numerical computation of P(t) in general, as $\Phi(t,\ \tau)$ needs to be determined first. The numerical integration of (B 45) is preferred to evaluate P(t). The last term in the right member of (B 46) represents the contribution of state noise to P(t).

7. Probabilistic Description of Measurements

Recalling the observation state relation in the form

$$\overline{y}(t) = H(t)\ \overline{x}(t) + \overline{V}(t) \qquad \text{for } t \geq t_0 \qquad (B\,47)$$

as in normal adjustment procedures, it is assumed that the measurement error $\overline{V}(t)$, $t \geq t_0$ is p-dimensional white noise with $E\{\overline{V}(t)\} = 0$ and has covariance

$$E\{[\overline{V}(t)][\overline{V}(\tau)]^\tau\} = R(t)\,\delta(t-\tau) \quad \text{for all } t, \tau \geq t_0 \tag{B48}$$

$R(t)$ is continuous and positive definite.

8. Classical Sequential Estimation

With the mathematical details given above, the next step is to take up the problem of estimation. The models used in the experiment are special cases of the formulations studied above. In classical sequential estimation, noise is compensated for only as indicated in Section 4.1, and no effort is made to model the parameters of the state noise. This estimation procedure has been given here though not used specifically in this study since the procedure for adaptive filtering follows from this procedure and clarifies the concepts underlying the Kalman filter algorithms.

With $G(t)$ taken as an identity matrix, the linear first-order differential equation for the state deviation in (B6) becomes

$$\dot{\overline{x}}(t) = A(t)\,\overline{x}(t) + \overline{W}(t) \tag{B49}$$

It is assumed that $t \geq t_0$, the initial state $\overline{x}(t_0) = \overline{x}_0$, and the state noise $\overline{W}(t)$ is an n-vector with the properties

$$E\{\overline{W}(t)\} = 0, \qquad E\{\overline{W}(t)\,\overline{W}(s)^\tau\} = Q(t)\,\delta(t-s)$$

where $Q(t)$ is the known $n \times n$ covariance matrix of state noise. $\overline{X}_0$ will not be perfectly known, and consequently the true solution $\overline{X}(t)$ will differ from the nominal solution $\overline{X}^*(t)$ obtained with a specified initial state $\overline{X}_0^*$. As a result, observations are taken to improve the estimate of $\overline{X}(t)$.

The observation vector $\overline{Y}_i$, at discrete times t_i, is related to the state by the functional form $\overline{Y}_i = O(\overline{X}_i, t_i) + \overline{V}_i$, $i = 1, \ldots, k-1, k$. $\overline{V}_i$ is the p-vector of observation errors with properties

$$E\{\overline{V}_i\} = 0 \qquad E\{\overline{V}_i\overline{V}_j^\top\} = R_i \delta_{ij} \qquad E\{\overline{X}(t_i)\overline{V}_j^\top\} = 0$$

R_i is a positive definite matrix which is assumed to be known. Linearization around the computed observation with respect to the nominal state $\overline{X}^*(t)$, yields the linear form

$$\overline{y}_i(t) = H_i \overline{x} + \overline{V}_i \qquad (B\,50)$$

where

$$H_i = \left(\frac{\partial O}{\partial \overline{X}_i}\right)_{\overline{X}_i^*}$$

which corresponds to equation (B 47) given earlier.

The solution of (B 49) as seen from equation (B 34) is of the form

$$\overline{x}(t) = \Phi(t, t_0)\,\overline{x}(t_0) + \int_{t_0}^{t} \Phi(t, \tau)\,\overline{W}(\tau)\,d\tau \qquad (B\,51)$$

To commence the estimation, say, from a discrete time t_{k-1}, the nominal state $\overline{X}^*(t_{k-1})$ and estimate of deviation $\hat{\overline{x}}(t_{k-1})$ are provided at time t_{k-1}, along with an associated $n \times n$ conditional covariance matrix of the state

$$\hat{P}_{k-1} = E\{(\overline{X}_{k-1} - \hat{\overline{X}}_{k-1})(\overline{X}_{k-1} - \hat{\overline{X}}_{k-1})^\top \mid \overline{Y}_{k-1}\} \qquad (B\,52)$$

where $\overline{Y}_{k-1}$ implies conditioning on all observations from $\overline{Y}_1$ through $\overline{Y}_{k-1}$. With this understanding $\hat{P}_{k-1}$ can be denoted by $\hat{P}(k-1/k-1)$ and $\hat{X}_{k-1}$ by $\hat{X}(k-1/k-1)$. To commence the algorithm at k = 1, the initial estimates of $\hat{P}_0$, even before the first observation vector is processed, is needed. In this study these estimates have been taken from the analyses in Chapter 4.

Similarly for k = 1, the initial estimate of the state $\hat{\overline{X}}_0$ is taken from the broadcast ephemeris.

Commencing at an arbitrary discrete time t_{k-1}, a procedure is considered for utilizing the observations $\overline{Y}_k$ at the next discrete time t_k to improve the estimate of the state. This is done in the following steps:

Step 1:

Given the nominal state $\overline{X}^*(t_{k-1})$ and the deviation $\hat{\overline{x}}(t_{k-1})$

$$\dot{\overline{X}}^* = F(\overline{X}^*, t), \quad \overline{X}^*(t_{k-1}) = \hat{\overline{X}}(t_{k-1})$$

and

$$\dot{\Phi}(k, k-1) = A(k)\Phi(k, k-1), \qquad \Phi(k-1, k-1) = I$$

are integrated numerically. The solutions will yield $\overline{X}^*(t_k)$ and $\Phi(k, k-1)$. The predicted state deviation

$$\hat{\overline{x}}(k/k-1) = \Phi(k, k-1)\hat{\overline{x}}(k-1/k-1) \tag{B53}$$

is then computed based on the concept of propagation of the mean, given in equation (B 39).

Step 2:

The predicted error covariance matrix of the state $\hat{P}(k/k-1)$ is computed from

$$\hat{P}(k/k-1) = \Phi(k/k-1)\hat{P}(k-1/k-1)\Phi^{\top}(k/k-1) + Q(k)$$

where

$$Q(k) = \int_{t_{k-1}}^{t_k} \Phi(t_k, \tau)Q(\tau)\Phi^{\top}(t_k, \tau)\,d\tau \qquad \text{vide equation (B 46)}$$

Analytical expressions for this have been derived in [Myers, 1973].

Step 3:

The observation vector $\overline{Y}(t_k)$ is now processed for estimation by first computing the observational deviation

$$\overline{y}_{(t_k)} = \overline{Y}_{(t_k)} - O(\overline{X}^*_{(t_k)} + \hat{\overline{x}}(k/k-1)) \tag{B54}$$

and the associated $H_{(t_k)}$ matrix for the observation state relation

$$\overline{y}_{(t_k)} = H_{(t_k)}\overline{x}(k/k) + V_{(t_k)} \tag{B55}$$

123

in which $\bar{x}(k/k)$ and $\bar{V}_{(t_k)}$ are the unknown state deviation and the observational error. Let $H_{(t_k)}$ be denoted as $H_{(k)}$ and $\bar{y}_{(t_k)}$ as $\bar{y}_{(k)}$.

Under the assumption that the estimate is a linear function of observations, and using the principle of minimum variance of the estimate as in normal least squares procedures, the following expression for the estimate of state at step k, after processing observations at t_k, is obtained

$$\hat{\bar{x}}(k/k) = \hat{\bar{x}}(k/k-1) + K(k)[\bar{y}_{(k)} - H_{(k)}\hat{\bar{x}}(k-1/k-1)] \tag{B 56}$$

where $K(k)$ is the $n \times p$ Kalman gain matrix given by

$$K_{(k)} = \hat{P}(k/k-1)H^{T}_{(k)}[H_{(k)}P_{(k/k-1)}H^{T}_{(k)} + R_{(k)}]^{-1} \tag{B 57}$$

This matrix is also called the filter gain. In (B 57) the matrix to be inverted is of size $p \times p$, the number of observations at t_k. The observation covariance matrix $R_{(k)}$ is assumed to be positive definite to ensure that the matrix in the brackets can be inverted. The new estimate of the state at t_k is

$$\hat{\bar{X}}_{(t_k)} = \bar{X}^{*}_{(t_k)} + \hat{\bar{x}}(k/k)$$

Step 4:

The new error covariance of the state based on the observations up to and including $\bar{Y}_{(t_k)}$ will be

$$\hat{P}(k/k) = [I - K_{(k)}H_{(k)}]\hat{P}(k/k-1) \tag{B 58}$$

and the algorithm is repeated for the next observation at t_{k+1}. To minimize the linearization errors, the current best estimate of the state is reinitialized as the nominal state vector for the next step. This procedure makes

$$\hat{\bar{X}}_{(t_k)} \quad \bar{X}^{*}_{(t_k)} + \hat{\bar{x}}(k/k)$$

the reinitialized nominal state for the next step, setting state deviation in Step 1 above to zero. This also simplifies computations.

124

It can be seen that the above estimation procedure which is at times known as first-order, nonadaptive filtering procedure with state noise compensation is very similar to a normal sequential least squares procedure, as applied to a dynamic situation. The inclusion of state noise is comparable to the procedure of weighting parameters in a solution. For example, we can compare equation (B 56) above to equation (27) of [Uotila, 1975]. This procedure treats state noise as a white noise process and takes cognizance of it in the adjustment procedure by assuming its statistical properties.

REFERENCES

Anderle, R.J. 1976. "Point Positioning Concept using Precise Ephemeris." Proceedings of the International Geodetic Symposium on Satellite Doppler Positioning, New Mexico State University, Las Cruces, N.M.

Anderson, T.W. 1971. The Statistical Analysis of Time Series. John Wiley Inc., New York.

Black, H.D. 1976. "Position Determination using the Transit System." Proceedings of the International Geodetic Symposium on Satellite Doppler Positioning, New Mexico State University, Las Cruces, N.M.

Blaha, G. 1971. "Inner Adjustment Constraints with Emphasis on Range Observations." Report No. 148 Department of Geodetic Science , The Ohio State University, Columbus, Ohio.

Brown, D.C. and J.E. Trotter 1969. "SAGA, A Computer Program for Short Arc Geodetic Adjustment of Satellite Observations." Report No. AFCRL-TR-69-0080, Air Force Cambridge Research Laboratories, Bedford, Mass.

Brown, D.C. and J.E. Trotter. 1973. "Extension to SAGA for Geodetic Reductions of Doppler Observations." Report No. AFCRL-TR-73-0177, Air Force Cambridge Research Laboratories, Bedford, Mass.

Brown, D.C. 1976. "Doppler Positioning by the Short Arc Method." Proceedings of the International Geodetic Symposium on Satellite Doppler Positioning, New Mexico State University, Las Cruces, N.M.

Fehlberg, E. 1968. "Classical Fifth-, Sixth-, Seventh- and Eighth-Order Runge-Kutta Formulas with Stepsize Control," NASA-TR-R-287. Aeronautics and Space Administration, Washington, D.C.

Hartwell, J.G. 1968. "A Power Series Solution for the Motion of an Artificial Satellite and its Concomitant Variational Equations." Report for GEOS Observation System Intercomparison Investigation, NASA Contract No. NAS-5-10588, Washington, D.C.

Hartwell, J.G. and T.R. Lewis. 1967. "Integration of Orbits and Concomital Variational Equations by Recurrent Power Series," Report for GEOS Observation System Intercomparison Investigation, NASA Contract No. NAS-5-10588, Washington, D.C.

Ingram, D.S. 1971. "Orbit Determination in the Presence of Unmodeled Accelerations." Report No. AMRL-1022. Applied Mechanics Research Laboratory, the University of Texas at Austin, Texas.

Jazwinsky, A.H. 1970. Stochastic Processes and Filtering Theory. Academic Press, New York.

Jenkins, G.M. and D.G. Watts, 1968. Spectral Analysis and its Applications, Holden-Day Series in Time Series Analysis, San Francisco.

Kouba, J. and D.E. Wells. 1976. "Semi-Dynamical Doppler Satellite Positioning." Bulletin Geodesique, Vol. 50, No. 1.

Kumar, M. 1976. "Monitoring of Crustal Movements in the San Andreas Fault Zone by a Satellite-Born Ranging System." Report No. 243 Department of Geodetic Science, The Ohio State University, Columbus, Ohio.

Krakiwsky, E.J. and A.J. Pope. 1967. "Least Squares Adjustment of Satellite Observations for Simultaneous Directions or Ranges." Report No. 86, Department of Geodetic Science, The Ohio State University, Columbus, Ohio.

Lerch, F.J., J.A. Richardson, and J.E. Brown. 1975. "Improvement in the Gravitational Potential Derived from Satellite Data (Goddard Earth Model, GEM 7)." Paper presented at the Annual Spring Meeting of the American Geophysical Union, Washington, D.C., June 16-20. E S Vol. 56, No. 6.

Meditch, J.S. 1969. Stochastic Optimal Linear Estimation and Control. McGraw-Hill Co., New York.

Moffett, J.B. 1973. "Program Requirements for Two Minute Integrated Doppler Satellite Navigation Solution." Technical Memorandum TG-819-(Rev. 2). Applied Physical Laboratory, The Johns Hopkins University, Silver Springs, Maryland.

Moritz, H. 1972. "Advanced Least Squares Methods." Report No. 175, Department of Geodetic Science. The Ohio State University, Columbus, Ohio.

Mueller, I. I. 1976. "Closing Summary" at the International Symposium on The Changing World of Geodetic Science, Report No. 250, Department of Geodetic Science, The Ohio State University , Columbus, Ohio.

Myers, K.A. 1973. "Filtering Theory Methods and Applications to the Orbit Determination Problem for Near-Earth Satellites." Report No. AMRL-1058. Applied Mechanics Research Laboratory, the University of Texas at Austin, Texas.

Piscane, V.L., B.B. Holland, and H.D. Black. 1973. "Recent (1973) Improvements in the Navy Navigation Satellite System." Navigation, Vol. 20, No. 3.

Pope, A.J. 1971. "Transformation of Covariance Matrices Due to Changes in Minimal Control." Paper presented at the American Geophysical Union fall meeting, San Francisco. EOS , Vol. 52, No. 11.

Rao, C.R. 1973. Linear Statistical Interference and its Applications, Second Edition, John Wiley Inc., New York.

Sims, T. 1972. "The NWL Ephemeris". Technical Report TR-2872, U.S. Naval Weapons Laboratory, Dahlgren, Virginia.

Staff of Applied Physics Laboratory. 1975-76. "Planned Improvements in the Transit System (1975)", Navigation, Journal of the Institute of Navigation, Vol. 22, No. 4.

Tapley, B.C. and V. Szebehely, 1972. "Statistical Orbit Determination Theory", Recent Advances in Dynamical Astronomy, Proceedings of the NATO Study Institute in Dynamical Astronomy, held in Cortina, D'ampezzo, Italy, 1972. D. Reidel Publishing Company, Boston.

Uotila, U.A. 1967. "Introduction to Adjustment Computations with Matrices." Department of Geodetic Science, Lecture Notes, The Ohio State University, Columbus, Ohio.

Uotila, U.A. 1975. "Sequential Solutions with Observation Equations." Department of Geodetic Science, Lecture Notes, The Ohio State University, Columbus , Ohio.

Vincenty, T. 1976. "Determination of North American Datum 1983 Coordinates of Map Corners." NOAA Technical Memorandum NOS. NGS-6. National Geodetic Survey, Rockville, Maryland.

Wells, D.E. 1974. "Doppler Satellite Control." Technical Report No. 29. University of New Brunswick, Fredericton, New Brunswick, Canada.

White, H.L., D.N. Huber, and J.L. Taylor, 1975. "Comparison between Naval Surface Weapons Center and Navy Astronautics Group Ephemerides for Geoceiver Positioning". Report No. TR-75-001, Defense Mapping Agency, Aerospace Center, St. Louis, Mo.